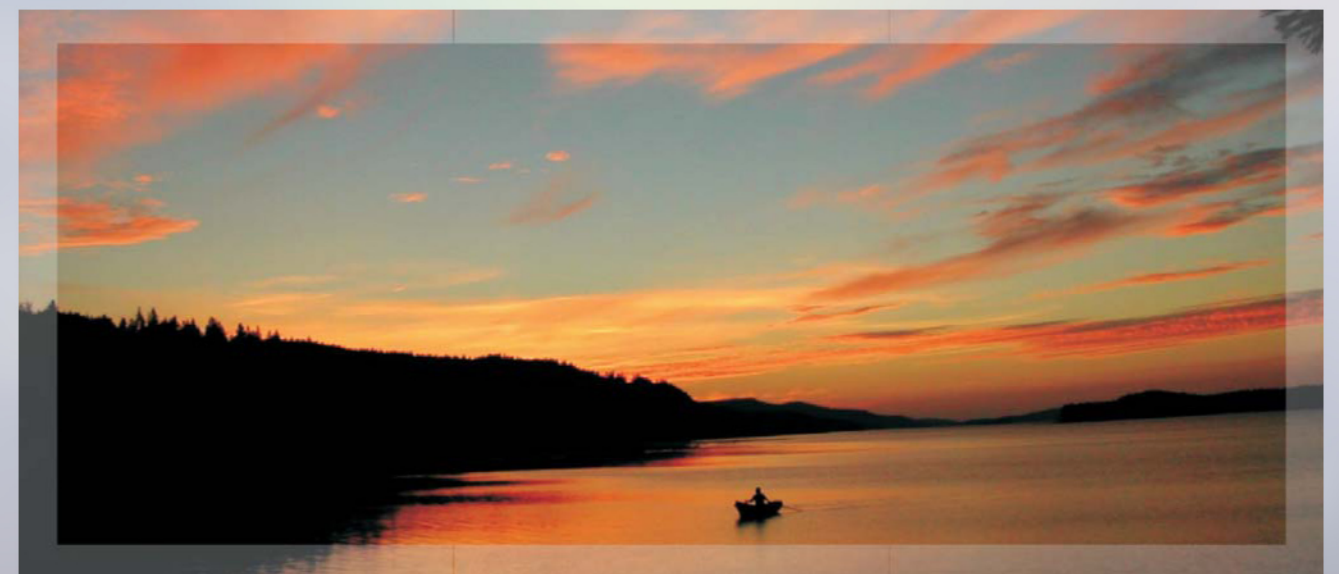


# Proceedings



## Fourth International Workshop **Nanocarbon Photonics and Optoelectronics**

28 July - 1 August 2014, Holiday Centre "Huhmari"  
Polvijärvi, Finland



University of Eastern Finland  
Institute of Photonics

# Proceedings

## Fourth International Workshop Nanocarbon Photonics and Optoelectronics Holiday centre "Huhmari", Polvijärvi, Finland

Editors:  
Yuri Svirko  
Alexander Obraztsov

Finland  
28 July - 1 August 2014



Sunday, July 27	Monday, July 28	Tuesday, July 29	Wednesday, July 30	Thursday, July 31	Friday, August 1	Saturday, August 2
ARRIVAL	Graphene	Photonics & Photovoltaics	Anticarb	Photonics & Optoelectronics	Synthesis & Characterization	DEPARTURE
7:00-9:00	Breakfast <b>8:50 OPENING</b>	Breakfast	Breakfast	Breakfast	Breakfast	Breakfast
9:00-10:30	J. M. Kim R. Fasel Coffee Break	W. Blau S. Maruyama Coffee Break	M. Kauranen M. Gonokami Coffee Break	M. Zheng H. Kataura Coffee Break	E. Kauppinen V. Kuznetsov Coffee Break	DEPARTURE
10:30-10:45	O. Shenderova A. Okotrub R. Shimano T. Makarova	Z. Sun A. Säynätjoki S. Maksimenko D. Lioubtchenko	G. Lanzani D. Golberg	T. Michel N. Izard L. Alvarez P. Fedotov	K. Eltsov Y. Li Y. Ohno A. Tonkikh	
10:45-12:15	Lunch	Lunch	Lunch	Lunch	Lunch	
12:15-14:00	A. Ferrari	Y. H. Lee		S. Purcell	M. Paillet	
14:00-14:45	A. Chernov D. Rybkovsky L. Karvonen	H. Yang I. Nefedov G. Mikheev	Workshop excursion Outokumpu mining museum	V. Klesch V. Korotceev Y. Shumin	T. Kaplas M. Qui M. Rybin	
14:45-15:30	Coffee Break	Coffee Break		Coffee Break	Coffee Break	Coffee Break
15:30-15:45	A. Jorio	A. Loiseau		J. Sipe	R. Ismagilov N. Valynets V. Vanyukov P. D'yachkov <b>CLOSING</b>	
15:45-16:30	J. Riikonen O. Sedelnikova	C. Gadermaier P. Obratsov		Y. Kato X. Gan		
16:30-17:10						
17:15-18:00						
18:00-19:30	Welcome Party	Dinner	Workshop reception <a href="#">Louhi Restaurant</a> , <a href="#">Huhmari</a>	Dinner	Boat trip to Hiekkasaari island including smoked salmon dinner	
19:30-21:00	Dinner	<a href="#">Poster session I</a>		<a href="#">Poster Session II</a>		

## NPO2014 Schedule-at-a-glance

## Workshop Co-Chairs

Yuri Svirko, University of Eastern Finland, Finland

Alexander Obraztsov, M.V. Lomonosov Moscow State University

## Program Committee

Hirofumi Kataura, AIST, Japan

Esko Kauppinen, Aalto University, Finland

Guglielmo Lanzani, Polytechnico di Milano, Italy

Elena Obraztsova, A. M. Prokhorov General Physics Institute, Russia

## Local Organizing Committee

Prof. Timo Jääskeläinen

Dr. Dmitry Lyashenko

Mrs. Hannele Karppinen

Mr. Timo Vahimaa

## NPO2014 Sponsor Organisations





**The municipality of POLVIJÄRVI** was founded in the year 1876 in the Eastern Finland. Polvijärvi is located about 40 km away from Joensuu. Currently the municipality is an active rural community with about 4.900 inhabitants. It offers a high-standard public services and offers excellent possibilities for leisure-time activities. The nearest Joensuu airport is 30 km away from Polvijärvi.

#### **The business services**

The municipality of Polvijärvi offers good business opportunities. New industrial areas have been built for companies. Recently, the training of entrepreneurs and cooperation between them have been in the centre of our interest. We expect growth especially in the wood processing industry and subcontract work. Tourism and agriculture are also very important. The lowering of the water level in Lake Höytiäinen in 1859 created a base for strong agriculture.

#### **Social services**

Polvijärvi offers high level social services for community members. These include fast placement of children to the day-care centres, well maintained public school and health care centre.

#### **Leisure-time services**

Leisure center that includes the ice hockey hall is situated in the center of Polvijärvi. The library offers a variety of services for community members. Many hospitable farms in the close vicinity of Polvijärvi offer delicious food, entertainment, activities for the whole family and cottages for rent. The holiday centre Huhmari is a place full of entertainment.

If you are interested in buying property in Finland we can offer you building sites for sell in the centre of Polvijärvi and in the surrounding small villages.

WELCOME to our municipality!

Polvijärventie 15, PL 6, FINLAND - 83701 POLVIJÄRVI

The municipal manager: **Mr Pauli Vaittinen**. Tel: +358-04010 46001,  
e-mail: pauli.vaittinen@polvijarvi.fi

The administrative manager: **Mrs Helena Kaasinen**. Tel: +358-04010 46002  
e-mail: helena.kaasinen@polvijarvi.fi

[www.polvijarvi.fi](http://www.polvijarvi.fi)

## Welcome to NPO2014

We are pleased to welcome you to the 4<sup>th</sup> International Workshop on Nanocarbon Photonics and Optoelectronics (NPO2014) that continues a series of meetings organized by the University of Eastern Finland. Since 2008 NPO Workshops bring together research leaders from both academia and industry to discuss the latest achievements in this rapidly developing area of modern physics and nanotechnology. The Workshops are also of strong educational importance allowing young researchers and students to attend lectures given by senior scientists and to be involved in intensive ideas exchange and networking. We hope that you will enjoy both scientific and social program of NPO2014.

Similar to previous Workshops, the NPO2014 has attracted about 100 researchers and students from around the globe. The Proceedings of the Workshops will be published in the special issue of Journal of Nanoelectronics and Optoelectronics and will be available for downloading.

We are grateful to our sponsors for their financial backing, which has allowed us to provide travel support to our lecturers and to reduce the participation fee. The Workshop venue is situated on the shores of lake Höytiäinen, whose broad waters and numerous islands offer magnificent scenery. We hope that the NPO2014 will expand on the success of previous Workshops and will provide its participants with the opportunity to enjoy the beauty of Finnish Lakeland.

Alexander Obraztsov  
Yuri Svirko  
*NPO2014 Co-Chairs*

# Contents

<b>Monday, July 28</b>	<b>1</b>	
9:00-9:45	<b>Convergence of nanotechnologies for the future photonics and other applications</b> Jong Min Kim, Seugnam Cha and Junginn Sohn, <i>Department of Engineering Science, University of Oxford, Oxford, UK</i> . . . . .	3
9:45-10:30	<b>Electronic and optical properties of atomically precise graphene nanoribbons</b> Roman Fasel, <i>EMPA, Swiss Federal Laboratories for Materials Science and Technology, Dben-dorf, Switzerland</i> . . . . .	6
10:45-11:10	<b>Fluorescent nanocarbon materials for bioimaging</b> O.A. Shenderova <sup>1,2</sup> , G. MvGuire <sup>1,2</sup> , I. Vlasov <sup>3</sup> , J.M. Rosenholm <sup>4</sup> , <sup>1</sup> <i>International Technol-ogy Center, Raleigh, NC</i> , <sup>2</sup> <i>Admas Nanotechnologies, Raleigh, NC</i> , <sup>3</sup> <i>General Physics Institute, Moscow</i> , <sup>4</sup> <i>Åbo Akademi University, Turku</i> . . . . .	7
11:10-11:35	<b>Electronic structure and optical properties of half-fluorinated graphite</b> A. V. Okotrub <sup>1</sup> , L. G. Bulusheva <sup>1</sup> , I.P. Asanov <sup>1</sup> , G.N.Chehova <sup>1</sup> , D.V. Pinakov <sup>1</sup> , T. L. Makarova <sup>2</sup> , <sup>1</sup> <i>Nikolaev Institute of Inorganic Chemistry SB RAS, Novosibirsk, Russia</i> , <sup>2</sup> <i>Umeå University, Umeå, Sweden</i> . . . . .	8
11:35-12:00	<b>Quantum Faraday effect in graphene</b> Ryo Shimano, <i>Cryogenic Research Center, The University of Tokyo, Tokyo, Japan</i> . . . . .	9
12:00-12:15	<b>Quantum nature of graphene magnetism</b> Tatiana L. Makarova and Andrei Shelankov, <i>Ioffe Physical-Technical Institute, St. Petersburg, Russia</i> . . . . .	10
14:00-14:45	<b>Raman spectroscopy in graphene and layered materials</b> Andrea Ferrari, <i>Cambridge Graphene Centre, Cambridge, UK</i> . . . . .	11
15:45-15:00	<b>H-terminated graphene nanoribbons and coronene stacks inside single-walled carbon nanotubes</b> Alexander I. Chernov <sup>1</sup> , Pavel V. Fedotov <sup>1</sup> , Albert G. Nasibulin <sup>2</sup> , Esko I. Kauppinen <sup>2</sup> , Vladimir L. Kuznetsov <sup>3</sup> , Elena D. Obraztsova <sup>1</sup> , <sup>1</sup> <i>A.M. Prokhorov General Physics Institute, Moscow, Russia</i> , <sup>2</sup> <i>Department of Applied Physics, Aalto University School of Science, Espoo, Finland</i> , <sup>3</sup> <i>Boreskov Institute of Catalysis SB RAS, Novosibirsk, Russia</i> . . . . .	12
15:00-15:15	<b>Transition between ring-shaped and parabolic valence band maximum in few-layer A<sub>3</sub>B<sub>6</sub> compounds</b> Dmitry V. Rybkovskiy, Alexander V. Osadchy, Elena D. Obraztsova, <i>A.M. Prokhorov General Physics Institute, Russian Academy of Sciences, 119991, Moscow, Vavilov Str., 38, Russia</i> . . . . .	13
15:15-15:30	<b>Investigation of optical nonlinearities in few-layer gallium selenide by multiphoton microscopy</b> Lasse Karvonen <sup>1</sup> , Antti Säynätjoki <sup>1</sup> , Soroush Mehravar <sup>2</sup> , Raul. D. Rodriquez <sup>3</sup> , Susanne Müller <sup>3</sup> , Dietrich R.T. Zahn <sup>3</sup> , Seppo Honkanen <sup>4</sup> , Robert Norwood <sup>2</sup> , Nasser Peyghambarian <sup>1,2,4</sup> , Khanh Kieu <sup>2</sup> , Harri Lipsanen <sup>1</sup> and Juha Riihonen <sup>1</sup> , <sup>1</sup> <i>Department of Micro and Nanosciences, Aalto University, Espoo, Finland</i> , <sup>2</sup> <i>College of Optical Sciences, University of Arizona, Tucson, USA</i> , <sup>3</sup> <i>Semiconductor Physics, Chemnitz University of Technology, Chemnitz, Germany</i> , <sup>4</sup> <i>Institute of Photonics, University of Eastern Finland, Joensuu, Finland</i> . . . . .	14
15:45-16:30	<b>Correlated Stokes-anti-Stokes photons in twisted bilayer graphene</b> Ado Jorio, <i>Departamento de Física, UFMG, Belo Horizonte, Brazil</i> . . . . .	15



16:30-16:55	<b>Rapid synthesis of monolayer graphene by photo-thermal chemical vapour deposition</b> Juha Riikonen <sup>1</sup> , Wonjae Kim <sup>1</sup> , Changfeng Li <sup>1</sup> , Jannatul Susoma <sup>1</sup> , Sanna Arpiainen <sup>2</sup> , Markku Kainlauri <sup>2</sup> , and Harri Lipsanen <sup>2</sup> , <sup>1</sup> <i>Department of Micro- and Nanosciences, Aalto University, Espoo, Finland</i> , <sup>2</sup> <i>VTT Technical Research Centre of Finland, Espoo, Finland</i> . . . . .	16
16:55-17:10	<b>Optical properties of graphitic material: effect of corrugation and stacking</b> Olga V. Sedelnikova <sup>1</sup> , Lyubov G. Bulusheva <sup>1</sup> , Andrey Chuvilin <sup>2</sup> , Igor P. Asanov <sup>2</sup> and Alexander V. Okotrub <sup>1</sup> , <sup>1</sup> <i>Nikolaev Institute of Inorganic Chemistry, SB RAS, Novosibirsk, Russia</i> , <sup>2</sup> <i>CIC nanoGUNE, San Sebastian, Spain</i> . . . . .	17
<b>Tuesday, July 29</b>		<b>19</b>
9:00-9:45	<b>Rational bottom-up assembly of tailored molecular aggregates on nanocarbon for high sensitivity nonlinear optical and light harvesting applications</b> Werner J. Blau, <i>School of Physics and CRANN, Trinity College Dublin, Dublin, Ireland</i> . . .	21
9:45-10:30	<b>CNT-Si heterojunction solar cells with structure-controlled single-wall carbon nanotube films</b> Shigeo Maruyama, <i>Department of Mechanical Engineering, The University of Tokyo, Tokyo, Japan</i> . . . . .	23
10:45-11:10	<b>Graphene based ultrafast lasers</b> Zhipai Sun, <i>Department of Micro- and Nanosciences, Aalto University, Finland</i> . . . . .	24
11:10-11:35	<b>Ultrafast fiber lasers enabled by carbon nanotubes and their applications</b> Khanh Kieu <sup>1</sup> and Antti Säynätjoki <sup>2</sup> , <sup>1</sup> <i>College of Optical Sciences, The University of Arizona, Tucson, USA</i> , <sup>2</sup> <i>Aalto University, Finland</i> . . . . .	25
11:35-12:00	<b>Electromagnetic response of carbon nanotubes and nanotube-based composites in terahertz range</b> S.A. Maksimenko <sup>1</sup> , G. Y. Slepyan <sup>2</sup> , M. V. Shuba <sup>1</sup> , P.P. Kuzhir <sup>1</sup> , <sup>1</sup> <i>Institute for Nuclear Problems, Belarusian State University, Minsk, Belarus</i> , <sup>2</sup> <i>Department of Physical Electronics, Tel Aviv University, Tel Aviv, Israel</i> . . . . .	26
12:00-12:15	<b>Suspended carbon nanotubes network MEMS varactor</b> Dmitri Lioubtchenko, Andrey Generalov, Ilya Anoshkin, Albert G. Nasibulin, Victor Ovchinnikov and Antti Räisänen, <i>Department of Radio Science and Engineering, Aalto University, Espoo, Finland</i> . . . . .	27
10:00-14:45	<b>Optical responses of graphene</b> Young Hee Lee and Seong Chu Lim, <i>IBS Center for Integrated Nanostructure Physics, Institute for Basic Science (IBS), Department of Energy Science, Department of Physics, Sungkyunkwan University, Suwon, Republic of Korea</i> . . . . .	28
14:45-15:00	<b>Broadband polarization dynamics control with aligned carbon nanotubes</b> Bo Fu <sup>1,2</sup> , He Yang <sup>1</sup> , Ya Chen <sup>1</sup> , Marco Mattila <sup>1</sup> , Zhenzhong Yong <sup>3</sup> , Qingwen Li <sup>3</sup> , Changxi Yang <sup>2</sup> , Ilkka Tittonen <sup>1</sup> , Harri Lipsanen <sup>1</sup> and Zhipai Sun <sup>1</sup> , <sup>1</sup> <i>Department of Micro- and Nanosciences, Aalto University, Espoo, Finland</i> , <sup>2</sup> <i>The State Key Laboratory of Precision Measurement Technology and Instruments, Department of Precision Instruments, Tsinghua University, Beijing, China</i> , <sup>3</sup> <i>Suzhou Institute of Nano-tech and Nano-bionics, Chinese Academy of Sciences, Suzhou, Jiangsu, China</i> . . . . .	29
15:00-15:15	<b>Asymmetric hyperbolic metamaterials for graphene nanophotonics</b> Igor Nefedov <sup>1</sup> , Leonid Melnikov <sup>2</sup> , Evgeny Nefedov <sup>1</sup> , <sup>1</sup> <i>Aalto University, Espoo, Finland</i> , <sup>2</sup> <i>Yuri Gagarin State Technical University of Saratov, Saratov, Russia</i> . . . . .	30
15:15-15:30	<b>Nanocarbon films based photovoltaic and optical devices</b> G. M. Mikheev, <i>Institute of Mechanics, Russian Academy of Sciences, Izhevsk, Russia</i> . . . . .	31
15:45-16:30	<b>Luminescence properties of h-BN materials: from bulk to 1D and 2D nano structures</b> Annick Loiseau, <i>ONERA, France</i> . . . . .	32
16:30-16:55	<b>Photophysics of semiconducting two-dimensional transition metal dichalcogenides</b> Christoph Gadermaier, <i>Department of Complex Matter and International Postgraduate School Jozef Stefan Institute, Ljubljana, Slovenia</i> . . . . .	34
16:55-17:10	<b>Optically induced terahertz emission from 3D topological insulators</b> Petr A. Obraztsov <sup>1,2</sup> , Pavel A. Chizov <sup>1</sup> , Oleg E. Tereshchenko <sup>3</sup> , Sergey V. Garnov <sup>1</sup> , Yuri Svirko <sup>2</sup> , <sup>1</sup> <i>A.M. Prokhorov General Physics Institute, Moscow, Russia</i> , <sup>1</sup> <i>Department of Physics</i>	

and Mathematics, University of Eastern Finland, Joensuu, Finland, <sup>1</sup>Institute of Semiconductor Physics, SB RAS, Novosibirsk, Russia . . . . . 35

**Poster session I** **37**

- PI.1 **Theoretical study of carbon nanotubes heat capacity in the frame of continuous theory of thin cylindrical shell dynamics**  
M. V. Avramenko, I. Yu. Golushko, S. B. Rochal, D. I. Levshov, Y. I. Yuzyuk, *Department of Nanotechnology, Faculty of Physics, Southern Federal University, Rostov-on-Don, Russia* . . . . . 39
- PI.2 **Extraction of carrier density and  $\pi$ - electron relaxation constant in terahertz wave transmission experiments with graphene sandwich structures**  
K. Batrakov<sup>1</sup>, P. P. Kuzhir<sup>1</sup>, S. A. Maksimenko<sup>1</sup>, S. Voronovich<sup>1</sup>, A. Paddubskaya<sup>2</sup>, J. Macutkevici<sup>3</sup>, T. Kaplas<sup>4</sup> and Y. Svirko<sup>4</sup>, <sup>1</sup>Research Institute for Nuclear problems of Belarusian State University, Belarus, <sup>2</sup>Center for Physical Science and technology, Vilnius, Lithuania, <sup>3</sup>Vilnius University, LT-00122 Vilnius, Lithuania, <sup>4</sup>Institute of Photonics, University of Eastern Finland, Joensuu, Finland . . . . . 40
- PI.3 **Raman spectroscopy for the characterization of multi-walled carbon nanotubes**  
S.N. Bokova-Sirosh<sup>1,2</sup>, E.D. Obratsova<sup>1,2</sup>, M. A. Shuvaeva<sup>3,5</sup>, A. V. Ishchenko<sup>3</sup>, D. V. Krasnikov<sup>3,5</sup> and V. L. Kuznetsov<sup>3,5,6,7</sup>, <sup>1</sup>A.M. Prokhorov General Physics Institute RAS, Moscow, Russia, <sup>2</sup>National Research Nuclear University MEPhI Moscow, Russia, <sup>3</sup>Boreskov Institute of Catalysis SB RAS, Novosibirsk, Russia, <sup>4</sup>Nikolaev Institute of Inorganic Chemistry, SB RAS, Novosibirsk, Russia, <sup>5</sup>Novosibirsk State University, Novosibirsk, Russia, <sup>6</sup>Novosibirsk State Technical University, Novosibirsk, Russia, <sup>7</sup>National Tomsk State University, Tomsk, Russia . . . . . 41
- PI.4 **Femtosecond charge transfer from MoS<sub>2</sub> to organic acceptor**  
T. Borzda<sup>1</sup>, N. Vujcic<sup>1,2</sup>, C. Gadermaier<sup>1</sup>, P. Topolovsek<sup>1</sup>, T. Mertelj<sup>1</sup>, D. Vella<sup>1</sup>, V. Vega Mayor<sup>1</sup>, D. Mihailovic<sup>1</sup>, <sup>1</sup>Department of Complex Matter, Jozef Stefan Institute, Ljubljana, Slovenia, <sup>2</sup>Institute of Physics, Zagreb, Croatia . . . . . 42
- PI.5 **In situ Raman monitoring of single-wall carbon nanotube filling with CuCl**  
T. V. Eremin<sup>1,2</sup>, A.A. Tonkikh<sup>2</sup>, E. D. Obratsova<sup>1,2</sup>, <sup>1</sup>Physics Department of M.V. Lomonosov Moscow State University, Moscow, Russia, <sup>2</sup>A.M. Prokhorov General Physics Institute, RAS, Moscow, Russia . . . . . 43
- PI.6 **The study of environmental and coupling effects in individual carbon nanotubes**  
D. Levshov<sup>1</sup>, M. V. Avramenko<sup>1</sup>, T. Michel<sup>2</sup>, R. Arenal<sup>3</sup>, Y. I. Yuzyuk<sup>1</sup>, J. L. Sauvajol<sup>2</sup>, <sup>1</sup>Faculty of Physics, Southern Federal University, Rostov-on-Don, Russia, <sup>2</sup>University Montpellier 2, Laboratoire Charles Coulomb, Montpellier, France, <sup>3</sup>Laboratorio de Microscopias Avanzadas, Instituto de Nanociencia de Aragon, Universidad de Zaragoza, Zaragoza, Spain . . . . . 44
- PI.7 **Multiwall carbon nanotube/silicon hybrids as a solar cell prototype**  
E. V. Lobiak<sup>1</sup>, D. S. Bychanok<sup>2</sup>, E.V. Shlyakhova<sup>1</sup>, A. V. Okotrub<sup>1</sup> and L. G. Bulusheva<sup>1</sup>, <sup>1</sup>Nikolaev Institute of Inorganic Chemistry, Siberian Branch of Russian Academy of Sciences, Novosibirsk, Russia, <sup>2</sup>Institute for Nuclear Problems, Belarus State University, Minsk, Belarus . . . . . 45
- PI.8 **Graphene passively mode-locking fiber laser**  
Man Jiang<sup>1</sup>, Diao Li<sup>1</sup>, Yali Liu<sup>2</sup>, Xuetao Gan<sup>1</sup>, Zhaoyu Ren<sup>1</sup> and Jintao Bai<sup>1</sup>, <sup>1</sup>Institute of Photonics and Photon-Technology, Department of Physics, Northwest University, Xi'an, China, <sup>2</sup>Department of Applied Physics, Northwestern Polytechnical University, Xi'an, China . . . . . 46
- PI.9 **Electronic and optical properties of graphene nanoribbons encapsulated in single-wall carbon nanotubes**  
A.V. Osadchy, D. V. Rybkovskiy, E. D. Obratsova, A. M. Prokhorov General Physics Institute of Russian Academy of Sciences, Moscow, Russia . . . . . 47
- PI.10 **Investigation of "fullerene-quantum dots" composite materials for solar cells applications**  
Sergey Pavlov, Demid Kirilenko, Alexei Nashchekin, *Ioffe Physical-Technical Institute of RAS, Saint-Petersburg, Russia* . . . . . 48
- PI.11 **Graphene for terahertz application**  
Yixuan Zhou, Zhaoyu Ren, Mei Qi, Xinlong Xu, and Jintao Bai, *Institute of Photonics and Photon-Technology, Northwest University, Xi'an, China* . . . . . 49
- PI.12 **Effect of polarization ellipticity on photovoltaic response of nanocarbon and Ag/Pd resistive films**

	A.S. Saushin <sup>1</sup> , R.G. Zonov <sup>1</sup> , A.G. Nasibulin <sup>2</sup> , G.M. Mikheev <sup>1</sup> , <sup>1</sup> <i>Institute of Mechanics UB RAS, Izhevsk, Russia</i> , <sup>2</sup> <i>Skolkovo Institute of Science and Technology, Skolkovo, Russia</i> . . . . .	50
PI.13	<b>Pump-probe WS<sub>2</sub> fundamental properties</b> V. Vega Mayoral <sup>1</sup> , D. Vella <sup>1</sup> , T. Borzda <sup>1</sup> , N. Vujicic <sup>1,2</sup> , P. Topolovsek <sup>1</sup> , M. Prijatelj <sup>1</sup> , C. Gadermaier <sup>1</sup> and D. Mihailovic <sup>1</sup> , <sup>1</sup> <i>Department of Complex Matter, Jozef Stefan Institute, Ljubljana, Slovenia</i> , <sup>2</sup> <i>Institute of Physics, Zagreb, Croatia</i> . . . . .	51
PI.14	<b>Femtosecond spectroscopy on MoS<sub>2</sub> films: effects of synthesis on the electron dynamics</b> D. Vella <sup>1</sup> , V. Vega Mayoral <sup>1</sup> , T. Borzda <sup>1</sup> , N. Vujicic <sup>1,2</sup> , P. Topolovsek <sup>1</sup> , M. Prijatelj <sup>1</sup> , C. Gadermaier <sup>1</sup> and D. Mihailovic <sup>1</sup> , <sup>1</sup> <i>Department of Complex Matter, Jozef Stefan Institute, Ljubljana, Slovenia</i> , <sup>2</sup> <i>Institute of Physics, Zagreb, Croatia</i> . . . . .	52
PI.15	<b>Influence of external conditions on the photovoltaic response single walled carbon nanotube films</b> R.G. Zonov <sup>1</sup> , G.M. Mikheev <sup>1</sup> , A.G. Nasibulin <sup>2,3</sup> , <sup>1</sup> <i>Institute of Mechanics UB RAS, Izhevsk, Russia</i> , <sup>2</sup> <i>Aalto University, Espoo, Finland</i> , <sup>3</sup> <i>Skolkovo Institute of Science and Technology, Skolkovo, Russia</i> . . . . .	53
<b>Wednesday, July 30</b>		<b>55</b>
9:00-9:45	<b>Nonlinear microscopy with focused vector fields</b> Martti Kauranen, M. Huttunen, G. Bautista, J. Mäkitalo, <i>Department of Physics, Tampere University of Technology, Tampere, Finland</i> . . . . .	57
9:45-10:30	<b>Materials with threefold rotational symmetry for polarization control of light</b> Makoto Kuwata-Gonokami, <i>Department of Physics, The University of Tokyo, Tokyo, Japan</i> . . . . .	58
10:45-11:30	<b>Organic and hybrid interface dynamics upon photoexcitation</b> Guglielmo Lanzani, <i>Center for Nano Science and Technology@PoliMi, Istituto Italiano di Tecnologia, and Department of Physics Politecnico di Milano, Milano, Italy</i> . . . . .	60
11:30-12:15	<b>Nanomaterial optical studies in a transmission electron microscope</b> Dmitri Golberg, <i>World Premier International Centre for Materials Nanoarchitectonics (WPI-MANA), National Institute for Materials Science (NIMS), Tsukuba, Japan</i> . . . . .	61
<b>Thursday, July 31</b>		<b>63</b>
9:00-9:45	<b>Purification of single-chirality carbon nanotubes for optical spectroscopy studies</b> Ming Zheng, <i>National Institute of Standards and Technology, Gaithersburg, USA</i> . . . . .	65
9:45-10:30	<b>Separation and optical properties of small-diameter single-chirality SWCNTs</b> Hiromichi Kataura <sup>1</sup> , Xiaojun Wei <sup>1</sup> , Yasuhiro Ito <sup>1</sup> , Takuya Hirakawa <sup>1</sup> , Shunjiro Fujii <sup>1</sup> , Astushi Hirano <sup>1</sup> , Yuhei Miyauchi <sup>2,3</sup> , Kazunari Matsuda <sup>2</sup> and Takeshi Tanaka <sup>1</sup> , <sup>1</sup> <i>Nanosystem Research Institute (NRI), AIST, Tsukuba, Japan</i> , <sup>2</sup> <i>Institute of Advanced Energy, Kyoto University, Japan, Kawaguchi, Japan</i> . . . . .	66
10:45-11:10	<b>Supramolecular organization of <math>\pi</math>-conjugated molecules monitored by single-walled carbon nanotubes</b> L. Alvarez <sup>1,2</sup> , R. Le Parc <sup>1,2</sup> , Y. Almadori <sup>1,2</sup> , P. Dieudonn-George <sup>1,2</sup> , R. Aznar <sup>1,2</sup> , B. Joussetme <sup>3</sup> , S. Campidelli <sup>3</sup> , J. Cambedouzou <sup>4</sup> , F. Fossard <sup>5</sup> , A. Loiseau <sup>5</sup> , T. Saito <sup>6</sup> and J-L. Bantignies <sup>1,2</sup> , <sup>1</sup> <i>Universit Montpellier 2, Laboratoire Charles Coulomb, Montpellier, France</i> , <sup>2</sup> <i>CNRS, Laboratoire Charles Coulomb, Montpellier, France</i> , <sup>3</sup> <i>CEA-Saclay, IRAMIS, NIMBE, Laboratoire d'Innovation en Chimie des Surfaces et Nanosciences (LICSEN), 1 Gif-sur-Yvette Cedex, France</i> , <sup>4</sup> <i>Institut de Chimie Sparative de Marcoule, Bagnols sur Cze, France</i> , <sup>5</sup> <i>Laboratoire d'tude des microstructures, CNRS-ONERA, Chtillon, France</i> , <sup>6</sup> <i>Nanotube Research Center, National Institute of Advanced Industrial Science and Technology (AIST), Tsukuba, Japan</i> . . . . .	67
11:10-11:35	<b>Carbon nanotubes photonics: enhancement of s-SWNT pl using silicon microring resonators</b> A. Noury, X. Le Roux, L. Vivien and N. Izard, <i>Institut d'Electronique Fondamentale, Univ. Paris Sud, Orsay, France</i> . . . . .	68
11:35-12:00	<b>Coupled vibrations in index-identified carbon nanotubes</b> Thierry Michel <sup>1</sup> , Dmitry Levshov <sup>1,2</sup> , Raul Arenal <sup>3</sup> , Matthieu Paillet <sup>1</sup> , Xuan Tinh Than <sup>1</sup> , Ahmed-Azmi Zahab <sup>1</sup> , Yuri I. Yuzyuk <sup>2</sup> , Jean- Louis Sauvajol <sup>1</sup> , <sup>1</sup> <i>Laboratoire Charles Coulomb, University of Montpellier-CNRS, Montpellier, France</i> , <sup>2</sup> <i>Faculty of Physics, Southern Federal Uni-</i>	

	<i>versity, Rostov-on-Don, Russia, <sup>3</sup>Laboratorio de Microscopias Avanzadas (LMA), Instituto de Nanociencia de Aragon (INA), Universidad de Zaragoza, Zaragoza, Spain . . . . .</i>	69
12:00-12:15	<b>Optical Spectral Features of CuCl@SWCNT Hybrids Synthesized via Gas-Phase Technique</b> P. V. Fedotov, A. A. Tonkikh, E. D. Obraztsova, A.M. Prokhorov, A. M. Prokhorov <i>General Physics Institute, Moscow, Russia . . . . .</i>	70
14:00-14:45	<b>Photo-stimulated field emission from individual Si nanowires</b> A. Derouet <sup>1</sup> , M. Choueib <sup>1,2</sup> , S. C. Cojocar <sup>3</sup> , A. Ayari <sup>1</sup> , P. Vincent <sup>2</sup> , P. Poncharal <sup>1</sup> , S. Perisanu <sup>1</sup> , R. Martel <sup>2</sup> and S. T. Purcell <sup>1</sup> , <sup>1</sup> <i>Institute Lumire Matire, Universit de Lyon 1, Villeurbanne, France, <sup>2</sup> Dpartement de chimie, Universit de Montral, Montral, Canada, <sup>3</sup>Laboratoire PICM, Ecole polytechnique, Palaiseau, France . . . . .</i>	71
14:45-15:00	<b>Field electron emission from single crystal diamond needles</b> V.I.Kleshch <sup>1</sup> , S. T. Purcell <sup>2</sup> , A. N. Obraztsov <sup>1,3</sup> , <sup>1</sup> <i>Department of Physics, M. V. Lomonosov Moscow State University, Moscow, Russia</i> , <sup>2</sup> <i>Institute Lumire Matire, Universit de Lyon 1, Villeurbanne, France, <sup>3</sup>Department of Physics and Mathematics, University of Eastern Finland, Joensuu, Finland . . . . .</i>	72
15:00-15:15	<b>Molibdenum disulfide covered CNT arrays for electrochemical applications</b> Victor Koroteev, L. G. Bulusheva, A. V. Okotrub, <i>Nikolaev Institute of Inorganic Chemistry SB RAS, Novosibirsk, Russia . . . . .</i>	73
15:15-15:30	<b>Simulation of electromagnetic properties in CNTs- and graphene-based nanomaterials and nanodevices</b> Yuri Shunin <sup>1,2</sup> , Yuri Zhukovskii <sup>1</sup> , Victor Gopeyenko <sup>2</sup> , Nataly Burluckaya <sup>2</sup> , Tamara Lobanova-Shunina <sup>3</sup> and Stefano Bellucci <sup>4</sup> , <sup>1</sup> <i>Institute of Solid State Physics, University of Latvia, Latvia, <sup>2</sup>Information Systems Management Institute, Latvia, <sup>3</sup>Riga Technical University, Aviation Institute, Latvia, <sup>4</sup>INFN - Laboratori Nazionali di Frascati, Frascati (Rome), Italy . . . . .</i>	74
15:45-16:30	<b>Calculation of optical nonlinearities in graphene</b> J.E. Sipe <sup>1</sup> , JinLuo Cheng <sup>1,2</sup> , and Nathalie Vermeulen <sup>2</sup> , <sup>1</sup> <i>Department of Physics and Institute for Optical Sciences, Toronto, Canada, <sup>2</sup>Brussels Photonics Team (B-PHOT), Department of Applied Physics and Photonics, Vrije Universiteit Brussel, Belgium . . . . .</i>	75
16:30-16:55	<b>Single-carbon-nanotube devices for integrated photonics</b> Yuichiro K. Kato, <i>Institute of Engineering Innovation, The University of Tokyo, Tokyo, Japan</i>	76
16:55-17:10	<b>Chip-integrated graphene optoelectronic devices</b> Xuetao Gan <sup>1,2</sup> , Ren-Jye Shiue <sup>2,3</sup> , Kin Fai Maki <sup>4</sup> , Tony F. Heinz <sup>2,4</sup> , Dirk Englund <sup>2,3</sup> , <sup>1</sup> <i>School of Science, Northwestern Polytechnical University, Xi'an, China, <sup>2</sup>Department of Electrical Engineering, Columbia University, New York, USA, <sup>3</sup>Department of Electrical Engineering and Computer Science, Massachusetts Institute of Technology, Cambridge, USA, <sup>4</sup>Department of Physics, Columbia University, New York, USA . . . . .</i>	77
<b>Poster session II</b>		<b>79</b>
P11.1	<b>Experimental study and computer simulation of the growth of single-crystal diamond microneedles</b> A. M. Alexeev <sup>1</sup> , F. T. Tuyakova <sup>2,3</sup> , R. R. Ismagilov <sup>1</sup> , A. N. Obraztsov <sup>1,2</sup> , <sup>1</sup> <i>Department of Physics, Lomonosov Moscow State University, Moscow, Russia, <sup>2</sup>Institute of Photonics, University of Eastern Finland, Joensuu, Finland, <sup>3</sup>Moscow State Institute of Radio Engineering, Electronics and Automation, Moscow, Russia . . . . .</i>	81
P11.2	<b>Synthesis of large area carbon nanotube arrays on Cu substrate for field emission cathodes</b> V. Arkhipov <sup>1</sup> , A. Guselnikov <sup>1</sup> , L. G. Bulusheva <sup>1</sup> , A. V. Okotrub <sup>1</sup> , V. Baryshevsky <sup>2</sup> , P. P. Kuzhir <sup>2</sup> , S. A. Maksimenko <sup>2</sup> , <sup>1</sup> <i>Nikolaev Institute of Inorganic Chemistry SB RAS, Novosibirsk, Russia, <sup>2</sup>Research Institute for Nuclear Problems, Belarusian State University, Minsk, Belarus</i>	82
P11.3	<b>Laser synthesis of 1D polyynic carbon chains</b> N. R. Arutyunyan <sup>1,2</sup> , V. V. Kononenko <sup>1</sup> , E. D. Obraztsova <sup>1,2</sup> , <sup>1</sup> <i>A.M.Prokhorov General Physics Institute, Moscow, Russia, <sup>2</sup>National Research Nuclear University MEPhI, Moscow, Russia . . . . .</i>	83
P11.4	<b>The separation of single-walled carbon nanotubes synthesized by arc discharge technique by type of conductivity</b> V. A. Eremina <sup>1,2</sup> , P. V. Fedotov <sup>1</sup> , E. D. Obraztsova <sup>1,2</sup> , <sup>1</sup> <i>Physics Department of M.V. Lomonosov</i>	

	<i>Moscow State University, Moscow, Russia, <sup>1</sup>A.M.Prokhorov General Physics Institute, Moscow, Russia . . . . .</i>	84
PII.5	<b>Hot filament chemical vapor deposition of nanographite films</b> D. I. Finkelstein <sup>1</sup> , A. M. Alexeev <sup>1</sup> , F. T. Tuyakova <sup>2,3</sup> , R. R. Ismagilov <sup>1</sup> , A. N. Obraztsov <sup>1,2</sup> , <sup>1</sup> <i>Department of Physics, Lomonosov Moscow State University, Moscow, Russia, <sup>2</sup>Institute of Photonics, University of Eastern Finland, Joensuu, Finland, <sup>3</sup>Moscow State Institute of Radio Engineering, Electronics and Automation, Moscow, Russia . . . . .</i>	85
PII.6	<b>Computer simulation of spatial-temporal behaviour of active species in an atmospheric pressure dielectric barrier discharge</b> R. R. Ismagilov <sup>1</sup> , A. M. Alexeev <sup>1</sup> , F. T. Tuyakova <sup>2,3</sup> , Kuo-Hui Yang <sup>4</sup> , A. N. Obraztsov <sup>1,2</sup> , <sup>1</sup> <i>Department of Physics, Lomonosov Moscow State University, Moscow, Russia, <sup>2</sup>Department of Physics and Mathematics, University of Eastern Finland, Joensuu, Finland, <sup>3</sup>Moscow State Institute of Radio Engineering, Electronics and Automation, Moscow, Russia . . . . .</i>	86
PII.7	<b>Properties of gas sensors based on graphene and single wall carbon nanotubes</b> I. I. Kondrashov <sup>1</sup> , P. S. Rusakov <sup>1</sup> , M. G. Rybin <sup>1</sup> , I. V. Sokolov <sup>1</sup> , A. S. Pozharov <sup>1</sup> , R. N. Rizakhanov <sup>2</sup> and E. D. Obraztsova <sup>1</sup> , <sup>1</sup> <i>A. M. Prokhorov General Physics Institute, Moscow, Russia, <sup>2</sup>Keldysh Research Center, Moscow, Russia . . . . .</i>	87
PII.8	<b>Boron nitride synthesis in afterglow phase of a discharge in molybdenum-dielectric powder</b> E.M.Konchekov, G. M.Batanov, V. D. Borzosekov, N. K. Kharchev, L. V. Kolik, A. A. Letunov, D. V. Malakhov, F. O. Milovich, E. A. Obraztsova, E. D. Obraztsova, A. E. Petrov, K. A. Sarkisian, N. N. Skvortsova, V. D. Stepakhin, <i>Prokhorov General Physics Institute of Russian Academy of Sciences, Moscow, Russia . . . . .</i>	88
PII.9	<b>Semiinsulating 6H-SiC substrate for graphen growth</b> A. A. Lebedev <sup>1</sup> , A. V. Vasil'ev <sup>2</sup> , Yu. N. Makarov <sup>2</sup> , S. S. Nagaluk <sup>2</sup> , A. N. Smirnov <sup>1</sup> , N. V. Agrinskaya <sup>1</sup> , Berezovets <sup>1,3</sup> , S. P. Lebedev <sup>1</sup> , D. P. Litvin <sup>1,2</sup> , <sup>1</sup> <i>A.F.Ioffe Institute, St.Petersburg, Russia, <sup>2</sup> Nitride Crystals Group, St.Petersburg, Russia, <sup>3</sup>International Laboratory of High Magnetic Fields and Low Temperatures, Wroclaw, Poland . . . . .</i>	89
PII.10	<b>Precleaning of copper foil prior to CVD synthesis of graphene</b> Changfeng Li, Wonjae Kim, Harri Lipsanen and Juha Riikonen, <i>Department of Micro and Nanosciences, Aalto University, Espoo, Finland . . . . .</i>	90
PII.11	<b>Chemical vapor deposition of isolated nanoscrolls with polygonal cross-section</b> S. A. Malykhin <sup>1</sup> , A. M. Alexeev <sup>1</sup> , F. T. Tuyakova <sup>2,3</sup> , R. R. Ismagilov <sup>1</sup> , A. N. Obraztsov <sup>1,2</sup> , <sup>1</sup> <i>Department of Physics, Lomonosov Moscow State University, Moscow, Russia, <sup>2</sup>Institute of Photonics, University of Eastern Finland, Joensuu, Finland, <sup>3</sup>Moscow State Institute of Radio Engineering, Electronics and Automation, Moscow, Russia . . . . .</i>	91
PII.12	<b>Liquid-phase exfoliation of flaky graphite</b> A. S. Pavlova <sup>1,3</sup> , E. A. Obraztsova <sup>2</sup> , C. Monat <sup>3</sup> , P. Rojo-Romeo <sup>3</sup> and E. D. Obraztsova <sup>1</sup> , <sup>1</sup> <i>A.M. Prokhorov General Physics Institute, Moscow, Russia, <sup>2</sup>Shemyakin-Ovchinnikov Institute of bioorganic chemistry RAS, Moscow, Russia, <sup>3</sup>Universit de Lyon, Lyon Institute of Nanotechnology, Ecole centrale de Lyon, Ecully, France . . . . .</i>	92
PII.13	<b>Gravitational effect on chemical vapor deposition of carbon materials in direct curent gas discharge plasma</b> N. O. Skovorodnikov <sup>1</sup> , A. M. Alexeev <sup>1</sup> , F. T. Tuyakova <sup>2,3</sup> , R. R. Ismagilov <sup>1</sup> , A. N. Obraztsov <sup>1,2</sup> , <sup>1</sup> <i>Department of Physics, Lomonosov Moscow State University, Moscow, Russia, <sup>2</sup>Institute of Photonics, University of Eastern Finland, Joensuu, Finland, <sup>3</sup>Moscow State Institute of Radio Engineering, Electronics and Automation, Moscow, Russia . . . . .</i>	93
PII.14	<b>Characterization of GaSe using Raman spectroscopy and atomic force microscopy</b> Jannatul Susoma, Changfeng Li, Harri Lipsanen and Juha Riikonen, <i>Department of Micro and Nanosciences, Aalto University, Espoo, Finland . . . . .</i>	94
PII.15	<b>Monocrystalline diamond probes for atomic force microscopy</b> F. T. Tyakova <sup>1</sup> , A. N. Obraztsov <sup>1,2</sup> , R. R. Ismagilov <sup>1</sup> , E. A. Obraztsova <sup>3</sup> , <sup>1</sup> <i>Institute of Photonics, University of Eastern Finland, Joensuu, Finland, <sup>2</sup>Department of Physics, Lomonosov Moscow State University, Moscow, Russia, <sup>3</sup>A.M. Prokhorov General Physics Institute, Moscow, Russia . . . . .</i>	95

**Friday, August 1****97**

- 9:00-9:45 **Floating catalyst CVD synthesis of SWNTs for thin film devices lessons learned and future directions**  
Esko I. Kauppinen, *Department of Applied Physics, Aalto University, Espoo, Finland* . . . . . 99
- 9:45-10:30 **Optimization of multi-walled carbon nanotube properties via variation of growth conditions and post synthesis treatments**  
Vladimir L. Kuznetsov<sup>1,2</sup>, <sup>1</sup>*Boreskov Institute of catalysis SB RAS and* <sup>2</sup>*Novosibirsk State University, Novosibirsk, Russia* . . . . . 100
- 10:45-11:10 **STM study of gold intercalation process under graphene monolayer on Ni(111)**  
S. L. Kovalenko, B. V. Andryushechkin and K. N. Eltsov, *A. M. Prokhorov General Physical Institute RAS, Moscow, Russia* . . . . . 101
- 11:10-11:35 **Chirality controlled growth of single-walled nanotubes**  
Yan Li, *Beijing National Laboratory for Molecular Science, Key Laboratory for the Physics and Chemistry of Nanodevices, State Key Laboratory of Rare Earth Materials Chemistry and Applications, College of Chemistry and Molecular Engineering, Peking University, Beijing China* 102
- 11:35-12:00 **Carbon nanotube transparent conductors and their device applications**  
Yutaka Ohno, *Department of Quantum Engineering, Nagoya University, Nagoya, Japan* . . . 103
- 12:00-12:15 **Transparent conductive films based on iodine- or CuCl-filled single-wall carbon nanotubes**  
A. A. Tonkikh<sup>1</sup>, V. I. Tsebro<sup>2</sup>, A. A. Dolgoborodov<sup>3</sup>, E. A. Obraztsova<sup>1</sup>, A. G. Nasibulin<sup>4</sup>, E. I. Kauppinen<sup>4</sup>, H. Kataura<sup>5</sup>, K. Suenaga<sup>5</sup>, A. L. Chuvilin<sup>6</sup>, E. D. Obraztsova<sup>1</sup>, <sup>1</sup>*A.M. Prokhorov General Physics Institut RAS, Moscow, Russia,* <sup>2</sup>*P.N. Lebedev Physical Institute RAS, Moscow, Russia,* <sup>3</sup>*Moscow Engineering Physics Institute, Russia,* <sup>4</sup>*Aalto University, Espoo, Finland,* <sup>5</sup>*National Institute of Advanced Science and Technology, Tsukuba, Japan,* <sup>6</sup>*CIC nanoGUNE Consolider, San Sebastian, Spain* . . . . . 104
- 14:00-14:45 **Reversible optical doping of graphene**  
Matthieu Paillet<sup>1,2</sup>, Antoine Tiberj<sup>1,2</sup>, Miguel Rubio-Roy<sup>3</sup>, Jean-Roch Huntzinger<sup>1,2</sup>, Prine Landois<sup>1,2</sup>, Mirko Mikolasek<sup>1,2</sup>, Sylvie Contreras<sup>1,2</sup>, Jean- Louis Sauvajol<sup>1,2</sup>, Erik Dujardin<sup>3</sup>, Ahmed-Azmi Zahab<sup>1,2</sup>, <sup>1</sup>*Universit Montpellier 2, Laboratoire Charles Coulomb, Montpellier, France,* <sup>2</sup>*CNRS, Laboratoire Charles Coulomb, Montpellier, France,* <sup>3</sup>*CEMES-CNRS, Universit de Toulouse, Toulouse, France* . . . . . 105
- 14:45-15:00 **Self-assembling graphene deposition technique on micron and sub-micron scale structures**  
Tommi Kaplas, Sepehr Ahmadi and Yuri Svirko, *Institute of Photonics, University of Eastern Finland, Finland* . . . . . 106
- 15:00-15:15 **Effects of hydrogen and temperature on scalable graphene growth by APCVD with C<sub>2</sub>H<sub>2</sub>**  
Mei Qi, Zhaoyu Ren, Yixuan Zhou, Weilong Li, Xinlong Xu, and Jintao Bai, *Institute of Photonics and Photon-Technology, Northwest University, Xi'an, China* . . . . . 107
- 15:15-15:30 **Nitrogen doping of graphene films grown by chemical vapour deposition via ammonia plasma treatment**  
M. G. Rybin<sup>1,2</sup>, A. Pereyaslavcev<sup>3</sup>, T. Vasilieva<sup>4</sup>, V. Maysnikov<sup>4</sup>, I. V. Sokolov<sup>1,3</sup>, E. D. Obraztsova<sup>1,2</sup>, <sup>1</sup>*A.M. Prokhorov General Physics Institute, Moscow, Russia,* <sup>2</sup>*National Research Nuclear University MEPhI, Moscow, Russia,* <sup>3</sup>*The Federal State Unitary Enterprise All-Russia Research Institute of Automatics, Moscow, Russia,* <sup>4</sup>*The Moscow Institute of Physics and Technology, Moscow, Russia* . . . . . 108
- 15:45-16:00 **TiO<sub>2</sub> nanographite composite film material**  
R. R. Ismagilov<sup>1</sup>, A. M. Alexeev<sup>1</sup>, F. T. Tuyakova<sup>2,3</sup>, A. N. Obraztsov<sup>1,2</sup>, <sup>1</sup>*Department of Physics, Lomonosov Moscow State University, Moscow, Russia,* <sup>2</sup>*Department of Physics and Mathematics, University of Eastern Finland, Joensuu, Finland,* <sup>3</sup>*Moscow State Institute of Radio Engineering, Electronics and Automation, Moscow, Russia* . . . . . 109
- 16:00-16:15 **Nanocarbon based composites vs fluorinated graphene: dielectric and electromagnetic properties**  
N. Valynets<sup>1</sup>, P. P. Kuzhir<sup>1</sup>, A. Paddubskaya<sup>1</sup>, M. V. Shuba<sup>1</sup>, S. A. Maksimenko<sup>1</sup>, V. Sysoev<sup>2</sup>, V. Tur<sup>2</sup>, L. G. Bulusheva<sup>2</sup>, A. V. Okotrub<sup>2</sup>, J. Macutkevic<sup>3</sup>, J. Banys<sup>3</sup>, F. Micciulla<sup>4</sup>, L. Coderoni<sup>4</sup>, S. Bellucci<sup>4</sup>, V. Fierro<sup>5</sup>, A. Celzard<sup>5</sup>, V. Ksenevich<sup>6</sup>, N. Gorbachuk<sup>6</sup>, T. Veselova<sup>6</sup>, N. Poklonski<sup>6</sup>, A. Wieck<sup>7</sup>, G. Rinaldi<sup>8</sup>, <sup>1</sup>*Research Institute for Nuclear Problems, Belarusian State University, Minsk, Belarus,* <sup>2</sup>*Nikolaev Institute of Inorganic Chemistry, SB RAS, Russia,* <sup>3</sup>*Department of Radiophysics, Vilnius University, Vilnius, Lithuania* <sup>4</sup>*Frascati National Laboratory, National*

	<i>Institute of Nuclear Physics, Frascati, Italy, <sup>5</sup>IJL UMR Universit de Lorraine CNRS 7198, ENSTIB, pinal Cedex, France, <sup>6</sup> Department of Physics, Belarusian State Univesity, Minsk, Belarus , <sup>7</sup>Department of Physics and Astronomy, Bochum Ruhr-University, Bochum, Germany, <sup>8</sup>University of Rome Sapienza, Rome, Italy . . . . .</i>	110
16:15-16:30	<b>Infrared optical limiting response in detonation nanodiamond clusters dispersed in heavy water</b> V. V. Vanyukov <sup>1</sup> , T. N. Mogileva <sup>2</sup> , G. M. Mikheev <sup>2</sup> , A. P. Puzyr <sup>3</sup> , V. S. Bondar <sup>3</sup> , Y. Svirko <sup>1</sup> , <sup>1</sup> <i>Institute of Photonics, University of Eastern Finland, Joensuu, Finland</i> <sup>2</sup> <i>Institute of Mechanics, Russian Academy of Science, Izhevsk, Russia</i> <sup>3</sup> <i>Institute of Biophysics, Russian Academy of Sciences, Krasnoyarsk, Russia</i> . . . . .	111
16:30-16:45	<b>Spin-orbit coupling and quantum conductance in carbyne -the most simple carbon nano-material</b> Pavel N. Dyachkov, Vasilij A. Zaluev, <i>Kurnakov Institute of General and Inorganic Chemistry RAS, Moscow, Russia</i> . . . . .	112
	<b>Author index</b>	<b>113</b>

## Monday, July 28







## CONVERGENCE OF NANOTECHNOLOGIES FOR THE FUTURE PHOTONICS AND OTHER APPLICATIONS

Jong Min Kim, Seungnam Cha and Junginn Sohn

*Department of Engineering Science, University of Oxford, Oxford, OX1 3PJ, UK*

*jong.kim@eng.ox.ac.uk*

### Abstract

We present the current and future nanotechnology, especially focusing on the convergence of nano with electronics, photonics, and energy/bio areas. Nano-electronics will cover the graphene and carbon nanotubes, and their applications in flexible and transparent electrodes, and transistors. Nano-photonics will include quantum-dot displays and other applications.

### 1. Introduction

In this paper, first, we discuss the recent trends in nano-electronics. This will address the nano carbon and its applications with graphene and carbon nanotubes (CNT), covering CNT displays, and lightings. Also, for the applications for the printable electronics, we discuss flexible and transparent electrodes with CNTs and graphene, printable and flexible transistors with organic TFT and CNTs, printable and flexible lighting element with nano carbons. Nano-photonics includes quantum-dot for the displays/lightings and GaN light emitting diode on the glass and the flexible substrates are shown with their images. The energy and bio areas will cover new applications.

### 2. Results and discussion

#### 2.1 Nanotechnology with nanocarbon

Nanocarbon materials, such as CNTs and graphene, have recently been studied intensively. The first example of nanocarbon applications was field emission displays (FEDs) using CNT material [1]. CNTs are used as electron emitters for field emission sources. These are implemented on the glass as paste. The triode-type electron sources are fabricated on the bottom glass, and the upper glass is coated with cathode luminescence (CL) phosphor. The two glass plates are sealed with glass packaging. The vacuum gap between the plates is maintained using micro-structured fibers as spacers. If CNTs are aligned with micro-size pixels of phosphor and an electrical field is applied, the phosphors are illuminated. This is known as a carbon-nanotube-based display (CNT FED, Fig. 1). FEDs have been studied from the mid-1990s, and up to 32-in diagonal full-color high-definition (HD) CNT-FEDs have now been reported [1]. Commercial application has been retarded, however, due to technical issues and the rapid development of competitive technologies such as liquid crystal display (LCD) and plasma display panels (PDPs) [2]. This technology has recently been modified for use as various electron source applications such as a high brightness CNT backlight unit (CNT BLU), X-rays, fluorescent lamps and THz.

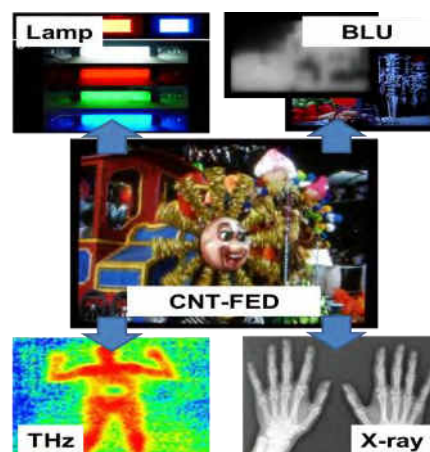


Figure 1. CNT-FED and various electron source applications using nano emitter technology.

Flexible displays require flexible and transparent electrodes. Indium–tin–oxide (ITO) is commonly used for transparent electrodes, but it is too brittle to be applied to flexible substrates. We reported a new technology using CNTs and graphene to create the necessary flexible and transparent materials (Fig. 2) [3]. This can be widely used in touch panels, displays, photovoltaic devices, flexible RF devices, and many other

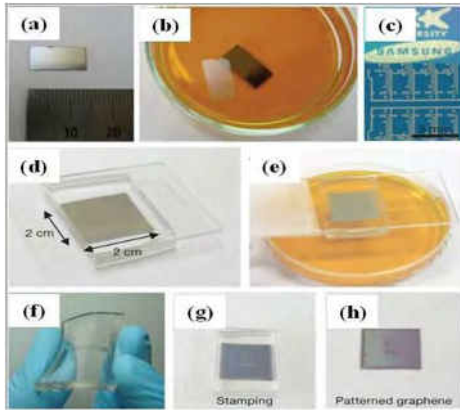


Figure 2. Large-scale pattern growth of grapheme.

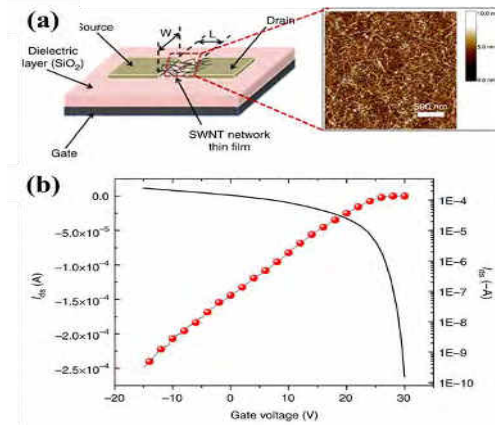


Figure 3. Schematic of a SWNT thin-film transistor.

photonic devices. If semiconducting-CNTs are sorted by surface functionalization via self-assembled monolayer technique, the high mobility of the resulting CNT-TFTs is reported. This technology can be used to prepare printable and flexible transistors as channel materials (Fig. 3).

## 2.2. Nanotechnology for next-generation photonics

Quantum dots have recently received considerable attention for the development of next-generation displays based on light-emitting diodes because quantum dot luminophores demonstrate high quantum yields, extremely narrow emission, spectral tunability and high stability, among other beneficial characteristics. Here we present new concept of display devices with the electro luminescence mode. Also, we show the demonstration of a large-area, full-colour quantum dot display, including in flexible form, using optimized quantum dot films, and with control of the nano-interfaces and carrier behavior (Fig. 4).

Printed quantum dot films exhibit excellent morphology, well-ordered quantum dot structure and clearly defined interfaces. These characteristics are achieved through the solvent-free transfer of quantum dot films and the compact structure of the quantum dot networks. Significant enhancements in charge transport/balance in the quantum dot layer improve electroluminescent performance. These findings suggest routes towards creating large-scale optoelectronic devices in displays, solid-state lighting and photovoltaics

In addition to demonstrating the light-emitting diode with quantum dots, we further demonstrate the fabrication of nearly single-crystalline GaN on amorphous glass

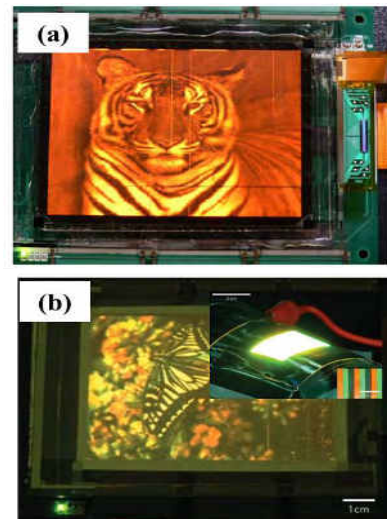


Figure 4. First quantum dot Full colour QD displays. Insert shows a QD display on flexible substrate [5].

substrates, in the form of pyramid arrays to overcome the size limitations of the sapphire substrate as well as to create larger, cheaper and efficient flat light sources (Fig. 5).

InGaN/GaN multiple-quantum wells formed on the GaN pyramid arrays exhibit a high internal quantum efficiency of 52%. LED arrays fabricated using these GaN pyramid arrays demonstrate reliable and stable area-type electroluminescent emission with a luminance of  $600 \text{ cd m}^{-2}$  [7]. This will be embedded on the large area glass and will be extended into new lighting areas

### 2.3 Nanotechnology for future applications

New concept of energy harvesting, e-nose, e-tongue, ordering system, and active hologram etc will be presented.

### 3. Summary

We have reported diverse applications of nanocarbon structures such as CNT and graphene. The core vacuum technology and emitter technology can be applied in various electron source applications. Nanocarbon film using graphene and CNT electrodes will be a future transparent electrode. Sorted semiconducting CNTs make potentially applicable printable CNT-FETs.

QD and GaN on glass and flexible substrate have been intensively studied for future large-scale optoelectronic devices in displays, solid-state lighting and photovoltaics. These convergence technologies will be creating new paradigm in future electronics, photonics, imaging areas, energy and bio areas.

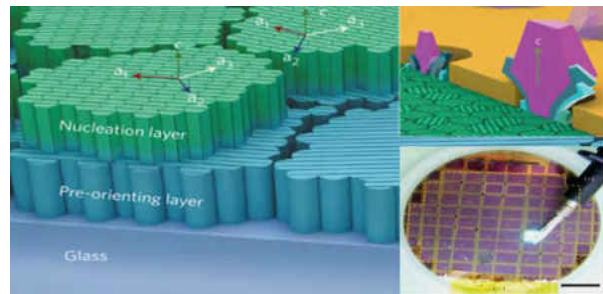


Figure 5. LED on Glass [6].

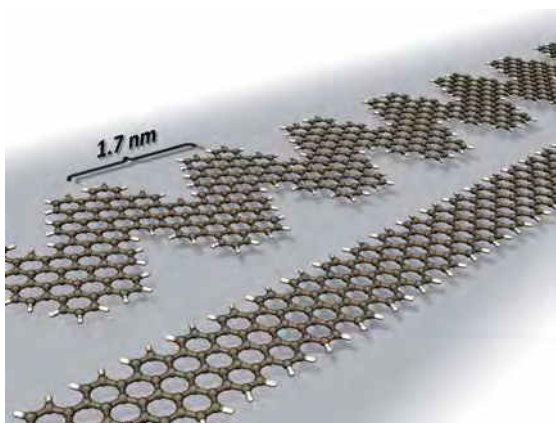
- [1] C. G. Lee et al., in *IMID Dig.* **1**, 303–304 (2002)
- [2] W. B. Choi, et. al. *Appl. Phys. Lett.* **75**, 3129, (1999)
- [3] K. S. Kim, et. al., *Nature* **457**, 706–710, (2009)
- [4] Hang Woo Lee et. al, *Nature Comm.* **2**, 1545 (2011)
- [5] Tae-Ho Kim et. al., *Nature Photonics* **5**, 176–182 (2011)
- [6] Jun Hee Choi et. al, *Nature Photonics* **5**, 763–769 (2011)

## ELECTRONIC AND OPTICAL PROPERTIES OF ATOMICALLY PRECISE GRAPHENE NANORIBBONS

Roman Fasel

*Empa, Swiss Federal Laboratories for Materials Science and Technology,  
8600 Dübendorf, Switzerland  
roman.fasel@empa.ch*

Graphene nanoribbons (GNRs) – narrow stripes of graphene – are predicted to be semiconductors with an electronic band gap that sensitively depends on the ribbon width. For armchair GNRs (AGNRs) the band gap is inversely proportional to the ribbon width, with an additional quantum confinement-related periodic modulation which becomes dominant for AGNRs narrower than  $\sim 3$  nm. This allows, in principle, for the design of GNR-based structures with specific and widely tunable properties, but requires structuring with atomic precision. The inability to produce graphene nanostructures with the needed precision has so far hampered the experimental investigation of narrow GNRs and their exploration in device configurations, which is in contrast to an impressive number of GNR-related computational studies.



In this presentation, I will review a recently developed bottom-up approach to the fabrication of atomically precise GNRs [1]. It is based on a surface-assisted synthetic route using specifically designed precursor monomers, and has made available ultra-narrow GNRs and related graphene nanostructures for experimental investigations of their structural, electronic and optical properties [1-8]. For the case of AGNRs of width  $N=7$  (7-AGNR), the electronic band gap and band dispersion have been determined with high precision

[7,8]. Optical characterization has revealed important excitonic effects [8], which are in good agreement with expectations for quasi-one-dimensional graphene systems. The versatility of the bottom-up approach also allows for the fabrication of substitutionally doped GNRs and heterostructures. First attempts at field effect transistor fabrication and characterization reveal serious challenges in patterning and contact fabrication that are related to the nanoscale dimensions of individual AGNRs.

- [1] J. Cai *et al.*, *Nature*, **466**, 470 (2010).
- [2] M. Bieri *et al.*, *Chem. Commun.*, 6919 (2009).
- [3] M. Bieri *et al.*, *J. Am. Chem. Soc.*, **132**, 16669 (2010).
- [4] M. Treier *et al.*, *Nature Chemistry*, **3**, 61 (2011).
- [5] S. Blankenburg *et al.*, *ACS Nano*, **6**, 2020 (2012).
- [6] P. Ruffieux *et al.*, *ACS Nano*, **6**, 6930 (2012).
- [7] L. Talirz *et al.*, *J. Am. Chem. Soc.* **135**, 2060 (2013).
- [8] J. Cai *et al.* ; R. Denk *et al.*, H. Söde *et al.*, submitted.

## FLUORESCENT NANOCARBON MATERIALS FOR BIOIMAGING

O.A. Shenderova<sup>1,2</sup>, G. MvGuire<sup>1,2</sup>, I. Vlasov<sup>3</sup>, J.M. Rosenholm<sup>4</sup>

<sup>1</sup> *International Technology Center, Raleigh, NC*, <sup>2</sup> *Adamas Nanotechnologies, Raleigh, NC*, <sup>3</sup> *General Physics Institute, Moscow*, <sup>4</sup> *Abo Akademi University, Turku*  
*oshenderova@itc-inc.org*

Being made from the major element of life, carbon nanostructures represent a special class of nanomaterials which raise minimum concern with regard to biocompatibility when integrated within biological systems. The focus of this talk will highlight two nanocarbon materials, nanodiamond (ND) particles and nano-graphene/graphite oxide (nGO), which recently emerged as multifunctional non-toxic alternatives to semiconductor quantum dots for biomedical imaging and carriers for drug delivery.

ND particles with the smallest crystal size of just a few nanometers are produced by detonation of carbon-containing explosives or by grinding microdiamond powders manufactured by static high-pressure, high-temperature synthesis [1]. Diamond particles have remarkable optical and mechanical properties in combination with biocompatibility, high specific surface area, and tunable surface structure. They are the least toxic of all carbon nanoparticles [1]. Foreign atoms can be incorporated into the lattice of ND particles, providing unique photoluminescent (PL) and spin properties. Challenges related to the large scale production of ND containing colour centres as well as material characterization and standardization toward development of a commercial product will be discussed. Multifunctional composites of PL ND and porous silica shell used for theranostic applications [2] as well as PL carbon dot-decorated NDs will be also discussed demonstrating synergistic advantages of combining nanostructured materials. We will also demonstrate in vivo multiphoton imaging capabilities using nGO produced by oxidation of graphitic structures using graphite intercalated acids [3].

Development of multimodal imaging probes based on 5-10nm ND and doping of ND with new functional elements are future directions for this field. The key issues that impact the fluorescent nanodiamond market with a particular emphasis on research and development, manufacturing and cost implications will be discussed.

[1] V.N. Mochalin, O. Shenderova, D. Ho, Y. Gogotsi, *Nature Nanotechnology*. 7 (2012) 11-23.

[2] E. Von Haartman, H. Jiang, A. Khomich, Shenderova O. et al. , *J. Mater. Chemistry B*, 1, (2013) 2358-2366

[3] S.C. Hens, W.G. Lawrence, A.S. Kumbhar, O. Shenderova, *J. Physical Chemistry C*. 116 (2012) 20015-20022.

## ELECTRONIC STRUCTURE AND OPTICAL PROPERTIES OF HALF-FLUORINATED GRAPHITE

A.V.Okotrub<sup>1\*</sup>, L.G. Bulusheva<sup>1</sup>, I.P. Asanov<sup>1</sup>, G.N.Chehova<sup>1</sup>, D.V. Pinakov<sup>1</sup>,  
T.L. Makarova<sup>2</sup>

<sup>1</sup>*Nikolaev Institute of Inorganic Chemistry SB RAS, 6303090, Novosibirsk, Russia*

<sup>2</sup>*Ioffe Physical Technical Institute RAS, 194021, St. Petersburg, Russia*

\*e-mail: spectrum@niic.nsc.ru

Graphite fluoride with a composition close to  $C_2F$  has been synthesized by fluorination of highly oriented pyrolytic and natural graphite using a  $BrF_3$  at room temperature. Depending on synthesis conditions graphite fluorides  $C_2F_x$  ( $x \leq 1$ ) with different composition can be obtained. The large interlayer spacing allows preparing intercalates with various molecules. Since the distance between the filled layers is 1.04 nm and the unfilled layers are separated by  $\sim 0.60$  nm, the obtained compound can be considered as a stack of the fluorinated graphenes. These fluorinated graphenes are large in area making it possible to study local destruction of the  $\pi$  conjugated system on the basal plane. It was shown that fluorine atoms form short chains, while non-fluorinated  $sp^2$  carbon atoms are organized in very narrow ribbons and aromatic areas with a size smaller than 3 nm [1, 2]. These  $\pi$  electron nanochains and nanoislands preserved after the fluorination process are likely responsible for the value of the energy gap of the compound of  $\sim 2.5$  eV. Variation in the size and the shape of  $\pi$  electron regions within the fluorinated graphene layers could be a way for tuning the electronic and optical characteristics of the graphene-based materials.

Electronic structure of graphite fluoride was probed using near edge x-ray absorption fine structure (NEXAFS) spectroscopy. The spectra measured near the C K- and F K-edges showed retention of delocalized  $\pi^*$ -system in graphite fluoride  $C_2F$ . The probable distribution of fluorine atoms on the graphite surface was determined from quantum-chemical modeling of the NEXAFS spectra [3]. The fluorine atoms were found to be easily detached from the  $C_2F$  surface under electron beam irradiation in a high vacuum or with a hydrazine vapor treatment. Changes of electronic structure under electron exposure were studied by Raman and optical reflection spectroscopy. The mechanism responsible for removal of fluorine atoms from dielectric matrix under electron irradiation has been proposed and substantiated using quantum chemical calculations.

[1] I.P. Asanov, L.G. Bulusheva, M. Dubois, N.F. Yudanov, A.V. Alexeev, T.L. Makarova, A.V. Okotrub, *Carbon*, **59**, 518 (2013).

[2] A. Vyalikh, L.G. Bulusheva, G.N. Chekhova, D.V. Pinakov, A.V. Okotrub and U. Scheler, *J. Phys. Chem. C*, **117**, 7940 (2013).

[3] A.V. Okotrub, N.F. Yudanov, I.P. Asanov, D.V. Vyalikh, and L.G. Bulusheva, *ACS Nano*, **7**, 65 (2013).

## QUANTUM FARADAY EFFECT IN GRAPHENE

Ryo Shimano

*Cryogenic Research Center, The University of Tokyo*

*Department of Physic, The University of Tokyo*

*Tokyo 113-0032, Japan*

*shimano@phys.s.u-tokyo.ac.jp*

Graphene exhibits intriguing electronic properties that arise from massless Dirac dispersion of electron. A striking example is the half-integer quantum Hall effect (QHE) which endorses the non-zero ( $\pi$ ) Berry's (topological) phase associated with the presence of Dirac cones. Then we can pose a question as to whether such an exotic topological phenomenon emerges in the optical response or not. This is an essential question since the topological protection that accounts for the quantized value of the Hall conductivity no longer exists in the AC responses. Moreover, it is unclear whether or not the carrier localization, which is crucial in realizing the quantum plateaus for the dc Hall current, sustains in the high frequency optical responses near the Landau-level transitions. Recently, a progress has been made in the theoretical study based on the exact diagonalization method, and the emergence of a plateau-like behaviour in the Hall conductivity even in the Landau-level transition energy, i.e., in the terahertz (THz) frequency regime has been predicted both in a conventional 2-dimensional electron gas system in GaAs and in graphene [1].

In this presentation, I will review our recent experimental study on the optical quantum Hall effect. Experimentally, the AC (optical) Hall conductivity can be measured through the magneto-optical effect such as Faraday effect and Kerr effect. By combining the THz time-domain spectroscopy (THz-TDS) with the polarization sensitive detection scheme [2,3], we have investigated the 'optical' quantum Hall effect or equivalently the quantum Faraday effect in a modulation-doped GaAs/AlGaAs single heterojunction [4] and in a monolayer graphene epitaxially grown on a SiC substrate [5]. In the GaAs/AlGaAs single heterojunction sample, a plateau-like structure is identified in the magnetic-field dependence of the Faraday rotation angle around the Landau-level filling of  $\nu=2$ , whereas the plateau-width was much narrower than that of dc regime. In contrast, the graphene sample exhibits a robust plateau-like structure, even showing the quantum steps between the Landau-level filling of  $\nu=2$  and  $\nu=6$ . The rotation angle was in the order of fine structure constant, and was consistent with the half-integer QHE.

- [1] T. Morimoto, Y. Hatsugai, and H. Aoki, *Phys. Rev. Lett.* **103**, 116803 (2009).
- [2] R. Shimano, Y. Ino, Yu. P. Svirko, M. Kuwata-Gonokami, *Appl. Phys. Lett.* **81**, 199 (2002).
- [3] Y. Ikebe, R. Shimano, *Appl. Phys. Lett.* **92**, 012111 (2008).
- [4] Y. Ikebe, T. Morimoto, R. Masutomi, T. Okamoto, H. Aoki, and R. Shimano, *Phys. Rev. Lett.* **104**, 256802 (2010).
- [5] R. Shimano, G. Yumoto, J. Y. Yoo, R. Matsunaga, S. Tanabe, H. Hibino, T. Morimoto, and H. Aoki, *Nature Commun.* **4**, 1841 (2013).



## QUANTUM NATURE OF GRAPHENE MAGNETISM

Tatiana Makarova & Andrei Shelankov

*Ioffe PTI, St. Petersburg, Russia*  
*tatiana.makarova@physics.umu.se*

. It is hard to imagine that something entirely new can be reported about graphene. It is even harder to expect that the novelty is related to graphene magnetism. Indeed, the community has had enough listening to the numerous theoreticians predicting that "carbon is magnetic", "zigzag edges are magnetic", "graphene is a spintronics material" etc. etc. It looks as if something is wrong with graphene: magnetism must be there but remains unobservable; both theories and common sense expect 1-dimensional antiferromagnetism whereas the experimental groups, with varied success, report either spin-half paramagnetism or vague signs of 3-dimensional ferromagnetic ordering.

We present the experimental evidence of magnetism in graphene nanochains and nanoislands embedded into fluorinated matrix produced by a mature technology [1,2]. The spontaneous spin alignment originates from (i) sectioning of the graphene basal plane by functionalization, which confines the electrons and (ii) the presence of  $sp^2$ - $sp^3$  interfaces as the spin sources. The quantum confinement of the electronic states induced by the presence of the fluorine interfaces leads to an enhancement of the Coulomb interactions and to stronger electron-electron correlations. Because of their 1D nature, these correlated states do not show long-range order but instead demonstrate magnetic behaviour typical for low-dimensional quantum spin systems, in accord with theories taking into account quantum nature of edge magnetism.

To quantify the experimental results in term of the spin coupling strength and the concentration of coupled spins, we have developed the quantum spin-ladder model in the limit of a strong intra-edge ferromagnetic interaction. Calculation showed that all carbon atoms are magnetic: about 10% bear spins, others participate in antiferromagnetic superexchange interactions. The experimentally measured exchange interaction between the spins separated by 3 carbon-carbon distances in the honeycomb lattice is 450 K. The high value of the exchange coupling allows the on/off switching between the nonmagnetic and magnetic states as a basic for graphene-based room-temperature operated spintronic devices. This experiment concludes the discussion about the existence of magnetic edge states in graphene and opens new horizons for this phenomenon.

[1] Asanov, I. P., Bulusheva, L. G., Dubois, M., Yudanov, N. F., Alexeev, A. V., Makarova, T. L., & Okotrub, A. V. Graphene Nanochains and Nanoislands in the Layers of Room-Temperature Fluorinated Graphite, *Carbon*, 59, 518–529 (2013).

[2] Vyalikh, A. Bulusheva, L.G., Chekhova, G.N. Pinakov, D.V., Okotrub, A.V., Scheler, U. "Fluorine patterning in room-temperature fluorinated graphite determined by solid-state NMR and DFT" *J. Phys. Chem. C* 117 (2013) 7940-7948

## RAMAN SPECTROSCOPY IN GRAPHENE AND LAYERED MATERIALS

Andrea C. Ferrari

*Cambridge Graphene Centre, Cambridge, 9 JJ Thomson Avenue, Cambridge CB3  
0FA, UK*

Raman spectroscopy is an integral part of graphene research[1-3]. It is used to determine the number and orientation of layers, the quality and types of edge, and the effects of perturbations, such as electric and magnetic fields, strain, doping, disorder and functional groups. This, in turn, provides insight into all sp<sup>2</sup>-bonded carbon allotropes, because graphene is their fundamental building block. I will review the state of the art, future directions and open questions in Raman spectroscopy of graphene. The essential physical processes will be described, in particular those only recently been recognized, such as the various types of resonance at play, and the role of quantum interference[3-6]. I will update all basic concepts and notations, and propose a terminology that is able to describe any result in literature[3]. Few layer graphene (FLG) with less than 10 layers do each show a distinctive band structure. There is thus an increasing interest in the physics and applications of FLG. I will discuss the interlayer shear mode of FLG, and show that the corresponding Raman peak, named C, measures the interlayer coupling[7]. A variety of layered materials can also be exfoliated to produce a whole range of two dimensional crystals [8,9]. Similar shear and layer breathing modes are present in all these materials, and their detection provides a direct probe of interlayer interactions. A simple chain model can be used to explain the results, with general applicability to any layered material [10].

- [1] A. C. Ferrari et al. Phys. Rev. Lett 97, 187401 (2006)
- [2] A. C. Ferrari et al. Solid State Comm. 143, 47 (2007)
- [3] A. C. Ferrari, D. M. Basko Nature Nanotech. 8, 235 (2013)
- [4] D. M. Basko, New J. Phys. 11, 095011 (2009)
- [5] M. Kalbac et al. ACS Nano 10, 6055 (2010)
- [6] C. F. Chen et al. Nature 471, 617 (2011)
- [7] P. H. Tan et al. Nature Materials 11, 294 (2012)
- [8] J. N. Coleman, et al. Science 331, 568 (2011).
- [9] F. Bonaccorso et al. Materials Today 15, 564 (2012)
- [10] X. Zhang et al. Phys. Rev. B 87, 115413 (2013)

## H-TERMINATED GRAPHENE NANORIBBONS AND CORONENE STACKS INSIDE SINGLE-WALLED CARBON NANOTUBES

Alexander I. Chernov<sup>1</sup>, Pavel V. Fedotov<sup>1</sup>, Albert G. Nasibulin<sup>2</sup>, Esko I. Kauppinen<sup>2</sup>,  
Vladimir L. Kuznetsov<sup>3</sup>, Elena D. Obraztsova<sup>1</sup>

<sup>1</sup> A.M. Prokhorov General Physics Institute, RAS, 38 Vavilov str., Moscow, Russia, 119991

<sup>2</sup> Department of Applied Physics, Aalto University School of Science, Espoo, Finland, P.O. Box 15100, FI-00076

<sup>3</sup> Borekov Institute of Catalysis SB RAS, Lavrentieva ave. 5, Novosibirsk, Russia, 630090

Presenting author e-mail address: [al.chernov@nsc.gpi.ru](mailto:al.chernov@nsc.gpi.ru)

Single-walled carbon nanotubes (SWCNTs) can serve as a template for formation of various structures inside. Depending on conditions the nanotube filling with coronene molecules may lead to creation of graphene nanoribbons (GNRs), coronene stacks, peapods or inner tubes [1]. When coronene molecules are converted into nanoribbons inside SWCNTs it results in formation of hydrogen-terminated GNRs. Molecules placed on the edges of the ribbons and the edge shape significantly influence on the electronic properties of GNRs. For instance, the nanometer wide H-terminated GNRs, which are formed inside SWCNTs, may have a large band gap of several eV and demonstrate a bright photoluminescence [2]. It is important to emphasize that the electronic structure of encapsulated structures can be controlled by tuning the host tube size. Using

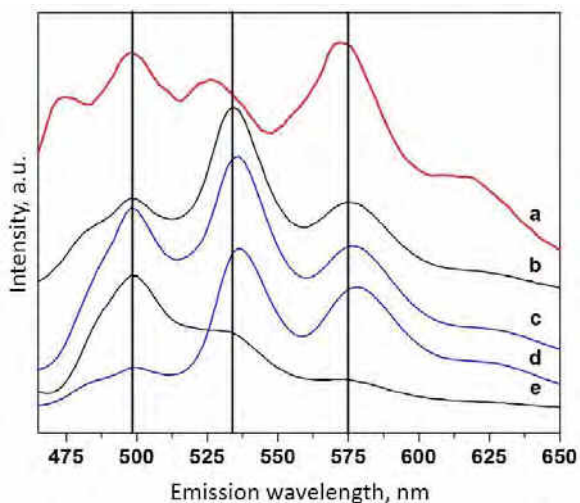


Fig. 1. The photoluminescence emission spectra of coronene stacks inside SWCNTs obtained with different experimental parameters such as nanotube average diameter and annealing temperature.

SWCNTs of various diameters allows tailoring the properties of the encapsulated material. In this work, we demonstrate the formation of coronene stacks (Fig. 1) or GNRs inside SWCNTs and study their optical properties by photoluminescence (PL) spectroscopy. We demonstrate the differences within the excitation PL maps between the spectral features of GNRs and coronene stacks inside the nanotubes and products which may be formed outside of nanotube interior. Optical investigation was supported by calculations of adsorption energy of coronene molecules inside and outside of nanotubes. Theoretical calculations demonstrate the most energetically favourable configurations of coronene molecules with respect to the diameter of host nanotubes.

Funding by RFBR grants 13-02-01354, 14-02-31829, 14-02-00777, RAS research projects and MESRF grants № 14.513.12.003, SP-7362.2013.3 is acknowledged.

[1] I. V. Anoshkin, A.V. Talyzin, et al., *ChemPhysChem*, doi: 10.1002/cphc.201301200 (2014).

[2] A. I. Chernov, P. V. Fedotov, et al., *ACS Nano* 7 (7), 6346 (2013).

## TRANSITION BETWEEN RING-SHAPED AND PARABOLIC VALENCE BAND MAXIMUM IN FEW-LAYER $A^3B^6$ COMPOUNDS

Dmitry V. Rybkovskiy, Alexander V. Osadchy, Elena D. Obraztsova  
*A.M. Prokhorov General Physics Institute RAS, 38 Vavilov Str., 119991 Moscow, Russia*  
*RybkovskiyD@gmail.com*

By performing first-principles electronic structure calculations in frames of the density functional theory we study the dependence of the valence band shape on the thickness of few-layer  $A^3B^6$  crystals (GaS, GaSe and InSe). We estimate the critical thickness of the transition from the bulk-like parabolic valence band to the ring-shaped band.

Direct supercell calculations show that the ring-shaped extremum (Fig.1) of the valence band appears in  $\beta$ -GaS and  $\beta$ -GaSe at the thickness below 6 tetralayers ( $\sim 4.6$  nm) and 8 tetralayers ( $\sim 6.4$  nm), respectively. Zone-folding calculations estimate the critical thickness of  $\beta$ -InSe equal to 28 tetralayers ( $\sim 23.6$  nm).

The origin of the ring-shaped valence band maximum can be understood in terms of the  $k$ - $p$  theory, that provides a link between the curvature of the energy bands and the distance between them. We explain the dependence of the band shape on the thickness, as well as the transition between two types of extremes, by the  $k$ -dependent orbital composition of the topmost valence band.

We show that in the vicinity of the critical thickness the effective mass of the holes in the  $A^3B^6$  compounds depends strongly on the number of tetralayers (Fig. 2). Below the critical thickness the hole effective masses are strongly  $k$ -dependent.

This work was supported by the SP-7452.2013.5 project and RAS research programs.

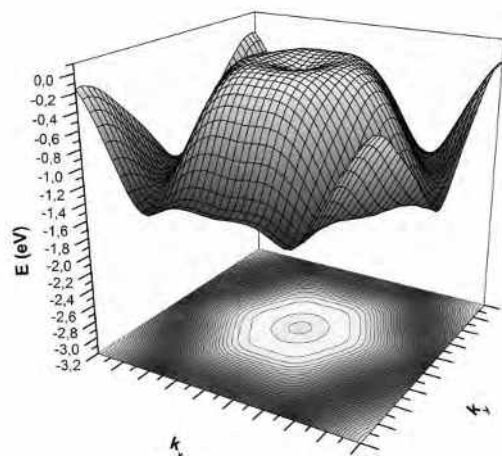


Fig. 1. The topmost valence band surface of a single GaS tetralayer together with the corresponding contour plot in the vicinity of the first Brillouin zone.

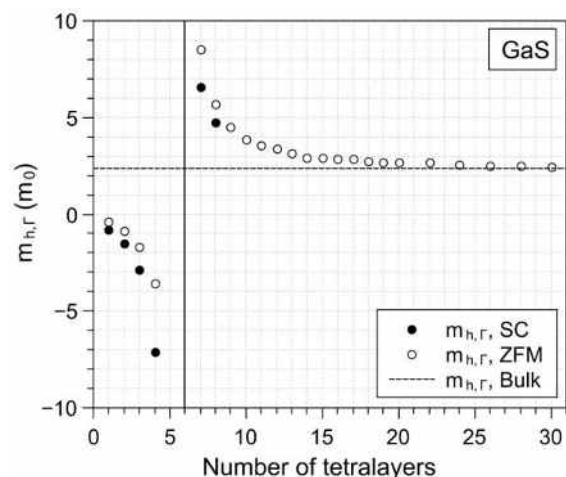


Fig. 2. The hole effective masses at  $\Gamma$  point of few-layer  $\beta$ -GaS, calculated with the supercell (SC, full circles) and zone-folding (ZFM, open circles) methods. The horizontal dotted line corresponds to the bulk hole effective mass, calculated within LDA.

## INVESTIGATION OF OPTICAL NONLINEARITIES IN FEW-LAYER GALLIUM SELENIDE BY MULTIPHOTON MICROSCOPY

Lasse Karvonen<sup>1</sup>, Antti Säynätjoki<sup>1</sup>, Soroush Mehravar<sup>2</sup>, Raul D. Rodriguez<sup>3</sup>, Susanne Müller<sup>3</sup>, Dietrich R.T. Zahn<sup>3</sup>, Seppo Honkanen<sup>4</sup>, Robert Norwood<sup>2</sup>, Nasser Peyghambarian<sup>1,2,4</sup>, Khanh Kieu<sup>2</sup>, Harri Lipsanen<sup>1</sup> and Juha Riihonen<sup>1</sup>

<sup>1</sup>*Aalto University, Department of Micro and Nanosciences, Tietotie 3, FI-02150 Espoo, Finland*

<sup>2</sup>*University of Arizona, College of Optical Sciences, 1630 E University Blvd, Tucson, AZ 85721, USA*

<sup>3</sup>*Chemnitz University of Technology, Semiconductor Physics, Chemnitz 09126, Germany*

<sup>4</sup>*University of Eastern Finland, Institute of Photonics, P.O. Box 111, FI-80101 Joensuu, Finland*

*lasse.karvonen@aalto.fi*

Due to the ever increasing demand for high speed data transfer, optical telecommunication is one of the key fields pursuing novel applications by exploiting second- and third-order optical nonlinearities. The optical nonlinearities of GaSe flakes with different number of layers were investigated using multiphoton microscopy with the excitation wavelength of 1560 nm [1], relevant for telecommunications. Strong second and third-harmonic generations were observed in few-layer gallium selenide flakes. The SHG and THG signals showed clear contrast between different numbers of GaSe layers. Figure 1 shows an RGB composite SHG-THG micrograph of the GaSe flake with different thicknesses. The red color in the RGB image represents the SHG

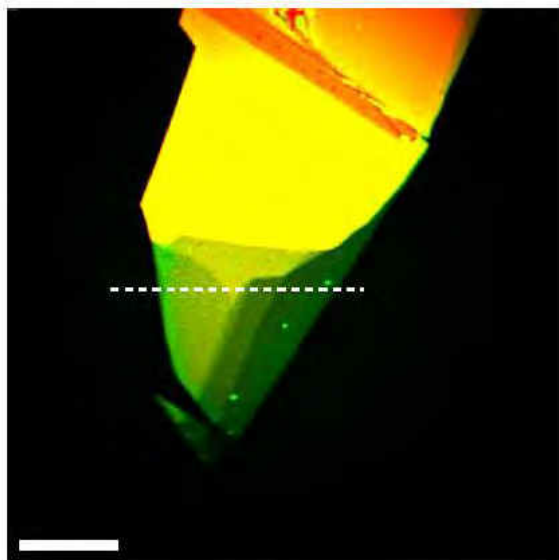


Fig. 1. RGB composite image generated from SHG and THG images (scale bar is 50  $\mu\text{m}$ ).

signal, and the green color represents the THG signal. The areas that simultaneously show a high intensity for both SHG and THG appear yellow in the composite image. Even the fourth-harmonic generation was detected from a  $\sim 40$  nm thick flake. Second-, third-, and fourth-harmonic generations were confirmed by spectral analysis. Strong nonlinear characteristics reported here for few-layer flakes demonstrate that GaSe is an intriguing material for telecommunication applications. These results contribute to the development of GaSe thin-layer flakes for next generation nonlinear applications satisfying the continuous need for device miniaturization.

[1] A. Säynätjoki, L. Karvonen, J. Riihonen, W. Kim, S. Mehravar, R. A. Norwood, N. Peyghambarian, H. Lipsanen, and K. Kieu, *ACS Nano*, 7, 8441 (2013).

## CORRELATED STOKES-ANTI-STOKES PHOTONS IN TWISTED BILAYER GRAPHENE

Ado Jorio

*Departamento de Física, UFMG, Belo Horizonte, MG, BRAZIL, 30.123-970*

*e-mail: adojorio@fisica.ufmg.br*

Twisted bilayer graphene (tBLG) is a two-graphene layers system with a mismatch angle  $\theta$  between the two hexagonal structures [1]. The interference between the two rotated layers generates a superlattice with a  $\theta$ -dependent wavevector that gives rise to van Hove singularities in the electronic density of states and activates phonons in the interior of the graphene Brillouin zone. Here we review the use of Raman spectroscopy [2] to study tBLG, exploring the  $\theta$ -dependent effects, corroborated by independent microscopy analysis. The phonon frequencies give a Raman signature of the specific tBLG, while their linewidths provide a straight forward test for tBLG structural homogeneity. Rich resonance effects, including single and multiple-resonances, intra- and inter-valley scattering events make it possible to accurately measure the energy of superlattice-induced van Hove singularities in the electronic joint density of states, as well as the phonon dispersion relation in tBLG, including the layer breathing vibrational modes.

With this knowledge in place, we produced a  $\theta = 11.3^\circ$  tBLG that works as an optomechanical cavity with a resonance wavelength of 575nm and a Q factor of 30, as defined by optical reflectivity measurements [3].

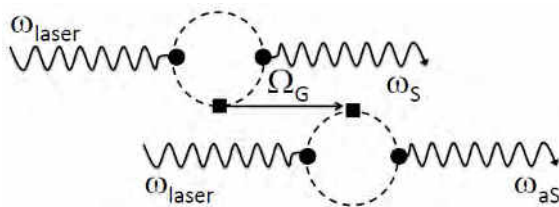


Fig. 1. The Stokes-anti-Stokes event.

By overlapping the resonance of the twisted bilayer with the anti-Stokes side band generated by the high energy optical phonon (G band) we achieve efficient generation of correlated Stokes and anti-Stokes Raman photons when excited by a few milliwatts of continuous wave laser radiation.

We estimate Stokes-anti-Stokes correlated photon generation to be  $10^{14}$  times more efficient than in bulk diamond. Our findings indicate that graphene can become a new source for correlated photons in quantum optics and information processing, and that the Stokes-anti-Stokes correlation has to be considered when using Raman spectroscopy to extract structural and transport properties of low-dimensional structures.

[1] Ado Jorio and Luiz Gustavo Cançado, *Solid Stat. Comm.* 175-176, 3–12 (2013)

[2] Ado Jorio and Luiz Gustavo Cançado, *PCCP* 14, 15246–15256 (2012)

[3] Ado Jorio et al. Unpublished.

## RAPID SYNTHESIS OF MONOLAYER GRAPHENE BY PHOTO-THERMAL CHEMICAL VAPOUR DEPOSITION

Juha Riikonen<sup>1\*</sup>, Wonjae Kim<sup>1</sup>, Changfeng Li<sup>1</sup>, Jannatul Susoma<sup>1</sup>, Sanna Arpiainen<sup>2</sup>, Markku Kainlauri<sup>2</sup>, and Harri Lipsanen<sup>1</sup>

<sup>1</sup> *Aalto University, Department of Micro- and Nanosciences, Micronova, Tietotie 3, FI-02150 Espoo, Finland*

<sup>2</sup> *VTT Technical Research Centre of Finland, Microsystems and Nanoelectronics, P.O. Box 1000, FI-02044 VTT, Espoo, Finland*

\* *juha.riikonen@aalto.fi*

Graphene is a remarkable material, which combines several intriguing properties. The overwhelming variety of different material properties and devices which have been demonstrated suggests that only the imagination of the researchers would be the limiting factor. In industrial point of view, however, material synthesis is a key challenge to be tackled before graphene based applications can reach the full market potential.

Chemical vapour deposition (CVD) is widely utilized method for thin film fabrication and is currently the most utilized method for the fabrication of large-area graphene monolayers. Typically used quartz tube furnace possesses some limitations due to hot-walls and high thermal mass. Here we present rapid monolayer graphene synthesis on copper utilizing photo-thermal CVD (PTCVD). In our system the halogen lamp heaters are placed outside the water-cooled stainless steel reactor and the temperature is monitored real-time using a pyrometer.

Utilizing our PTCVD process monolayer graphene can be grown on copper in about 30 s [1]. Graphene films are continuous as revealed by optical microscopy and scanning electron microscopy (SEM). In addition,  $\mu$ -Raman spectroscopy displays uniformly the fingerprint of high crystalline quality and low defect density as evidenced by  $2D/G > 2$  and practically non-existent D-band not only in single spectrum but also in mapping histograms. Grain size was determined to be 3-5  $\mu\text{m}$  by making grain boundaries visible via copper oxidation due to enhanced UV treatment of graphene on copper. To assess the true viability of such rapidly grown graphene for example in terms of grain boundary stitching, monolayer film were used in variety of different field-effect devices fabricated on  $\text{SiO}_2/\text{Si}$  substrates. Measurements of graphene field-effect transistors (FETs) revealed high field-effect mobility reaching values above  $3000 \text{ cm}^2/\text{Vs}$  in ambient air at room temperature. Additionally, complex CMOS-like transistor structures with local top and bottom gates were also fabricated. Both nFET-pFET and pFET-nFET configurations were realized by electrostatic control of the graphene channels and, consequently, inverter and voltage controlled resistor performance was observed, respectively [2]. As evidenced by our experimental findings, rapid monolayer synthesis of high-quality graphene makes PTCVD a potential candidate for cost-effective graphene fabrication.

[1] J. Riikonen, W. Kim, C. Li, O. Svensk, S. Arpiainen, M. Kainlauri, H. Lipsanen, *Carbon*, 62 (2013) 43-50.

[2] W. Kim, J. Riikonen, C. Li, Y. Chen, H. Lipsanen, *Nanotechnology*, 24 (2013) 395202-1-5.

## OPTICAL PROPERTIES OF GRAPHITIC MATERIAL: EFFECT OF CORRUGATION AND STACKING

Olga V. Sedelnikova, Lyubov G. Bulusheva, Andrey Chuvilin, Igor P. Asanov, and Alexander V. Okotrub

*Nikolaev Institute of Inorganic Chemistry, SB RAS, Novosibirsk, Russia*

*CIC nanoGUNE, San Sebastian, Spain*

*o.sedelnikova@gmail.com*

Graphene, a one-atom-thick material, is very promising material for a wide range of practical applications. Ideal graphene has the linear dispersion of  $\pi$ -bands around the K point and has the highest electron mobility of any known materials. However, it appears that graphene surface could contain structural defects which may change electronic, transport and optical properties, and this is the main concept of nanoengineering of defect structures on graphene. Particularly, due to high flexibility of graphene layer, its ability to match the support morphology, investigation effect of corrugation of graphene on electronic and plasmonic properties becomes an important task.

Theoretical investigations showed that deformation of graphitic surface can change electronic band structure and electron excitation properties notably. The density of states depends sensitively on the local curvature of corrugated layer [1] affecting optical response. The bending of graphite layer was found to remove restrictions on the electron transitions being forbidden in the flat material for certain light polarization. As a result, new peaks appear in the optical absorption spectrum and EEL spectrum of both rippled graphene and graphite [2, 3]. Moreover corrugation results in red shift of  $\pi$  and  $\pi+\sigma$  plasmon modes as well as  $\pi\rightarrow\pi^*$  transition peak. Recently this effect was detected experimentally using optical absorption and X-ray photoelectron spectroscopy. The obtained data showed that plasmon and absorption peaks of onion-like carbon, where agglomerates of carbon onions are jointed by several highly corrugated graphite layers, are downshifted in comparison with graphite samples [4]. The performed results showed that both optical absorption and plasmonic properties of graphite-like structures can be controlled by simple deformation of network without any topological changes that could potentially be used in optoelectronic devices.

Bilayer graphene with rotational faulting is also referred as turbostratic. The distinction from Bernal stacking gives rise to electronic decoupling of the graphene layers. As a result bilayer material can exhibit linear energy dispersion around the Fermi level similar to single-layer graphene. By carrying out EEL spectroscopy and theoretical calculation, we observed appearance of specific feature in plasmon spectra of twisted bilayer graphene in comparison with sample with Bernal stacking.

[1] O. V. Sedelnikova, L. G. Bulusheva and A. V. Okotrub, *Synthetic Metals*, **160**, 1848 (2010).

[2] O. V. Sedelnikova, L. G. Bulusheva and A. V. Okotrub, *The Journal of Chemical Physics*, **134**, 244707 (2011).

[3] O. V. Sedelnikova, L. G. Bulusheva and A. V. Okotrub, *Fullerenes, Nanotubes and Carbon Nanostructures*, **20**, 558 (2012).

[4] O. V. Sedelnikova, L.G. Bulusheva, I. P. Asanov, I. V. Yushina and A. V. Okotrub, *Applied Physics Letters*, **104**, 161905 (2014).





## Tuesday, July 29



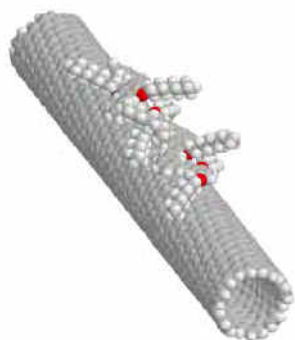


## RATIONAL BOTTOM-UP ASSEMBLY OF TAILORED MOLECULAR AGGREGATES ON NANOCARBON FOR HIGH SENSITIVITY NONLINEAR OPTICAL AND LIGHT HARVESTING APPLICATIONS

Werner J. Blau

*School of Physics and CRANN, Trinity College Dublin  
Dublin 2, Ireland*

Nanocarbons, i.e. single-walled nanotube (SWNT) and graphene surfaces can mediate the self-assembly of polymers and large conjugated organic and organometallic, e.g. dye, molecules on their surfaces and thereby create organised molecular structures



which would not form in solution or free space. Such aggregates, supramolecular assemblies of dye molecules, can possess sharp optical absorption bands and large optical cross sections so that they can photosensitise nanocarbon devices with high selectivity and sensitivity. In addition, these aggregates can modify the intrinsic electronic structure of the underlying nanocarbons locally and thereby generate locally defined electronic structures which are not available in neat nanocarbon particles. This is of particular relevance to emerging graphene electronics, which is one of the most promising

technologies for going beyond current CMOS, as detailed in the 2010 update of the ITRS International Technology Roadmap for Semiconductors.

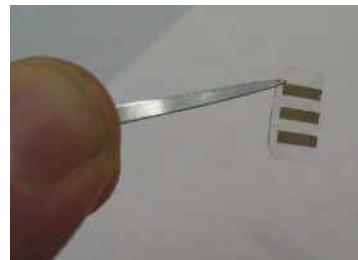
Dye aggregates are assembled on graphene sheets and nanotubes in dispersions and on thin films, in which we can exploit their extraordinary field effect mobility to detect optical absorption events. It is now possible to prepare defect-free, clean (down to atomic scale) nanotube and graphene devices [1]. Intimate interaction between dye molecules and atomically clean device surfaces enables aggregate assembly.

The following are fundamental scientific issues that can be addressed while developing dye aggregate-functionalized nanotube and graphene nonlinear optical and light harvesting devices:

- Structure of dye aggregates on nanotube and graphene surfaces.
- Impact of direct  $\pi$ - $\pi$  interaction between dye molecules and graphitic surfaces.
- Fundamental mechanism of photosensitisation of nanotubes and graphene sheets using tailored dye aggregates, as measured by ultrafast nonlinear optical and photoconduction responses.
- Fundamental mechanism of local modulation of nanotube and graphene electronic structure through aggregate electric fields and polymerised aggregate pressure.
- Impact of intense electric field near nanotube surface on dye aggregates with large linear and hyper-polarisability.

Photonic devices fabricated using nanoscale materials are essential building blocks in developing novel linear and nonlinear optical applications, especially light sources, photodetectors and solar cells.

- For nonlinear optical applications, the major challenge is to increase the optical absorption cross section of the material to enable large ultrafast response in the near-infrared. For graphene and carbon nanotube optical limiters, for instance, excessively high light intensity is required to induce a useful effect [2].
- For nanoscale photodetectors (and solar cells), the major challenge is to increase the optical absorption cross section of the material to enable detection at low light intensities. For carbon nanotube photodetectors, high light intensities of  $1 \text{ kW/cm}^2$  are required to induce photoconductivity [3]. Such small sensitivities reduce their utility. Therefore there is a dire need to tailor and increase the sensitivity of the ultrafast nonlinear optical response as well as the efficiency of nanoscale light-harvesting.



Semiconducting carbon nanotubes exhibit significant nonlinear optical response [2] and can detect light as they are direct band gap materials [4]. However, for SWNTs produced using chemical vapour deposition, band gaps range approximately from 0.8-0.4 eV. No synthesis technique is available to produce nanotubes with mono-disperse diameters. Therefore, the characteristic optical absorption cut-off wavelengths vary from 1.4 to 2.8  $\mu\text{m}$  without any control at the synthetic level. This renders any efforts to engineer the optical responses of nanotube-based sensors *futile*. However, polar dye aggregates on nanocarbon surfaces will modify the local electronic structure through a Stark effect and therefore generate locally modulated electrical and optical properties. Furthermore, if we can assemble polymerisable molecular aggregates on such surfaces, the bond length changes involved in the polymerisation process will apply a relatively large local pressure thereby modulating the local electronic structure. This process may be particularly interesting in converting semimetallic graphene particles to semiconducting ones.

[1] Ishigami, M, Chen JH, Cullen WG, Fuhrer MS, and Williams ED, Nano Letters, 2008, 7, p. 1643

[2] Wang J, Chen Y, Blau WJ, J Mater Chem, 2009, 19, p. 7425

[3] Freitag, M, Avouris PH et al., Nano Letters, 2003, 3, p. 1067

[4] Avouris, PH, Freitag M, and Perebeinos V, Nature Photonics, 2008, 2, p. 341

## CNT-SI HETEROJUNCTION SOLAR CELLS WITH STRUCTURE-CONTROLLED SINGLE-WALL CARBON NANOTUBE FILMS

Shigeo Maruyama

*Department of Mechanical Engineering, The University of Tokyo 113-8656, Japan  
maruyama@photon.t.u-tokyo.ac.jp*

Single-walled carbon nanotubes (SWNTs) with outstanding electronic, optical, mechanical, and thermal properties are expected to be the most promising materials for next-generation energy devices as well as optical and electronic devices. However, the structure controlled assembly of SWNTs for various devices is still challenging. In this study, we discuss two different SWNT assemblies for SWNT-Si heterojunction solar cells.

We proposed a water-vapor treatment to build up SWNTs to a self-assembled micro-honeycomb network for the application of solar cells [1]. The micro-honeycomb network consists of vertical aggregated SWNT walls and a buckypaper bottom (quasi 2 dimensional random network). This hierarchical structure exhibits lower sheet resistance and higher optical transmittance compared with the buckypaper. The heterojunction solar cell was fabricated by dry depositing the SWNT film to the 3 mm by 3 mm n-type silicon substrate. The pristine SWNT-Si heterojunction solar cell shows a record-high fill factor of 72 % as well as a power conversion efficiency (PCE) of 6 % without tuning the diameter or height of original vertically aligned SWNTs [2]. The PCE remains stable for months in ambient condition. A PCE exceeding 10 % is achieved in the dry state after dilute nitric acid treatment.

On the other hand, heterojunction solar cells using highly transparent-conductive SWNT films from controlled bundle-diameter and long bundle length [3] are also promising. Here, SWNTs were synthesized by the thermal decomposition of ferrocene vapor in a carbon monoxide atmosphere, with the average diameter of approx. 2 nm. The dry-deposited SWNT films showed a sheet resistance of 117  $\Omega$ /sq. at the transmittance of 91 % over the AM1.5G spectrum. Our preliminary test result shows the PCE of 11 %. These solar cells are stable after 1 year, which is attributed to the high-purity pristine SWNTs. The updated performance of these solar cells and the detailed mechanism will be discussed.

- [1] K. Cui, T. Chiba, S. Omiya, T. Thurakitseree, P. Zhao, S. Fujii, H. Kataura, E. Einarsson, S. Chiashi, S. Maruyama, *J. Phys. Chem. Lett.*, **4**, 2571, (2013).
- [2] Y. Murakami, S. Chiashi, Y. Miyauchi, M. Hu, M. Ogura, T. Okubo, S. Maruyama, *Chem. Phys. Lett.*, **385**, 298, (2004).
- [3] A. G. Nasibulin, A. Kaskela, K. Mustonen, A. S. Anisimov, V. Ruiz, S. Kivistö, S. Rackauskas, M. Y. Timmermans, M. Pudas, B. Aitchison, M. Kauppinen, D. P. Brown, O. G. Okhotnikov, E. I. Kauppinen, *ACS Nano*, **5**, 3214, (2011).
- [4] K. Cui, A. S. Anisimov, T. Chiba, S. Fujii, H. Kataura, A. G. Nasibulin, S. Chiashi, E. I. Kauppinen, S. Maruyama, *J. Mater. Chem. A*, submitted, (2014).

## GRAPHENE BASED ULTRAFAST LASERS

Zhipei Sun

*Department of Micro- and Nanosciences, Aalto University, FI-00076, Finland*

*Zhipei.sun@aalto.fi*

Graphene is a promising saturable absorber for various applications in ultrafast photonics [1], due to its ultrafast and strong nonlinear optical response over a broad spectral range [1-3]. Here, I review the fabrication and characterization of graphene saturable absorbers [2-7]. They are successfully used to mode-lock various lasers (*e.g.*, fiber [2-5,7], semiconductor [8], waveguide [9], and solid-state [11] lasers) in a broad spectral range (*e.g.*, 0.9[8], 1 [9], 1.5 [2-3,10], and 2  $\mu\text{m}$  [11]) [12]. We report the realization of mode-locked tuneable fiber lasers [13], tuneable between 1529 and 1559 nm [13]. We also present stretched-pulse fibre lasers [14] generating  $\sim 174$  fs pulses and solid-state laser with high power outputs, exceeding 2 W [15]. Finally, we present ultrafast pulse generation, covering 1, 1.5 and 2  $\mu\text{m}$  [16], exhibiting the intrinsic broadband ( $>1000$  nm) operation property of graphene. Our experiments [17] can lead to novel light sources meeting the wavelength (*e.g.*, fully covering  $\sim 1$  to 2  $\mu\text{m}$  [16], and beyond [17-18]), pulse duration (sub-100fs to ns [19]), repetition rate (up to GHz [8-9] and THz [20]), quality and power (up to 2W [15,21]) requirements for many applications, such as micro-machining and optical tomography, opening new opportunities in metrology, spectroscopy and biomedical diagnostics [22].

- [1] F. Bonaccorso et. al., *Nat. Photonics*, **4**, 611 (2010).
- [2] T. Hasan et. al., *Adv. Mat.* **21**, 3874 (2009).
- [3] Z. Sun et. al, *ACS Nano* **4**,803 (2010).
- [4] F. Bonaccorso et.al., *Materials Today*, **15**, 564 (2012).
- [5] F. Bonaccorso et.al., *Optical Materials Express*, **4**, 63 (2014).
- [6] F. Torrisi, et al., *ACS Nano* **6**, 2992 (2012).
- [7] T. Hasan, et al., *Phys. Stat. Sol. (b)* **247**, 2953 (2010).
- [8] C. A. Zaugg, *Opt. Express* **21**, 31548 (2013).
- [9] R. Mary, et. al., *Opt. Express* **21**, 7943 (2013).
- [10] D. Popa, et al., *Appl. Phys. Lett.* **98**, 073106 (2011).
- [11] M. Zhang, et al., *Opt. Express* **20**, 25077 (2012); A. A. Lagatsky, et. al., *Appl. Phys. Lett.* **102**, 013113 (2013).
- [12] Z. Sun et al., *Physica E*, **44**, 1082 (2012).
- [13] Z. Sun et al., *Nano Res.* **3**,653 (2010).
- [14] D. Popa, *Appl. Phys. Lett.* **97**, 203106 (2010); Z. Sun, *Nano Res.* **3**, 404 (2010).
- [15] L. Li, et al., *Appl. Phys. Express* **6**, 082701 (2013).
- [16] B. Fu, et. al., *IEEE JSTQE*. **20**, DOI: 10.1109/JSTQE.2014.2302361 (2014).
- [17] A. Martinez, Z. Sun, *Nat. Photonics* **7**, 842 (2013).
- [18] X. Liu, et. al., *Sci. Rep.* **3**, 2718 (2013); C. E. S. Castellani, et. al., *Opt. Lett.* **36**, 3996 (2011); Z. Sun et. al., *Nat. Photonics* **5**, 446 (2011).
- [19] D. Popa, et al. *Appl. Phys. Lett.* **101**, 153107 (2012); E. J. R. Kelleher, et al. *Appl. Phys. Lett.* **95**, 111108 (2009); E. J. R. Kelleher, et al. *Opt. Lett.* **34**, 3526-3528 (2009).
- [20] D. Mao, et. al., *Sci. Rep.* **3**, 3223 (2013).
- [21] Z. Sun et al. *Appl. Phys. Lett.* **95**, 253102 (2009).
- [22] Y. Chen, et. al., *Advanced Materials Interfaces* **1**, 1300008 (2014).

## ULTRAFAST FIBER LASERS ENABLED BY CARBON NANOTUBES AND THEIR APPLICATIONS

Khanh Kieu<sup>1</sup> and Antti Säynätjoki<sup>2</sup>

<sup>1</sup>*College of Optical Sciences, The University of Arizona, Tucson, Arizona 85721 USA*

<sup>2</sup>*Aalto University, Finland*

*kkieu@optics.arizona.edu*

Mode-locked lasers which generate femtosecond or picosecond pulses are important tools in modern scientific research and technological applications. These lasers are notorious for their high cost, bulkiness, and complexity in day-to-day operation. The discovery of carbon-based nano-materials (carbon nanotubes and graphene) as an effective saturable absorber (SA) for mode-locking may have changed the situation. It is now possible to build very compact, low cost, and reliable femtosecond fiber lasers working in a wide range of wavelengths with the use of this new SA technology. I will review the latest ultrafast fiber laser systems that we have developed using carbon nanotubes. The emphasis will be put not only on the excellent performance of the developed lasers but also on their commercialization path where long term operation and stability are crucial. A newly developed laser is only useful when it is successfully used in a real application. For that reason, I will also discuss the latest results that we have been able to achieve through the use of the laser systems that we have developed. In particular, I will discuss the application of these lasers in multiphoton microscopy of nonlinear materials, photonic devices as well as biological tissues.

### References:

1. Christian W. Freudiger, Wenlong Yang, Gary R. Holtom, Nasser Peyghambarian, X. Sunney Xie, Khanh Q. Kieu, "Stimulated Raman microscopy with a robust fiber laser source," *Nature Photonics* **8**,153–159 (2014)
2. Chur Kim, Sangho Bae, K. Kieu, and Jungwon Kim, "Sub-femtosecond timing jitter, all-fiber, CNT-mode-locked Er-laser at telecom wavelength," *Opt. Express* **21**, 26533-26541 (2013)
3. K. Kieu, S. Mehravar, R. Gowda, R. A. Norwood, and N. Peyghambarian, "Label-free multiphoton imaging using a compact femtosecond fiber laser mode-locked by carbon nanotube saturable absorber," *Biomed. Opt. Express* **4**, 2187-2195 (2013)
4. A. Säynätjoki, L. Karvonen, J. Riikonen, W. Kim, S. Mehravar, R. Norwood, N. Peyghambarian, H. Lipsanen, and K. Kieu, "Rapid Large-Area Multiphoton Microscopy for Characterization of Graphene", *ACS Nano*, in press, (2013) DOI:10.1021/nm4042909
5. T. N. Nguyen, K. Kieu, A. V. Maslov, M. Miyawaki, and N. Peyghambarian, "Normal dispersion femtosecond fiber optical parametric oscillator," *Opt. Lett.* **38**, 3616-3619 (2013)
6. K. Kieu, L. Schneebeli, E. Merzlyak, J. M. Hales, A. DeSimone, J. W. Perry, R. A. Norwood, and N. Peyghambarian, "All-optical switching based on inverse Raman scattering in liquid-core optical fibers," *Opt. Lett.* **37**, 942-944 (2012).
7. K. Kieu, J. Jones and N. Peyghambarian, "Generation of Few-Cycle Pulses From an Amplified Carbon Nanotube Mode-Locked Fiber Laser System," *PTL*, **22**, 1521-1523 (2010)
8. K. Kieu and F. W. Wise, "Soliton thulium fiber laser with carbon nanotube saturable absorber", *PTL* **21**, 128-130, (2008)
9. K. Kieu and F. W. Wise, "All-fiber normal-dispersion femtosecond laser," *Opt. Express* **16**, 11453-11458 (2008)
10. K. Kieu and M. Mansuripur, "Femtosecond laser pulse generation with a fiber taper embedded in carbon nanotube/polymer composite," *Opt. Lett.* **32**, 2242-2244 (2007)



## ELECTROMAGNETIC RESPONSE OF CARBON NANOTUBES AND NANOTUBE-BASED COMPOSITES IN TERAHERTZ RANGE

S.A. Maksimenko<sup>1</sup>, G. Y. Slepyan<sup>2</sup>, M. V. Shuba<sup>1</sup>, P.P. Kuzhir<sup>1</sup>

<sup>1</sup>*Institute for Nuclear Problems, Belarusian State University, Minsk, Belarus*

<sup>2</sup>*Department of Physical Electronics, Tel Aviv University, Tel Aviv, Israel*  
*sergey.maksimenko@gmail.com*

Thin carbon nanotube (CNT) films have attractive electronic and optical properties motivating their wide application as e.g. transparent flexible electrodes and polarizers. Especially it is important in terahertz range where the response from individual tube is very small and cannot be detected while far infrared and terahertz conductivity of CNT films demonstrates a non-Drude behavior, which can be interpreted by imposing some resonant term over the Drude conductivity law.

Electromagnetic scattering theory is applied to calculate polarizabilities of finite-length single- and multi-walled carbon nanotubes (SW- and MWCNTs) in terahertz and IR ranges. The influence of the length and diameter of a MWCNT and electron relaxation time on the regime of the CNT interaction with an electromagnetic field is analyzed. We demonstrate theoretically the dominant role of finite length effect in the non-Drude conductivity of CNT films due to the strong slowing down of surface polariton [1,2]. Significant screening effect is demonstrated to be inherent to MWCNTs films at gigahertz frequencies while it practically disappears in the THz range. The main features of the gigahertz and terahertz spectra of effective permittivity and electromagnetic interference shielding efficiencies of a MWCNT-based composite observed previously in experiments are systematized and described.

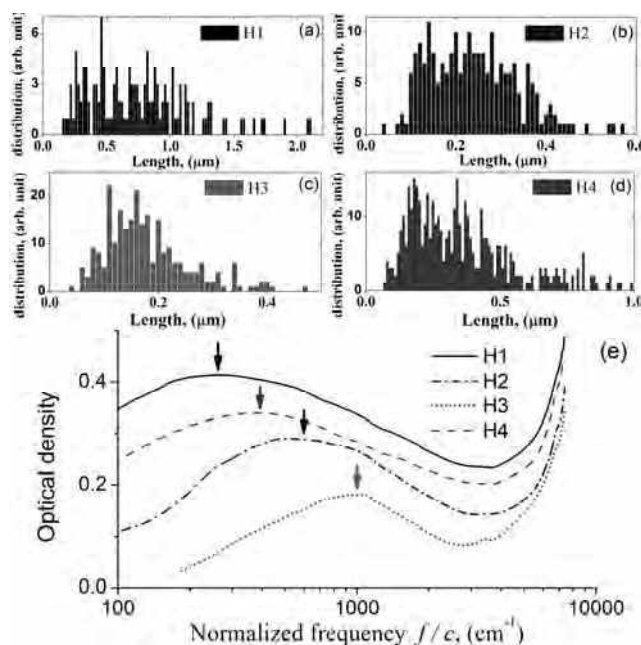


Figure 1 presents the experimental evidence of the finite-length effect in the FIR spectra of SWCNT films [3]. The peak in FIR conductivity of SWCNT thin film shifts into the high frequency range with decreasing SWCNT length. Thus, experimental results demonstrate the phenomena of localized plasmon resonance in SWCNTs and prove theoretically predicted antenna effect in SWCNTs in terahertz and far-infrared ranges.

Fig. 1. Length distributions of SWCNT bundles in four samples and optical-density spectra of these samples. Arrows indicate the THz conductivity peaks [3].

[1] G.Ya. Slepyan, *et al.*, Phys. Rev. B **60**, 17136 (1999).

[2] G. Ya. Slepyan, *et al.*, Phys. Rev. B **81**, 205423 (2010).

[3] M. V. Shuba, *et al.*, Phys. Rev. B **85**, 165435 (2012).

## SUSPENDED CARBON NANOTUBES NETWORK MEMS VARACTOR

Dmitri Lioubtchenko, Andrey Generalov, Ilya Anoshkin, Albert Nasibulin, Victor Ovchinnikov, and Antti Räsänen

*Aalto University, Department of Radio Science and Engineering*

*dmitri.lioubtchenko@aalto.fi*

Carbon nanotubes (CNT) have outstanding electrical and mechanical properties, which makes them very promising to use in future microelectromechanical systems (MEMS). While single CNT have a very high Young's modulus close to 1 TPa, the CNT networks can have very low Young's modulus values in the range of 1 – 10 GPa [1] in contrast with conventional metals with Young's modulus in the range of 100 – 200 GPa. This is because individual CNTs can move within the network, so the deformation of individual CNTs plays a little role in the overall deformation of the network. Using CNT networks with low Young's modulus in MEMS will result in lower actuating voltages compared to other materials. We present in this article a design and experimental verification of a CNT network MEMS varactor.

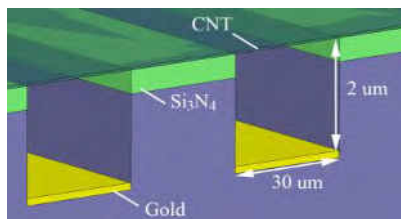


Fig. 1. Design of the CNT MEMS

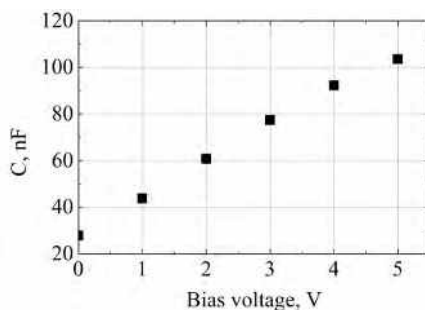


Fig. 2. Measured capacitance change.

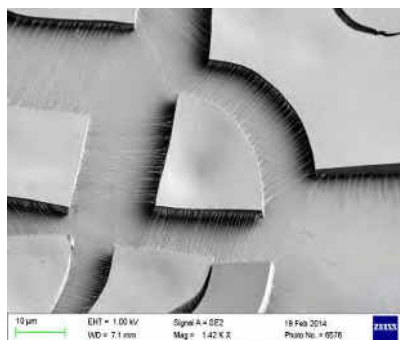


Fig. 3. Single – standing CNTs.

The design of the CNT MEMS varactor is presented in Fig. 1. The grooves are etched in high resistive silicon substrate with silicon nitride layer at the top for insulation. The lower parts of grooves are covered with gold and the CNT network with 30 nm thickness is placed at the top of the structure, hence the capacitance is created between lower gold patches and upper CNT layer.

The measurements of the capacitance change versus bias voltage were carried out using Agilent semiconductor device analyser at frequencies 1 kHz – 5 MHz. The measured C-V curve is shown in Fig. 2.

An interesting phenomenon was observed after special treatments of CNT layer (Fig. 3). CNTs happened to be very well aligned between the contact islands. This structure seems to be very perspective for future CNT MEMS varactors.

[1] D. Acquaviva et. al, "Capacitive nanoelectromechanical switch based on suspended carbon nanotube array," *Applied Physics Letters*, **97**, 233508 (2010).

## OPTICAL RESPONSES OF GRAPHENE

Young Hee Lee<sup>\*</sup> and Seong Chu Lim

*IBS Center for Integrated Nanostructure Physics, Institute for Basic Science (IBS),  
Department of Energy Science, Department of Physics, Sungkyunkwan University,  
Suwon, Republic of Korea*

*leeyoung@skku.edu*

Unlike one-dimensional carbon nanotubes where optical responses strongly rely on van Hove singularities in their electronic structures, two-dimensional graphene dominates optical responses uniquely by a linear band dispersion near K-point. Graphene on SiO<sub>2</sub>/Si substrate shows persistent positive and negative photoconductivity, which is associated with carrier-carrier scattering in graphene and charge scattering from trap sites in SiO<sub>2</sub> substrate. In general, graphene reveals both photoelectric and thermoelectric effect in typical transistor structures. In our approach, the graphene device on a suspended SiN membrane was constructed to maximize thermoelectric effect. For photothermoelectric detection of light using multilayer graphene (MLG), the input light was converted into thermoelectric voltage. The temperature difference between the suspended central hot SiN membrane region and SiO<sub>2</sub> substrate was about 3~5 K, which was enough to measure thermopower of graphene device. This transduction mechanism exhibits a wide range of optical response from mid-infrared to visible light and, more surprisingly, uniform responsivity, which originates from a linear band dispersion attributing to constant optical absorption of graphene from mid-IR to visible range. If time is allowed, we will further discuss optical responses on carbon nanotubes hybridized with CdSe-ZnS core-shell quantum dots (QDs), which revealed optical stark shift.

## BROADBAND POLARIZATION DYNAMICS CONTROL WITH ALIGNED CARBON NANOTUBES

Bo Fu<sup>1,2</sup>, He Yang<sup>1</sup>, Ya Chen<sup>1</sup>, Marco Mattila<sup>1</sup>, Zhenzhong Yong<sup>3</sup>,  
Qingwen Li<sup>3</sup>, Changxi Yang<sup>2</sup>, Ilkka Tittonen<sup>1</sup>, Harri Lipsanen<sup>1</sup>, and Zhipei Sun<sup>1</sup>

<sup>1</sup> Department of Micro- and Nanosciences, Aalto University, FI-00076 Aalto, Finland

<sup>2</sup> The State Key Laboratory of Precision Measurement Technology and Instruments, Department of Precision Instruments, Tsinghua University, Beijing 100084, China

<sup>3</sup> Suzhou Institute of Nano-tech and Nano-bionics, Chinese Academy of Sciences, Suzhou, Jiangsu 215125, China

E-mail: he.2.yang@aalto.fi

Carbon nanotubes have anisotropic optical absorption properties<sup>[1]</sup> due to the unique confinement in one-dimension<sup>[2]</sup>. Such properties can be utilized for various applications. For example, aligned carbon nanotubes have been demonstrated as a simple and compact polarizer, exhibiting a unique broadband (*e.g.*, from UV<sup>[3]</sup> to THz spectral range<sup>[4]</sup>) property. Here, we demonstrate a high-performance aligned carbon nanotube polarizer for broadband polarization control in fiber lasers at 1 and 1.5  $\mu\text{m}$ .

Our aligned carbon nanotube was fabricated on glass substrate by drawing from a CNT array<sup>[5]</sup>. Its optical microscopy image is shown in Fig 1(a). During the experiment, this device was inserted into different fiber laser systems (*i.e.*, at 1.0 and 1.5  $\mu\text{m}$ ) for polarization control. With the CNT device, the output average power presented linear-polarized characteristics with an extinction ratio up to 15 dB, shown in Fig 1(b) and (c). The degree of polarization (DOP) was also calculated to characterize polarizer performance in the two different fiber laser systems.

In conclusion, we demonstrate that the aligned nanotube device, working as a high-performance polarizer, has been utilized in the broadband fiber laser system to modulate the laser output characteristics. It shows that such CNT devices can be used for various photonic applications, which require the linearly-polarized light sources.

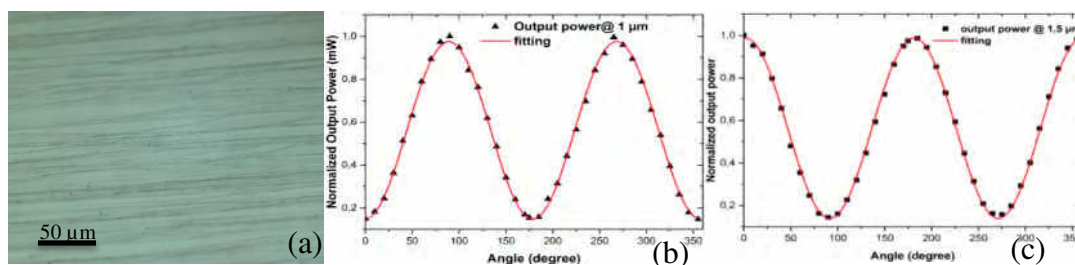


Fig. 1 (a) the optical microscopy image of aligned carbon nanotube (b) the normalized output average power at 1  $\mu\text{m}$  (c) the normalized output average power at 1.5  $\mu\text{m}$

- [1]. Y. Murakami, et al., *Physics Review Letter*. **94**, 087402 (2005)
- [2]. P. Avouris et al., *Nature Photonics* **2**, 341 (2008)
- [3]. S. Shoji et al., *Physics Review B* **77**, 153407 (2008)
- [4]. L. Ren et al., *Nano Letter*. **12**, 787 (2012)
- [5]. J. Di, et al., *Small* **9**, 1367 (2013)

## ASYMMETRIC HYPERBOLIC METAMATERIALS FOR GRAPHENE NANOPHOTONICS

Igor Nefedov<sup>1</sup>, Leonid Melnikov<sup>2</sup>, Evgeny Nefedov<sup>1</sup>  
<sup>1</sup>Aalto University, P.O. Box 13000, FI-00076, Aalto, Finland  
<sup>2</sup>Yuri Gagarin State Technical University of Saratov,  
 77, Politekhnikeskaya, 410054, Saratov, Russia  
 igor.nefedov@aalto.fi

In this paper we demonstrate possibilities, offered by graphene-based asymmetric hyperbolic metamaterials (HMM), for photonics. Asymmetric HMMs (AHMMs) are media with optical axes, tilted with respect to interfaces. Asymmetry appears as a difference in properties of waves propagating upward and downward to interfaces that causes unusual properties of AHMMs [1]. The first example relates to the total absorption which can be achieved in an optically ultrathin layer of AHMM, made of graphene sheets [1]. The second effect under discussion is a high-directive thermal emission from AHMMs, see Fig. 1 (left). The tilt angle for graphene sheets equals to  $35^\circ$ , period of a graphene multilayer lattice is 2 nm and the emission wavelength is 4.7  $\mu\text{m}$ . Changing the chemical potential of graphene we can control the emission direction. Such thermal emitters can be used as partially coherent IR sources.

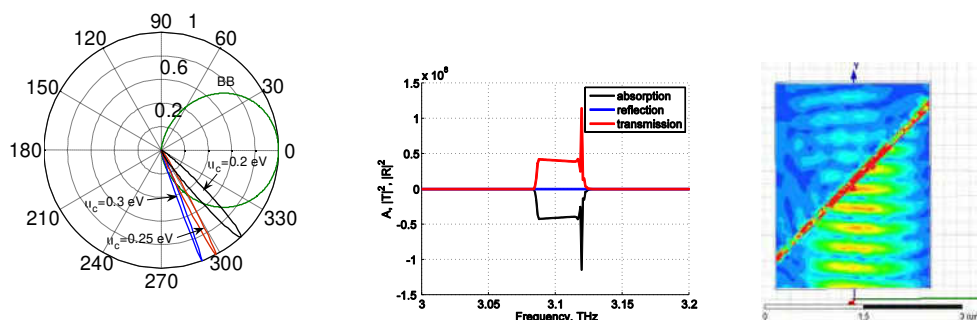


Fig. 1. **Left:** Thermal emission from the graphene AHMM. Radiation pattern, calculated for different values of the chemical potential. Green curve shows black body (BB) radiation. **Center:** Transmission, reflection and absorption of the THz radiation, passed through the AHMM slab. **Right:** Amplification of the Gaussian beam in the graphene AHMM slab (HFSS simulation).

It was shown [2] that if graphene is pumped either by optical illumination or by injection of electrons and holes, the electron and hole densities in graphene can substantially exceed their equilibrium values that results in the negative real part of graphene conductivity. In order to provide a coupling of THz radiation with graphene and realize the THz amplification, authors of [3] proposed to use a periodic array of resonant nanocavities. We suggest a more efficient way for the coupling of non-equilibrium plasmons with incoming THz radiation that allows a wide-band, non-resonant amplification in AHMM, see Fig. 1 (center and right).

[1] I. S. Nefedov<sup>1</sup>, C. A. Valaginnopoulos and L. A. Melnikov, *Journal of Optics*, **15**, 114003 (2013).

[2] A. A. Dubinov, V. Ya. Aleshkin, V. Mitin, T. Otsuji, and V. Ryzhii, *J. Phys. Condens. Matter.*, **23**, 145302 (2011).

[3] V. V. Popov, O. V. Polischuk, S. A. Nikitov, V. Ryzhii, T. Otsuji and M. S. Shur, *Journal of Optics*, **15**, 114009 (2013).

## NANOCARBON FILMS BASED PHOTOVOLTAIC AND OPTICAL DEVICES

G.M. Mikheev

*Institute of Mechanics, Russian Academy of Sciences, Izhevsk, Russia*  
*mikheev@udman.ru*

Investigations of the laser radiation interaction with carbon nanostructures revealed a lot of interesting nonlinear optical phenomena. One of them is a photon-drag effect. A photovoltaic current produced due to the momentum transfer from the incident photons to the charge carriers during the interband or intraband energy transitions is known as the photon-drag effect [1]. The photon-drag effect was observed in the nanographite (NG) films [2-4], carbon nanotube yarns [5], graphene [6] and single walled carbon nanotube (SWCNT) films [7]. In the nanocarbon films, this phenomenon is observed as the surface currents that uniquely depend on the incident angle and the polarization of the exciting radiation. Here we present the application examples of the angle- and polarization-dependent photovoltaic phenomena for designing a fast-response photo detector, angle sensor and polarization analyzer based on the NG and SWCNT films.

We have also demonstrated the possibility of laser image recoding on the detonation nanodiamond (DND) films for obtaining the diffractive structures. We used purified DND powder samples with an average particle sizes of 38, 50, 110, and 320 nm. The semitransparent films were obtained on the glass substrates by vaporization of the DND aqueous suspension. The DND films were exposed to the 632.8 nm laser light focused by  $10\times$  and  $50\times$  objectives. The laser beam power was of the order of 8.5 mW. The short-term laser irradiation of the films led to blackening of the exposed surface area. The threshold incident intensity for film blackening was about  $600 \text{ W}\cdot\text{cm}^{-2}$ . Scrolling the film in a horizontal plane under the incident beam, we obtained a continuous black line. In the future, this phenomenon can be used for recording the images via blackening of the DND film under the effect of the laser beam scanned in a programmed manner. The conceptual feasibility of such recording has been demonstrated by the examples of a square and diffraction grating written on the DND films [8].

- [1] A. M. Danishevskii, A. A. Kastalskii, S. M. Ryvkin, I. D. Yaroshetskii, *Sov. Phys. JETP* **31**, 292–295 (1970).
- [2] G. M. Mikheev, R. G. Zonov, A. N. Obratsov, Y. P. Svirko, *Appl. Phys. Lett.*, **84**, 4854–4856 (2004).
- [3] Mikheev G. M., Styapshin V. M., Obratsov P.A., et al. *Quantum Electron*, **40**, 425–430 (2010).
- [4] P. A. Obratsov, G. M. Mikheev, S. V. Garnov, et al., *Appl. Phys. Lett.*, **98**, 091903 (2011).
- [5] A. N. Obratsov, D. A. Lyashenk, S. Fang, et al. *Appl. Phys. Lett.*, **94**, 231112 (2009).
- [6] J. Karch, P. Olbrich, M. Schmalzbauer, et al. // *Phys. Rev. Lett.*, **105**, P. 227402 (2010).
- [7] Mikheev G. M., A. G. Nasibulin, R. G. Zonov, et al. *Nano Lett.*, **12**, 77-83 (2012).
- [8] G. M. Mikheev, K. G. Mikheev, T. N. Mogileva, et al. *Quantum Electron*, **44**, 1–3 (2014).

## STRUCTURE AND SPECTROSCOPIC PROPERTIES OF BN 1D AND 2D NANOSTRUCTURES

A.Pierret,<sup>1,2</sup>, L. Schué<sup>1,3</sup>, F. Fossard<sup>1</sup>, S. Moldovan<sup>4</sup>, O. Ersen<sup>4</sup>, F. Ducastelle<sup>1</sup>,  
J. Barjon<sup>3</sup> and A. Loiseau<sup>1</sup>

<sup>1</sup>LEM, ONERA-CNRS, Châtillon, France

<sup>2</sup>CEA-CNRS-UJF group "Nanophysique et Semiconducteurs", Grenoble, France

<sup>3</sup>GEMaC, UVSQ-CNRS, Versailles, France

<sup>4</sup>IPCMS, Univ. Strasbourg-CNRS, Strasbourg, France

Annick Loiseau <annick.loiseau@onera.fr>

Hexagonal boron nitride (h-BN) is a wide band gap semiconductor (6.4eV), which can be synthesized, as its carbon analog graphite, as bulk crystallites, nanotubes and nanosheets. Investigation of their optoelectronic properties is made difficult because of the paucity of high quality samples and suitable investigation tools. These structures meet nevertheless a growing interest for deep UV LED and graphene engineering. A deeper understanding of the interplay between the structural and luminescence properties of different BN structures and how these properties can be further exploited for their characterization are therefore highly needed.

Such studies are now possible thanks to the recent development of dedicated photoluminescence (PL) and cathodoluminescence (CL) experiments running at 4K and adapted to the detection in the far UV range (up to 6eV) [1]. We can also combine various TEM techniques and CL experiments in a FEG-SEM with a spatial resolution of 3nm on the same nano-object. With these tools, we investigated the structure and luminescence of various structures, from high quality crystals [2], exfoliated nanosheets to multi-wall nanotubes [3].

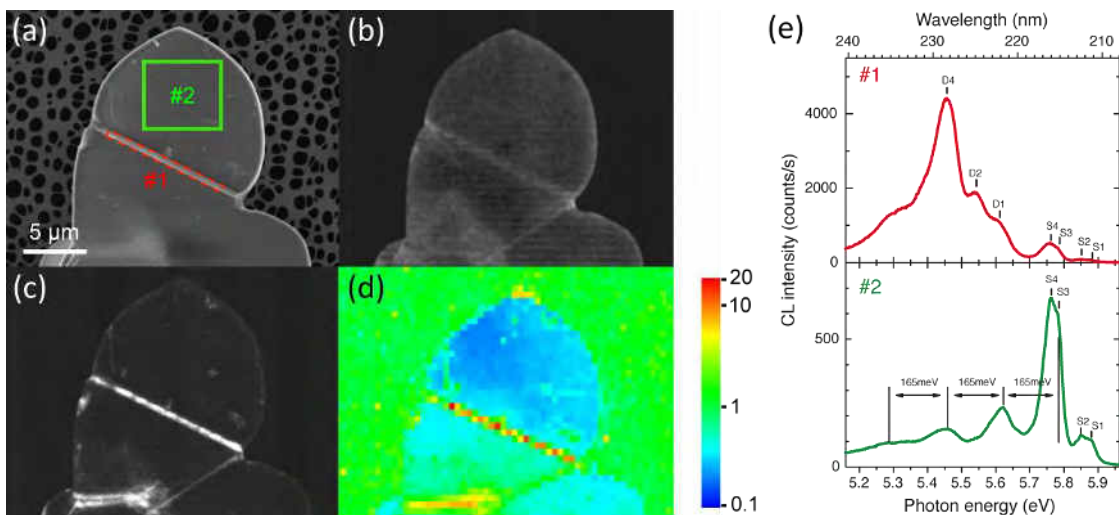


Figure 1: (a) SEM image of a h-BN crystallite; (b), (c) Corresponding CL images recorded (b) on the main S line (S3-S4), and (c) on the main D line (D4). (d) Map of the D/S ratio. (e) CL spectra recorded in the areas #1 (grain boundary) and #2 (middle of the grain), indicated in (a).

As a result, BN materials present original optical properties, governed by excitonic effects in the 5.5–6eV energy range. Two kinds of excitonic luminescence have been identified and are called S and D lines [4]. As revealed from CL-TEM analyses, D lines are issued from defective areas (Fig 1), so that D/S ratio can be used as a qualification parameter of the defect density [5]. This procedure has been applied to understand the first luminescence studies of few layers individual BN flakes [5].

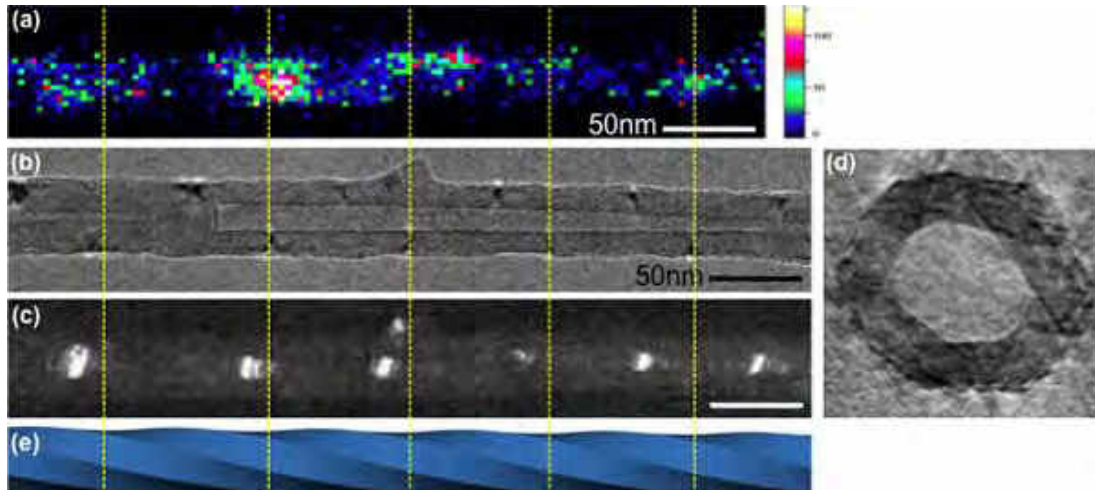


Figure 2: Images of a BN nanotube: (a) 3nm spatially resolved CL image recorded at 5.49 eV (226 nm); (b), (c) Corresponding TEM images in (b) bright-field mode, and (c) dark-field mode on the (100) reflection. (d) Heptagonal tube cross-section obtained by tomography experiment. (e) Structure of the tube as deduced from (b-d) images.

Concerning nanotubes, CL images reveal that the luminescence in the 5.5–6eV energy range is strongly inhomogeneous and oscillating. Thanks to a deep investigation combining different TEM techniques, we have shown that the tubes display a complex twisted faceted structure and that the twist period is correlated with the luminescence oscillations (Fig 2). Furthermore, we could show that excitons, responsible for the spectacular localization of the luminescence, are trapped to specific defects, twisted along with the faceting structure.

Finally, low-loss EELS providing an alternative approach to the nature of electronic excitations [6], we will show how it is an efficient tool to investigate the local structure and optical properties with an energy resolution below 100meV of different BN layers and nanotubes.

- [1] P. Jaffrennou et al., *Phys. Rev. B* 77 (2008) 235422
- [2] T. Taniguchi et al., *J. Cryst. Growth* 303 (2007) 525
- [3] C. Tang et al., *Chem. Commun.* 12 (2002) 1290
- [4] K. Watanabe et al., *Phys. Rev. B* 79 (2009) 193104
- [5] A. Pierret et al., *Phys. Rev. B* 89 (2014) 035414
- [6] R. Arenal et al., *Phys. Rev. Lett.* 95 (2005) 127601



## PHOTOPHYSICS OF SEMICONDUCTING TWO-DIMENSIONAL TRANSITION METAL DICHALCOGENIDES

Christoph Gadermaier

*Department of Complex Matter and International Postgraduate School*

*Jozef Stefan Institute*

*Jamova 39, 1000 Ljubljana, Slovenia*

*christoph.gadermaier@ijs.si*

Recent progress in the exfoliation of layered materials and the nanofabrication of functional structures has revived the interest in two-dimensional materials with properties complementary to graphene, in particular transition metal dichalcogenides (TMDs) such as MoS<sub>2</sub>. Depending on the coordination and oxidation state of the metal atoms, TMDs can be metallic, semimetallic, or semiconducting. In addition, superconductivity and charge-density wave effects have been observed in some TMDs. A transistor and a logical circuit device based on a monolayer of MoS<sub>2</sub> have recently been demonstrated.

The functional properties of any material are determined by its response to external stimuli, which drive it out of equilibrium. Hence, fundamental understanding is gained from studying relaxation processes. A salient question in semiconducting TMDs is the electronic nature of photoexcited states, which determines their optoelectronic and energy harvesting functionalities. On the one hand, there are imperative indications for excitons as the primary photoexcitations, with a binding energy that strongly increases with decreasing number of layers, reaching 0.5 – 1 eV for the monolayer. On the other hand, efficient photovoltaics and highly sensitive photodetectors based on monolayer MoS<sub>2</sub> transistors have been demonstrated, which both require mobile carriers created by the absorption of light.

Here we use femtosecond optical spectroscopy to show that a significant fraction of the photoexcited excitons in MoS<sub>2</sub> dissociates within a few ps. We discuss the implications of the excitation wavelength and layer number dependence for the possible dissociation mechanism and present preliminary results on the electron dynamics in heterostructures with an increased charge separation efficiency.

## OPTICALLY INDUCED TERAHERTZ EMISSION FROM 3D TOPOLOGICAL INSULATORS

Petr A. Obraztsov<sup>1,2</sup>, Pavel A. Chizov<sup>1</sup>, Oleg E. Tereshchenko<sup>3</sup>, Sergey V. Garnov<sup>1</sup>,  
Yuri P. Svirko<sup>2</sup>

<sup>1</sup>*A.M. Prokhorov General Physical Institute RAS, 38 Vavilov Stret, 119991 Moscow, Russia*

<sup>2</sup>*Institute of Photonics, University of Eastern Finland, Joensuu, Finland*

<sup>3</sup>*Institute of Semiconductor Physics, SB RAS, Novosibirsk, Russia*

*p.obraztsov@gmail.com*

The chalcogenides  $\text{Bi}_2\text{Se}_3$  and  $\text{Bi}_2\text{Te}_3$  have long been known as narrow-bandgap semiconductors suitable for high-performance infrared detectors and for thermoelectric applications. Recent discovery of topologically protected surface states in these layered compounds made them a benchmark of three-dimensional topological insulator (3D TI) [1]. It has been theoretically predicted that 3D TI have insulating bulk and conducting surface. The metallic conductivity at TI surface is determined by the surface states that can be described by Dirac-like equation for massless particles similarly to electrons in graphene. The gapless band structure of TI surface have been directly imaged by angle-resolved photoemission and tunneling spectroscopy.

We report experimental observation of terahertz emission from bulk crystals and epitaxial thin films of three-dimensional topological insulators  $\text{Bi}_2\text{Se}_3$  and  $\text{Bi}_2\text{Te}_3$  under excitation with femtosecond laser pulses centered at 800 nm. The excitation of any surface of the 3D topological insulator with obliquely incident arbitrary polarized femtosecond laser pulse induces THz response which depends on the polarization state and incidence angle of the excitation light. The performed polarization sensitive measurements suggest separate contributions from bulk and surface of  $\text{Bi}_2(\text{Se},\text{Te})_3$  crystal to the THz generation process. The bulk contribution does not feel the polarization state of the incidence light and decreases with reducing the topological insulator crystal thickness. The surface contribution, on the contrary, is extremely sensitive to the excitation light helicity and linear polarization rotation due to unusual band structure of topological insulator surface. The topologically protected surface states cause very pronounced polarization dependence in agreement with the recent theoretical [2] and experimental [3,4] studies on light induced spin and electron currents in materials having Dirac-cone band structure.

[1]. H. Zhang, C.-X. et.al., *Nature Physics* **5**, 398-402 (2009).

[2]. A. Junck, G. Refael, F. von Oppen *Phys. Rev. B* **88**, 075144. (2013).

[3]. J.W. McIver et.al. *Nature Nanotechnology* **7**, 96–100 (2012).

[4]. P.A. Obraztsov et. al., *Scientific Reports* **4**, 4007 (2014).



## Poster session I





## THEORETICAL STUDY OF CARBON NANOTUBES HEAT CAPACITY IN THE FRAME OF CONTINUOUS THEORY OF THIN CYLINDRICAL SHELL DYNAMICS

M. V. Avramenko<sup>\*</sup>, I. Yu. Golushko, S. B. Rochal, D. I. Levshov, Yu. I. Yuzyuk

*Department of Nanotechnology, Faculty of Physics, Southern Federal University,  
Rostov-on-Don, 344090, Russia*

*\* avramenko.marina@gmail.com*

Since their discovery [1], carbon nanotubes (CNTs) have held the researchers' attention due to their unique fundamental properties and high potential for various applications [2–4]. The use of CNTs in the rapidly developing field of nanotechnology requires simple and clear models for comprehensive interpretation of their characteristics. In particular, low-frequency vibrational spectrum of CNTs (both single- and double-walled) is well-described in the frame of the continuous theory of thin cylindrical shell dynamics [5]. Considering graphene sheet as a two-dimensional membrane of no macroscopic thickness, the authors of this approach obtain user-friendly equations for further application in quantitative studies of corresponding CNTs properties.

In our work we use the results of this recently developed theory [5] in order to study one of the fundamental thermal characteristics of CNTs, namely their heat capacity. Firstly, we analyze the key points of existing approaches for heat capacity studies and draw an inference about the facts which make questionable the validity of those models. Then we carry out our calculations for (10, 10) nanotube and find the temperature dependence of its heat capacity in the low-temperature region. Finally, we discuss the form of the obtained dependence and compare it with available experimental data.

Thus, we demonstrate that the continuous theory [5] appears to be a quite simple and convenient tool for CNTs theoretical studies and, in particular, for analysis of their heat capacity.

[1] S. Iijima, *Nature* **354**, 56–58 (1991).

[2] R. Saito, G. Dresselhaus and M.S. Dresselhaus, *Physical Properties of Carbon Nanotubes* (Imperial College Press, London, 1998).

[3] S. Reich, C. Thomsen and P. Ordejon, *Elastic Properties and Pressure-induced Phase Transitions of Single-walled Carbon Nanotubes*, Vol. **235** (Wiley Online Library, 2003).

[4] A. Jorio, M.S. Dresselhaus and G. Dresselhaus, *Carbon Nanotubes: Advanced Topics in the Synthesis, Structure, Properties and Applications*, Vol. **111** (Springer, Berlin, 2008).

[5] S. B. Rochal, V. L. Lorman and Yu. I. Yuzyuk, *Physical Review B* **88**, 235435-6 (2013).

## EXTRACTION OF CARRIER DENSITY AND $\pi$ - ELECTRON RELAXATION CONSTANT IN TERAHERTZ WAVE TRANSMISSION EXPERIMENTS WITH GRAPHENE SANDWICH STRUCTURES

K. Batrakov,<sup>1</sup> P. Kuzhir,<sup>1</sup> S. Maksimenko,<sup>1</sup> S. Voronovich,<sup>1</sup> A. Paddubskaya,<sup>2</sup> J. Macutkevicius,<sup>3</sup> T. Kaplas,<sup>4</sup> and Y. Svirko<sup>4</sup>

<sup>1</sup>Research Institute for Nuclear problems of Belarusian State University, Belarus

<sup>2</sup>Center for Physical Science and technology, LT-01108 Vilnius, Lithuania

<sup>3</sup>Vilnius University, LT-00122 Vilnius, Lithuania

<sup>4</sup>Institute of Photonics, University of Eastern Finland, Joensuu FI-80101, Finland  
kbatrakov@gmail.com

We report experiment and theoretical results on terahertz wave transmission through sandwich structure which consists of graphene mono-layers interlaced by submicron layers of polymethyl methacrylate (PMMA) (see Fig.1 for schematic structure of produced experimental samples). The graphene/PMMA sandwich production consists of the following steps. The first graphene monolayer is synthesized by chemical vapor deposition (CVD) at 1000 C in methane atmosphere on the copper catalyst and then spin coated by the 600-800 nm thick PMMA layer. Next, Cu is wet etched in ferric chloride. The obtained PMMA film with deposited graphene is washed in distilled water. After drying the next graphene layer is deposited on the top of the PMMA. This procedure allows us to fabricate sandwich-like coatings containing several graphene layers.

Measurements of THz transmission for free standing graphene/PMMA sandwiches (one and three graphene layers, not supported by quartz substrate) were performed in the frequency range from 100 GHz to 3 THz, by time domain terahertz spectrometer (EKSPLA, Vilnius Lithuania) based on femtosecond laser (wavelength 1  $\mu$ m, pulse duration less than 150 fs) and GaBiAs photoconductive switch as THz emitter and detector. Free standing graphene/PMMA was used in experiments to prevent interference effects and strong transmission coefficient oscillations due to substrate boundaries.

Measurements demonstrated the remarkably high absorption of terahertz waves by graphene sheets. Comparison of experimental data (points on Fig.1) with calculated ones (theoretical curves on Fig.1) gave the following results for used in our measurements graphene samples: graphene chemical potential  $\mu=0.14$  eV and relaxation parameter  $\gamma=13$  THz. These values correspond to carrier density  $n \sim 10^{12}$  cm<sup>-2</sup> and free path length of  $\pi$ -electrons  $\sim 100$  nm.

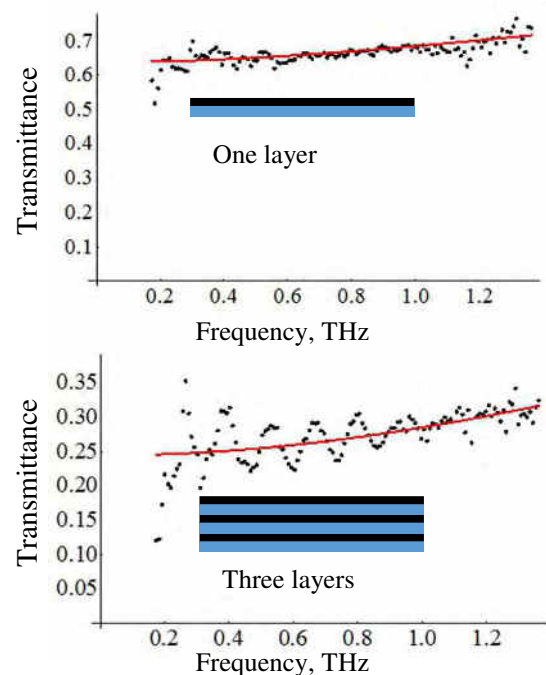


Fig.1. Transmission for the one- and three-layer sandwich structure as function of frequency. Dots and red solid line represent results of the experiment and theory, respectively.

## RAMAN SPECTROSCOPY FOR THE CHARACTERIZATION OF MULTI-WALLED CARBON NANOTUBES

S.N. Bokova-Sirosh<sup>1,2</sup>, E.D. Obraztsova<sup>1,2</sup>, M. A. Shuvaeva<sup>3,5</sup>, A. V. Ishchenko<sup>3</sup>, D. V. Krasnikov<sup>3,5</sup> and V. L. Kuznetsov<sup>3,5,6,7</sup>

<sup>1</sup>*A.M. Prokhorov General Physics Institute RAS, 38 Vavilov str., 119991, Moscow, Russia*

<sup>2</sup>*National Research Nuclear University «MEPhI», Kashirskoe shosse, 31, Moscow, Russia*

<sup>3</sup>*Boreskov Institute of Catalysis SB RAS, Lavrentieva ave. 5, Novosibirsk, 630090, Russia*

<sup>4</sup>*Nikolaev Institute of Inorganic Chemistry, SB RAS, Lavrentieva ave. 3, Novosibirsk, 630090, Russia*

<sup>5</sup>*Novosibirsk State University, Pirogova ave. 2, Novosibirsk, 630090, Novosibirsk, Russia*

<sup>6</sup>*Novosibirsk State Technical University, K. Marx ave. 20, 630092, Novosibirsk, Russia*

<sup>7</sup>*National Tomsk State University, 36, Lenina Avenue, Tomsk, 634050, Russia  
sofia@kapella.gpi.ru*

Development of new materials and technologies of their production is currently one of the determining factors of the scientific and economic development. One of the priorities of modern materials are nanomaterials and nanotechnology. Multi-walled carbon nanotubes are unique material, as they have partially quantum properties of single-walled nanostructures, improved mechanical properties, but along with those, the cost of production is significantly lower than for their single-walled counterparts.

Raman spectroscopy is very effective for the diagnostics of various forms of carbon nanomaterials, such as single- and double-wall nanotubes, graphene, ultrafine nanodiamond, etc. In this work a possibility of the Raman spectroscopy for diagnostics of multi-walled carbon nanotubes has been used. The Raman spectra registration has been made in the spectral range 1150 - 2900  $\text{cm}^{-1}$ : D (disorder-induced), G (graphite) and 2D (two-phonon scattering)-bands. Two series of multi-walled carbon nanotubes synthesized on basis of two types of catalyst Fe-Co-CaO and Fe-Co- $\text{Al}_2\text{O}_3$  have been investigated. Variable parameter of synthesis was the addition of promoting additives (100 – 400 ppm  $\text{H}_2\text{O}$ ).

*This research was partially supported by the RAS research programs and RFBR 13-02-90715 mol\_rf\_nr and RFBR-13-02-01354.*



## FEMTOSECOND CHARGE TRANSFER FROM MoS<sub>2</sub> TO ORGANIC ACCEPTOR

T. Borzda<sup>1</sup>, N. Vujicic<sup>1,2</sup>, C. Gadermaier<sup>1</sup>, P. Topolovsek<sup>1</sup>, T. Mertelj<sup>1</sup>, D. Vella<sup>1</sup>,  
V. Vega Mayoral<sup>1</sup>, D. Mihailovic<sup>1</sup>

<sup>1</sup>Department of Complex Matter, Jozef Stefan Institute, Jamova 39, 1000 Ljubljana, Slovenia

<sup>2</sup>Institute of Physics Bijenička 46, Zagreb, Croatia

tetiana.borzda@ijs.si

MoS<sub>2</sub> has been shown to have a strong photovoltaic effect [1] and can be used in high sensitivity photodetectors [2]. However, because of the high excitonic binding energy [3] we can expect that the efficiency of such devices can be improved by using MoS<sub>2</sub> in a donor-acceptor configuration.

I will present the femtosecond study of the photo-excitation dynamics of MoS<sub>2</sub> intermixed with different organic acceptor materials. Excitons are efficiently dissociated to free charges on the time scale about few ps and electrons are transfer to acceptor material.

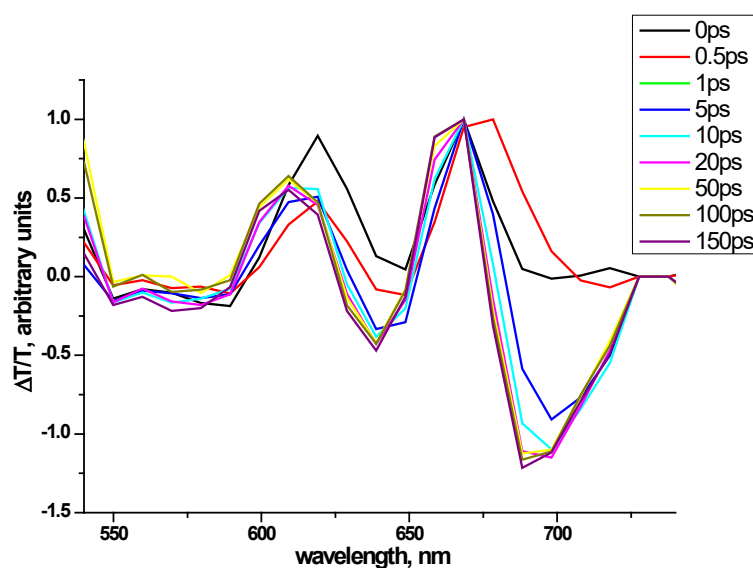


Fig. 1. Differential transmission spectra of mixture of MoS<sub>2</sub> with acceptor material at different time delays

[1] E. Fortin and W. M. Sears, *Journal of Physics and Chemistry of Solids*, Vol 43, No 9, 881-884 (1982).

[2] O. Lopez-Sanchez, D. Lembke, M. Kayci, A. Radenovic, A. Kis, *Nature Nanotechnology*, 8, 497-501 (2013).

[3] T. Cheiwchanhangij, W. R. Lambrecht, *Phys. Rev. B*, 85 (2012).

## IN SITU RAMAN MONITORING OF SINGLE-WALL CARBON NANOTUBE FILLING WITH CuCl

T. V. Eremin<sup>1,2</sup>, A.A. Tonkikh<sup>2</sup>, E. D. Obraztsova<sup>1,2</sup>

<sup>1</sup>Physics Department of M.V. Lomonosov Moscow State University, Moscow, Russia

<sup>2</sup>A.M.Prokhorov General Physics Institute, RAS, Moscow, Russia

timaeremin@yandex.ru

Filling of internal channels of single-wall carbon nanotubes (SWNTs) with different substances leads to change of their electronic and optical properties. Particularly, a Fermi level of hybrid structures, such as I@SWNT and CuCl@SWNT, is downshifted in comparison with the initial value for empty nanotubes. A corresponding charge transfer is observed according to the suppression of  $E_{11}$  band in the optical absorption spectrum. (Fig.1)[1]. The changes in Raman spectra are, mainly, the shifts of tangential and radial breathing modes. The Raman spectra (in the "breathing" mode spectral range) of pristine and filled with CuCl (during 13 hours) SWNTs are shown in Fig.2.

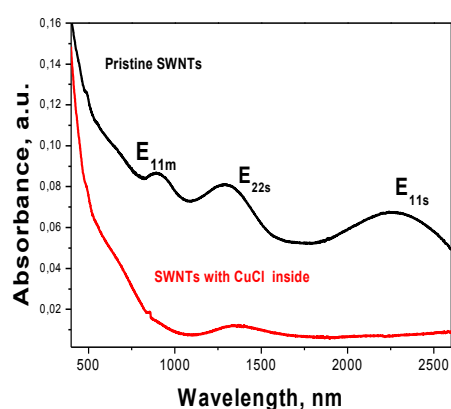


Fig.1. UV-vis-NIR absorbance spectra of pristine and filled with CuCl SWNTs.

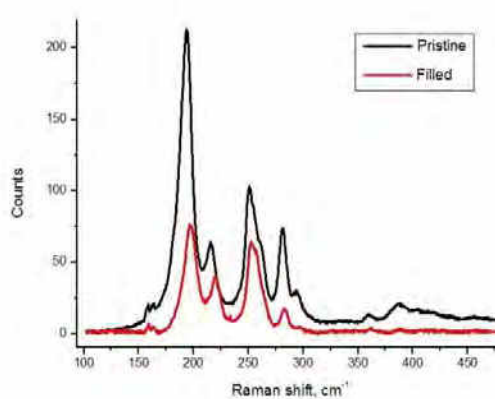


Fig.2 The Raman spectra of pristine and filled with CuCl SWNTs (RBM modes).

However, there is also a considerable interest to monitor the step-by-step Raman spectrum modification while the filling time is increased. This is the aim of this work.

Copper chloride (CuCl) was used as a filler. CuCl powder and chemically vapor deposited SWNT film on a quartz substrate were placed in a special hermetic chamber with optical windows. The temperature inside was maintained at 200 °C. This temperature provides a gaseous CuCl penetration into nanotube internal channels. In situ Raman measurements were carried out via a glass illuminator placed in the chamber top cover.

*The work was supported by RFBR projects 14-02-31829, 14-02-31818 and 13-02-01354.*

[1] A.A. Tonkikh, E. D. Obraztsova, E. A. Obraztsova, A.V. Belkin, and A. S. Pozharov "Optical spectroscopy of iodine-doped single-wall carbon nanotubes of different diameter", Phys. Status Solidi B, 249 (2012) 2454-2459.

## THE STUDY OF ENVIRONMENTAL AND COUPLING EFFECTS IN INDIVIDUAL CARBON NANOTUBES

D. Levshov<sup>1</sup>, M. Avramenko<sup>1</sup>, T. Michel<sup>2</sup>, R. Arenal<sup>3</sup>, Y. Yuzyuk<sup>1</sup>, J.-L. Sauvajol<sup>2</sup>

<sup>1</sup>*Faculty of Physics, Southern Federal University, Rostov-on-Don, Russia*

<sup>2</sup>*University Montpellier 2, Laboratoire Charles Coulomb, Montpellier, France*

<sup>3</sup>*Laboratorio de Microscopias Avanzadas, Instituto de Nanociencia de Aragon,  
Universidad de Zaragoza, Zaragoza, Spain  
dmitry.levshov@gmail.com*

In this work, we present a study of environmental and coupling effects in individual single-walled and multi-walled carbon nanotubes (CNTs). The individual free-standing CNTs were synthesized by catalytic chemical vapour deposition method on dedicated substrates and then analysed by Raman spectroscopy, High-resolution electron microscopy (HRTEM) and Electron diffraction (ED).

The combined Raman-ED approach has allowed us to probe unambiguously specific features that can never be derived from ensemble measurements. For instance, we estimated the effect of environment and van-der-Waals interaction on the intrinsic vibrational and optical properties of CNTs. We showed that the coupling between the concentric layers in multi-walled nanotubes plays a major role in the conditions of the observation of low-frequency Radial Breathing-Like Modes (RBLMs) and high-frequency G-modes in Raman spectra. Firstly, the low frequency range is understood in terms of collective in-phase and out-of-phase RBLMs in the framework of discrete [1] and continuous [2] theoretical models. We argue that the continuous approach [2] gives the best fit of our experimental data. Secondly, we discuss the behaviour of G-modes in the Raman spectra of individual double-walled nanotubes as a function of tube diameter and interlayer distance.

Finally, Raman resonance profiles of RBLMs and G-modes performed on free-standing DWNTs with tunable lasers are reported. Such experiments allow us to measure transition energies of each layer and thus to precise the resonance chart in the presence of coupling effect.

[1] V. N. Popov, L. Henrard, *Breathing-like phonon modes of multiwalled carbon nanotubes*, Phys. Rev. B 65, 235415 (2002).

[2] S.B. Rochal, V.L. Lorman, Yu.I. Yuzyuk, *Two-dimensional elasticity determines the low-frequency dynamics of single- and double-walled carbon nanotubes*, Phys. Rev. B 88, 235435 (2013).

## MULTIWALL CARBON NANOTUBE/SILICON HYBRIDS AS A SOLAR CELL PROTOTYPE

E.V. Lobiak,<sup>1</sup> D.S. Bychanok,<sup>2</sup> E.V. Shlyakhova<sup>1</sup>, A.V. Okotrub,<sup>1</sup> and L.G. Bulusheva<sup>1</sup>

<sup>1</sup>*Nikolaev Institute of Inorganic Chemistry, Siberian Branch of Russian Academy of Sciences, 3 Academician Lavrentiev ave., 630090 Novosibirsk, Russia*

<sup>2</sup>*Institute for Nuclear Problems, Belarus State University, 11 Bobruiskaya str., 220030 Minsk, Belarus*

*e-mail: [lobjaka@gmail.com](mailto:lobjaka@gmail.com)*

Silicon solar cells, which are produced by industry in a large scale, are based on the p-n junction. The main problem with the creation of such elements is a difficulty in the formation of thin Si layers and the electrical current supply. To solve this problem a combination of semiconductor material, such as silicon, with electrically conductive carbon nanotubes (CNTs) was offered in recent years. Conductive properties of CNTs depend on their structure. For example, defects in CNT walls provide the p-type conductivity.

In the present work, hybrid structures from silicon and multiwall CNTs were obtained using an aerosol-assisted variant of the catalytic chemical vapor deposition (CCVD) method. The iron polyoxomolybdate  $[\text{H}_4\text{Mo}_72\text{Fe}_{30}\text{O}_{254}(\text{CH}_3\text{COO})_{10}\{\text{Mo}_2\text{O}_7(\text{H}_2\text{O})\}\{\text{H}_2\text{Mo}_2\text{O}_8(\text{H}_2\text{O})\}_3(\text{H}_2\text{O})_{87}]\cdot 80\text{H}_2\text{O}$ , called keplerate, was used as a catalyst precursor. The size of the metal frame  $\{\text{Fe}_{30}\text{Mo}_{72}\}$  is about 2.5 nm which gives a high chance to obtain thin CNTs. The acetonitrile and alcohol/acetone mixture were used as sources of carbon for the growth of CNTs. The keplerate was dissolved in the sources of carbon (0.1 wt. %) and then injected into a tubular CVD reactor. The synthesis was carried out at temperatures of 800 °C, 900 °C and 1050 °C for 30 min. As a result, a very thin layer of CNTs was formed on the surface of the 10x10 mm<sup>2</sup> silicon substrate (Fig. 1).

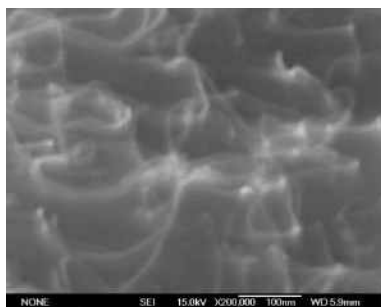


Fig. 1. SEM image of carbon materials synthesized at 1050 °C from a mixture of ethanol and acetone using keplerate as a catalyst source.

The CNT/Si hybrid materials were tested as solar cell prototypes. We measured the current-voltage characteristics derived cells. During the experiment, the open circuit voltage, short circuit current, resistance of the sample under illumination and without that were measured. The data were normalized to the area of the photocell.

The most promising results were obtained using CNTs synthesized from a mixture of ethanol and acetone taken in equal ratio at 1050 °C. The Raman scattering investigation showed that these CNTs are the most defective in the considered set which indicates their highest p-type conductivity.

This work was supported by RFBR 14-03-32089 number.

## GRAPHENE PASSIVELY MODE-LOCKING FIBER LASER

Man Jiang<sup>1</sup>, Diao Li<sup>1</sup>, Yali Liu<sup>1</sup>, Xuetao Gan<sup>2</sup>, Zhaoyu Ren<sup>1</sup> and Jintao Bai<sup>1</sup>

<sup>1</sup>*Institute of Photonics & Photon-Technology, Department of Physics, Northwest University, Xi'an 710069, China*

<sup>2</sup>*Department of Applied Physics, Northwestern Polytechnical University, Xi'an 710072, China*  
*e-mail address: jjmfish@163.com*

Recently, the unique band structure, outstanding linear and nonlinear optical properties of graphene make it a promising material in optical applications such as novel saturable absorbers(SAs)[1-2]. In the most of researches, graphene nanosheets or graphene-polymer films were usually used for generating pulsed lasers[3-4], in order to obtain more robust operation of pulse laser, we chose the method that the evanescent field of processed fiber coupled with graphene to enhance the interaction of graphene with light.

The single mode fibers(SMF) were etched using an HF acid of 10% concentration until the diameter of SMF reduced to  $\sim 5 \mu\text{m}$ , and then graphene grown by CVD method was wrapped around the processed fiber, which can be used as a SA. Here, we demonstrated a stable mode-locked pulse by employing the last graphene SA in the Er-doped fiber laser. In the laser cavity,  $\sim 1 \text{ m}$  Er-doped fiber is used as a laser gain medium, and a  $\sim 974\text{nm}$  laser diode (LD) is used as a pump via 974/1550 fiber wavelength division multiplexer(WDM) coupler. An optical isolator is used to ensured the unidirectional operation of the ring laser, and a polarization controller (PC) is employed to match the state of polarization of the propagating light in the cavity. A fused 10/90 coupler is utilized as output coupler. Finally, Self-starting, single pulse mode-locking was facilitated. The laser produced 3 ps pules at  $1.55 \mu\text{m}$  at a repetition rate of 260MHz.

The work was supported by the National Natural Science Foundation of China (Nos 61177059 and 61275105).

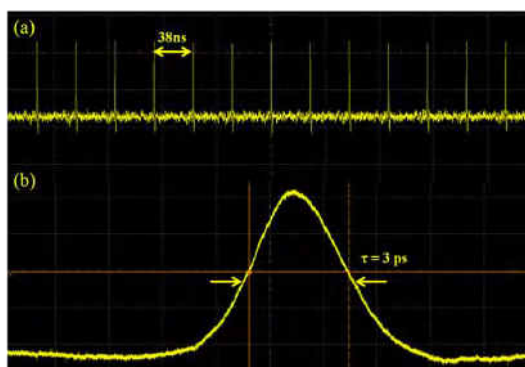


Fig.1 mode-locking pulses train (a), and a single pulse (b).

- [1] F. Bonaccorso, Z. Sun, T. Hasan and A. C. Ferrari, *Nature Photonics*, **4**, 611 (2010).
- [2] Z. Sun et.al., *ACS Nano*, **4**, 803 (2010).
- [3] Z. Sun, T. Hasan and A. C. Ferrari, *Physica E*, **44**, 1082 (2012).

## ELECTRONIC AND OPTICAL PROPERTIES OF GRAPHENE NANORIBBONS ENCAPSULATED IN SINGLE-WALL CARBON NANOTUBES

A.V. Osadchy, D. V. Rybkovskiy, E. D. Obratsova

A. M. Prokhorov *General Physics Institute of Russian Academy of Sciences,  
119991, Vavilov str., 38, Moscow, Russia*  
e-mail: aosadchy@kapella.gpi.ru

In this work, has been performed theoretical studies of the band structure and optical properties of graphene nanoribbons encapsulated in single-wall carbon nanotubes. The simulation was performed using methods based on density functional theory and GW approximation [1,2]

Electronic dispersion curves has been obtained for different geometries of graphene nanoribbons encapsulated in single-wall carbon nanotubes (Fig. 1). The band gap dependence on the nanoribbon width has been calculated in GW and LDA approximations (Fig. 2).

The obtained information agrees well with the results of recently published experimental studies [3,4] and have been used for analysis of the photoluminescence spectra of synthesized samples of graphene nanoribbons inside nanotubes.

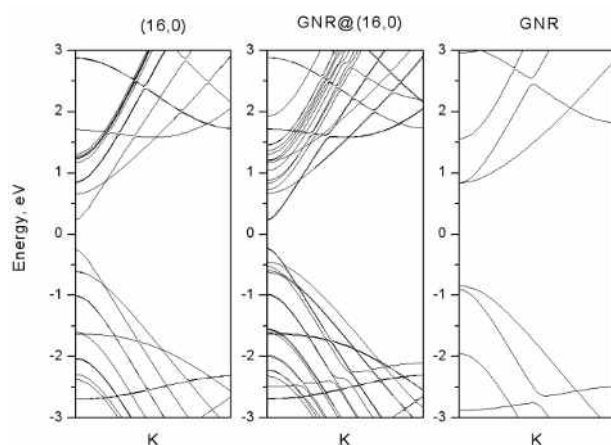


Fig. 1. Electronical dispersion curves for isolated (16,0) nanotube, nanoribbon encapsulated in nanotube, and isolated nanoribbon width 4.4 nm

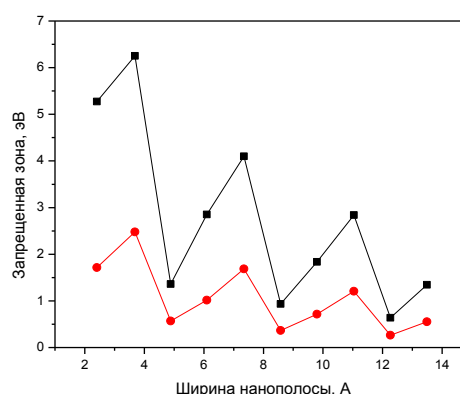


Fig. 2. Band gap dependencies for nanoribbons using GW (bottom) and LDA (top) approxiamtions

*This work was supported by RFBR 13-02-01354. SP-7452.2013.5 and RAS Research Programs.*

- [1] P. Giannozzi et al., *J. Phys. Condens Matter* 21, 395502 (2009).
- [2] Arno Schindlmayr, P. Garcia-Gonzalez, et al., *Phys. Rev. B* 64, 235106 (2001)
- [3] A. V. Talyzin, et al., *Nano Letters*, 2011, 11, 4352.
- [4] A.I. Chernov, P.V. Fedotov et al., *ACS Nano* 7 (2013) 6346.

## INVESTIGATION OF "FULLERENE-QUANTUM DOTS" COMPOSITE MATERIALS FOR SOLAR CELLS APPLICATIONS

Sergey Pavlov, Demid Kirilenko, Alexei Nashchekin  
*Ioffe Physical-Technical Institute of RAS, Saint-Petersburg, Russia*  
*e-mail: pavlov\_sergey87@mail.ru*

We present the structure and electrical properties study of  $C_{60}$  fullerene-quantum dot nanocomposite. It's known [1] that being dissolved in mixed solvents fullerenes form stable clusters. Varying concentration of the fullerene solution and proportion of various solvents it's possible to produce clusters with sizes up to several hundred nanometers. Furthermore, mixing fullerene solution with a quantum dots (QD) solution the composite material can be prepared. In such material photoinduced charge transfer efficiency is increased due to  $C_{60}$  is a good acceptor [2], so the composite can be used in thin-film photovoltaic.

In the work toluene solution with known concentration of colloidal QDs CdSe/CdS/ZnS was mixed with  $C_{60}$  toluene solution. The obtained solution was slowly injected in larger amount of acetonitrile to form composite clusters with size about 100 nm (Fig. 1, left).

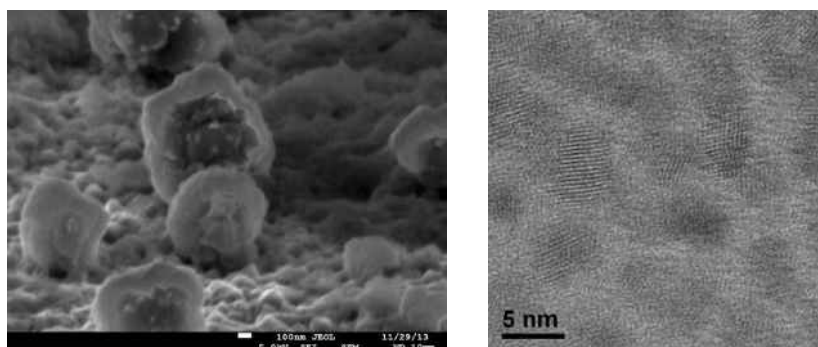


Fig. 1.  $C_{60}$ /QD cluster SEM (left) and TEM (right) image.

By electrophoretic deposition there was prepared up to 2  $\mu\text{m}$  thick films consisting of fullerene based composite clusters. Energy-dispersive spectra and TEM images (Fig. 1, right) demonstrate the 5 nm QDs distributed in fullerene matrix.

Electrical measurements was performed after deposition of composite onto photolithographic planar contacts fabricated on Si/SiO<sub>2</sub> dielectric substrate. In  $C_{60}$ /QD composite value of measured current was an order of magnitude higher, then in pristine  $C_{60}$ , and increased when affected by visible light.

- [1] R. G. Alargova, S. Deguchi and K. Tsujii, *J. Am. Chem. Soc.*, **123**, 10460 (2001).
- [2] P. Brown and P. V. Kamat, *J. Am. Chem. Soc.*, **130**, 8890, (2008).

## GRAPHENE FOR TERAHERTZ APPLICATION

Yixuan Zhou, Zhaoyu Ren, Mei Qi, Xinlong Xu, and Jintao Bai  
*Institute of Photonics & Photon-Technology, Northwest University, Xi'an 710069,  
China*

[rzy@nwu.edu.cn](mailto:rzy@nwu.edu.cn)

As one of the most rapid growing field, terahertz (THz) technology has stimulated many applications, ranging from time-domain spectroscopy (TDS), biological imaging, to high-speed communications. Hence, there is an urgent demand of THz devices, such as THz source, detector, and modulator. Recently, many new proof-of-concept graphene-based THz modulators have been proposed. Our work is as follows: Firstly, we studied the controllable preparation of large-area, high quality CVD graphene [1]. In addition, we have prepared nitrogen doped graphene [2] and graphene oxide. Secondly, THz-TDS has been employed to investigate these materials' THz properties. The experiment combined with theory proved that randomly stacked multilayer graphene, which has extended variation range of the THz conductivity, can be treated as multiple electronically decoupled monolayer graphene in the THz region [3]. Meanwhile, both nitrogen doped graphene [2] and graphene oxide have sensitive THz responses. Last but not the least, the excellent tunable THz conductivity of these materials makes them probably to be used in broadband THz application. We have examined the potential of stacked multilayer graphene as broadband THz antireflection coating in experiment and theory [3]. The reflected pulses from the quartz and silicon substrates were observed to change with the layer number and chemical doping degree of the graphene coating. We also studied the hybridization of graphene with THz metamaterials, which leads to an ultrasensitive and strong interaction. This ultrasensitive interaction is proved to be relevant to the electrical conductivity of graphene overlayer. And we have also proposed a device based on tunable magnetoplasmons in gated monolayer graphene for THz wave modulation and isolation [4, 5]. A superior modulation depth and giant magneto-optic rotation due to the cyclotron effect in the classical regime by intraband transitions in graphene offer an effective, uniform, and flexible tunability for THz wave.

The work was supported by National Natural Science Foundation of China (61275105, 61177059, 11374240), International Cooperative Program (201410780), Shaanxi Natural Science Basic Research Plan (2012KJXX-27, 12JK0990), Education Ministry Ph.D. Programs Foundation (20136101110007, 20126101120029), and Key Laboratory Science Research Plan of Shaanxi Education Department (11JS106, 13JS101).

[1] M. Qi, Z. Ren, Y. Jiao, Y. Zhou, X. Xu, W. Li, J. Li, X. Zheng and J. Bai, *J. Phys. Chem. C* **117** (27), 14348-14353 (2013).

[2] J. Li, Z. Ren, Y. Zhou, X. Wu, X. Xu, M. Qi, W. Li, J. Bai and L. Wang, *Carbon* **62**, 330-336 (2013).

[3] Y. Zhou, X. Xu, F. Hu, X. Zheng, W. Li, P. Zhao, J. Bai and Z. Ren, *Applied Physics Letters* **104** (5), 051106 (2014).

[4] Y. Zhou, X. Xu, H. Fan, Z. Ren, J. Bai and L. Wang, *Physical Chemistry Chemical Physics* **15** (14), 5084-5090 (2013).

[5] Y. Zhou, X. Xu, H. Fan, Z. Ren, X. Chen and J. Bai, *Journal of the Physical Society of Japan* **82** (7), 074717 (2013).



## EFFECT OF POLARIZATION ELLIPTICITY ON PHOTOVOLTAIC RESPONSE OF NANOCARBON AND Ag/Pd RESISTIVE FILMS

A.S. Saushin<sup>1</sup>, R.G. Zonov<sup>1</sup>, A.G. Nasibulin<sup>2</sup>, G.M. Mikheev<sup>1</sup>

<sup>1</sup>*Institute of Mechanics UB RAS, 34 T. Baramzinoy st., Izhevsk, Russia*

<sup>2</sup>*Skolkovo Institute of Science and Technology, 100 Novaya st., Skolkovo, Odintsovsky district, Moscow Region, Russia 143025*

*alex@udman.ru*

Recently a significant amount of papers dedicated to the study of photovoltaic phenomena which are sensitive to the sign of polarization, have been published [1-3]. Such research are interesting in terms of the polarization analyzer creation without optical elements. Here we present new results of the study of the photovoltaic phenomena in the single-walled carbon nanotube films and the Ag/Pd-films, depending on the sign of polarization in the visible range of radiation.

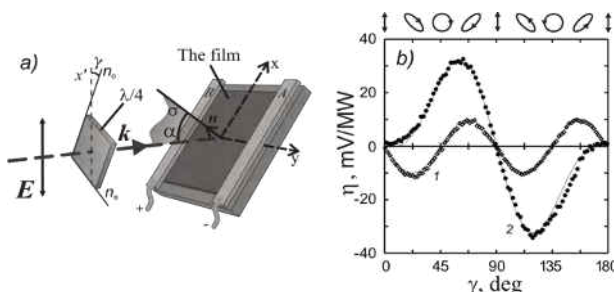


Fig. 1. *a* – the scheme of the experiments. *b* – dependences of the conversion factor  $\eta$  on the angle of rotation of the quarter wave plate for single-walled carbon nanotube films 1 and Ag/Pd-films 2.

The 532 nm pulsed linearly polarized laser radiation was used in the experiments. The pulse duration was of 15 ns. The angle  $\gamma$  of rotation of the quarter wave plate set an ellipticity and the sign of the polarization of incident light. The films were disposed such that the electrodes attached to the films were parallel to the plane of the laser light incidence (Fig. 1a).

The figure 1b represents the results obtained that can be described with the following:

$$\eta = \eta_1 \sin(2\gamma) + \eta_2 \sin(4\gamma), \quad (1)$$

where  $\eta_1$ ,  $\eta_2$  – coefficients responsible for circular and linear contributions to the photovoltaic signal, respectively. For the Ag/Pd-films  $\eta_1 = 24 \text{ mV} / \text{MW}$ ,  $\eta_2 = -13 \text{ mV} / \text{MW}$ , while for the single-walled carbon nanotube films  $\eta_1 = 0$ ,  $\eta_2 = -10 \text{ mV} / \text{MW}$ . Thus in the nanotube films the circular contribution is missing and the signal amplitude and polarity are defined by the direction and the ratio of polarization ellipse axes. The similar results were obtained for the nanographite films [4]. It means that in contrast to the Ag/Pd-films, the single-walled carbon nanotube films do not possess of the sensitivity to sign of circular polarization.

This study was supported by the RFBR (project no. 13-08-01031).

[1] T. Hatano, T. Ishihara, S.G. Tikhodeev and N.A. Gippius, *Phys. Rev. Lett.*, **103**, 103906 (2009).

[2] G.M. Mikheev, V.A. Aleksandrov, A.S. Saushin, *Tech. Phys. Lett.*, **37**, 551 (2011).

[3] J. Karch, P. Olbrich, M. Schmalzbauer et al., *Phys. Rev. Lett.*, **105**, 227402 (2010).

[4] G.M. Mikheev, V.M. Styapshin, P.A. Obratsov, E.A. Khestanova, S.V. Garnov, *Quantum Electronics*, **40** (5), 425 (2010).

## PUMP-PROBE WS<sub>2</sub> FUNDAMENTAL PROPERTIES

*V. Vega Mayoral<sup>1</sup>, D. Vella<sup>1</sup>, T. Borzda<sup>1</sup>, N. Vujicic<sup>1,2</sup>, P. Topolovsek<sup>1</sup>, M. Prijatelj<sup>1</sup>,  
C. Gadermaier<sup>1</sup> and D. Mihailovic<sup>1</sup>*

<sup>1</sup> *Department of Complex Matter, Jozef Stefan Institute, Ljubljana, Slovenia*

<sup>2</sup> *Institute of Physics, Zagreb, Croatia*

*victor.vega@ijs.si*

Some of the most fundamental electronic relaxation processes occur on the femto- and picosecond time scales. Here we use time resolved optical spectroscopy to study the photoexcitation dynamics in semiconducting few-layer WS<sub>2</sub>.

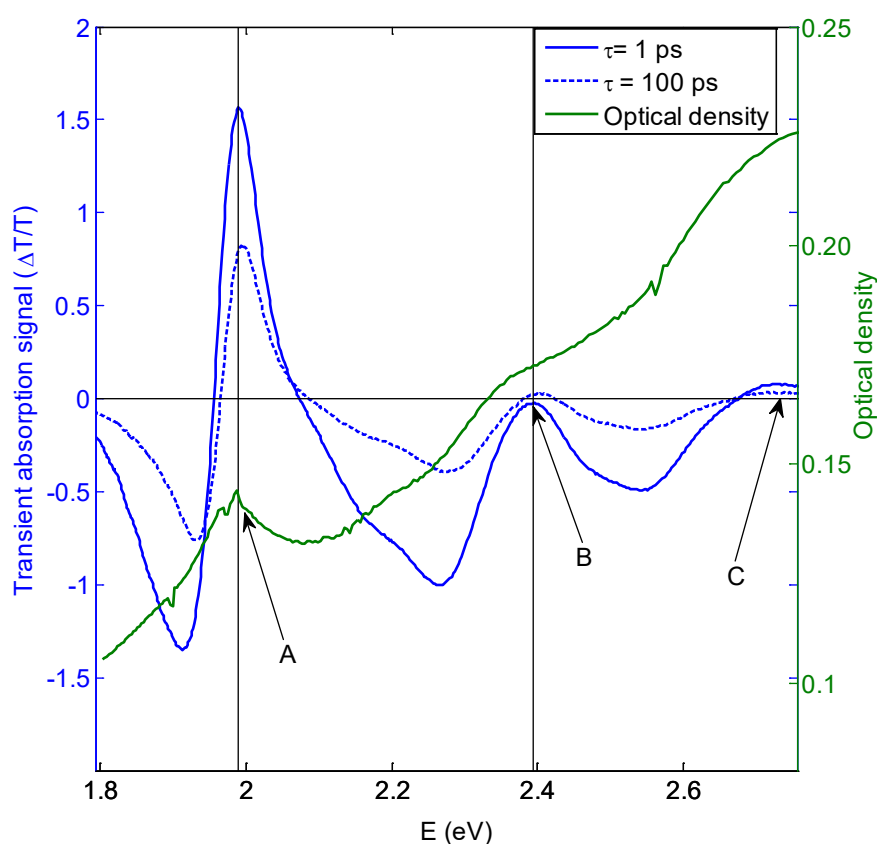


**Fig 1:** WS<sub>2</sub> optical density and transient absorption spectra.

We determine exciton lifetimes and observe charge generation, which highlights the scope of WS<sub>2</sub> for photovoltaic and photodetector applications, similar to reported results on MoS<sub>2</sub> [1]. The larger spectral separation of the A and B exciton peaks (Fig 1) allows the disentanglement of previously unresolved dynamics of overlapping signatures of different photoexcited states.

[1] H. Shi, R. Yan, S. Bertolazzi, J. Brivio, B. Gao, A. Kis, D. Jena, H. G. Xing and L. Huang. *ACS Nano*, **7**, 1072-1082 (2013).

## FEMTOSECOND SPECTROSCOPY ON MoS<sub>2</sub> FILMS: EFFECTS OF SYNTHESIS ON THE ELECTRON DYNAMICS

D. Vella<sup>1</sup>, V. Vega Mayoral<sup>1</sup>, T. Borzda<sup>1</sup>, N. Vujicic<sup>1,2</sup>, P. Topolovsek<sup>1</sup>, M. Prijatelj<sup>1</sup>,  
C. Gadermaier<sup>1</sup>, and D. Mihailovic<sup>1</sup>

<sup>1</sup>Department of Complex Matter, Jozef Stefan Institute, Ljubljana, Slovenia

<sup>2</sup>Institute of Physics, Zagreb, Croatia

daniele.vella@ijs.si

Currently, many different methods for exfoliating TMDs and obtain films covering macroscopic areas are explored. The influence of different intercalants, surfactants, etc on the electronic and optical properties of semiconducting TMDs is little known. Here we exploit ultrafast spectroscopy to study MoS<sub>2</sub> [1] from different liquid exfoliation and film deposition methods, as pristine films as well as blended into the inert transparent polymer PMMA. In particular, we find that ionic surfactants such as sodium cholate increase charge carrier generation (see Fig. 1). We also explore modulating the charge photogeneration via an electric field in an interdigitated electrode structure.

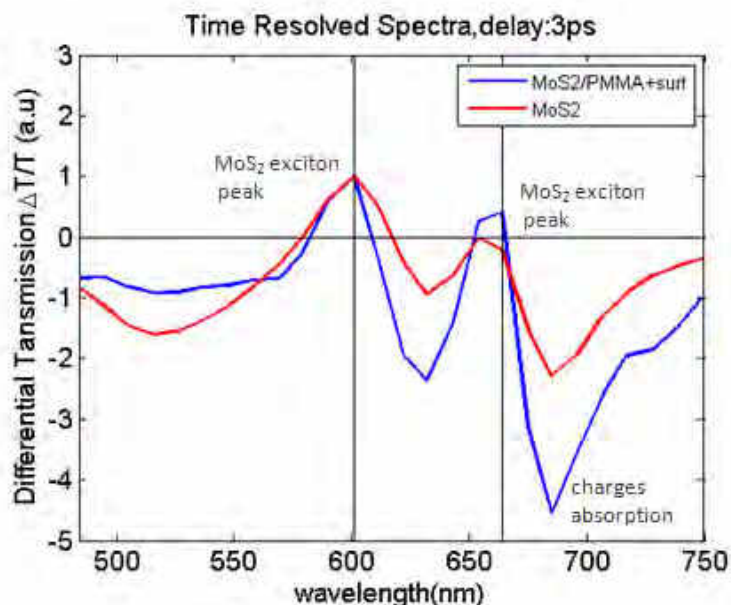


Fig. 1

[1] H. Shi, R. Yan, S. Bertolazzi, J. Gao, A. Kis, D. Jena, H. G. Xing, and L. Huang, *ACS NANO*, **7**, 1072-1080 (2013).

## INFLUENCE OF EXTERNAL CONDITIONS ON THE PHOTOVOLTAIC RESPONSE SINGLE WALLED CARBON NANOTUBE FILMS

R.G. Zonov<sup>1</sup>, G.M. Mikheev<sup>1</sup>, A.G. Nasibulin<sup>2,3</sup>

<sup>1</sup>*Institute of Mechanics UB RAS, 34, str. T. Baramzinoy, Izhevsk, Russia 426067*

<sup>2</sup>*Aalto University, P.O.Box 15100, 00076, Espoo, Finland*

<sup>3</sup>*Skolkovo Institute of Science and Technology, 100 Novaya st., Skolkovo,*

*Odintsovsky district, Moscow Region, Russia 143025*

*e-mail:zov@udman.ru*

We have recently demonstrated that single-walled carbon nanotube (SWCNT) films synthesized by an aerosol method [1] possess unique photovoltaic properties as well as sensitivity for the polarization of laser radiation [2]. These films can be used as high-speed photodetector, the polarization analyzer of the laser radiation or the goniometric device. However, external conditions may adversely affect the photovoltaic response. Here we report recent investigation of the light-induced electric currents generation in SWCNT films under different conditions of the external environment.

In our experiments copper electrodes were attached to the surface of the SWCNT film on a polyester substrate. The substrate with the film on a special copper holder was placed in a vacuum chamber and heated by using nichrome wire heater. The SWCNT film was irradiated by linear-polarized laser pulses of the Q-switched YAG:Nd<sup>3+</sup>-laser (pulse duration - 20 ns, pulse energy – less than 1 mJ) and the voltage generated between the electrodes was registered by a digital oscilloscope. Preliminary experiments showed that the voltage of the photovoltaic response decreases under vacuum and may finally changes to the opposite sign with the initial amplitude. However, after annealing the SWCNT film at temperature of 473 K photovoltaic voltage returns to its original value.

Among others the treatment of the SWCNT film surface with a solvent such as alcohol affects the photovoltaic response. As in the previous case, the voltage of the photovoltaic response reverses its sign after the treatment with alcohol and returned to the original value either after some period of time or after heat treatment.

Experiments on the photoelectric conversion ratio of different gases (such as hydrogen, nitrogen, carbon dioxide and other) in the environment did not reveal any regular dependence.

In the report possible mechanisms leading to changes in the polarity of the photovoltaic response are discussed.

This study was supported by the RFBR (project no. 13-02-96037).

[1] Moisala, A.; Nasibulin, A. G.; Brown, D. P.; Jiang, H.; Khriachtchev, L.; Kauppinen, E. I. *Chemical Engineering Science*, **61**, 4393-4402 (2006).

[2] G. M. Mikheev, A. G. Nasibulin, R. G. Zonov, A. Kaskela, E. I. Kauppinen, *Nano Letters*, **12**, 77-83 (2012).



## Wednesday, July 30





## NONLINEAR MICROSCOPY WITH FOCUSED VECTOR FIELDS

Martti Kauranen, M. Huttunen, G. Bautista, J. Mäkitalo  
*Department of Physics, Tampere University of Technology, PO Box 692,  
FI-33101 Tampere, Finland  
martti.kauranen@tut.fi*

Nonlinear optical processes can provide several new contrast mechanisms for microscopy. Focusing of a polarized laser beam gives rise to a spatially varying three-dimensional vector field in the focal volume. In this paper, we show, using several different examples, that this provides completely new capabilities in the characterization of the structural properties of materials at microscopic resolution.

Thin films of chiral molecules respond differently to left- and right-hand circular polarizations. For second-harmonic generation (SHG), this leads to a different response for the circularly-polarized components of fundamental light. In traditional surface nonlinear optics, however, chirality is difficult to separate from in-plane anisotropy. We first show that SHG with focused circular polarizations at normal incidence provides an unambiguous probe of surface chirality, using both organic thin films [1] and metal nanostructures [2] as model samples. In the latter case, the surface defects of the metal nanostructures give rise to fluctuating signals, but the circular-difference response stays relatively constant, allowing the handedness of the individual nano-objects to be recognized. These techniques can also be generalized for handed superpositions of radial and azimuthal polarizations.

More recently, we have used polarization based nonlinear microscopy to study individual nano-objects. We have shown that SHG with radial and azimuthal polarizations is sensitive to the morphology of metal nanobumps and nanocones [3]. We have also observed SHG from individual single-walled carbon nanotubes [4]. The origin of this signal could be chirality or defects and needs to be addressed in future work. We have also shown that THG microscopy with polarized light can be used to address the composition and order of lipid droplets. Surprisingly, signals depending on linear polarization do not necessarily imply anisotropy, whereas circular polarizations are sensitive to ordering.

Coupling of light to sharp nanotips usually requires a polarization component along the tip axis, complicating experimental geometries. We show that nano-objects with lowered symmetry allow more convenient geometries to be used [5]. SHG microscopy with radial and azimuthal polarizations further reveals that efficient excitation requires that the three-dimensional field vector be tailored for the modes of the particle.

- [1] M. J. Huttunen et al., *J. Phys. Chem. Lett.* **1**, 1826 (2010)
- [2] M. J. Huttunen et al., *Opt. Mat. Express* **1**, 46 (2011).
- [3] G. Bautista et al., *Nano Lett.* **12**, 3207 (2012).
- [4] M. J. Huttunen, et al., *New J. Phys.* **15**, 083043 (2013).
- [5] M. J. Huttunen et al., submitted to *Opt. Lett.*



## MATERIALS WITH THREEFOLD ROTATIONAL SYMMETRY FOR POLARIZATION CONTROL OF LIGHT

Makoto Kuwata-Gonokami

*Department of Physics, The University of Tokyo, Hongo, Tokyo 113-0033 Japan  
gonokami@phys.s.u-tokyo.ac.j*

Symmetry of materials plays an important role in polarization-sensitive optical phenomena. In coherent nonlinear light scattering processes, the conservation laws of angular momentum determine the polarization state of the scattered photon [1]. The angular momenta of the electromagnetic field ( $\mathbf{J}^{EM}$ ), material excitations ( $\mathbf{J}^{ex}$ ), and the crystalline lattice ( $\mathbf{J}^c$ ) are related by  $\mathbf{J}^{EM} + \mathbf{J}^{ex} + \mathbf{J}^c = 0$ . When light propagates along a threefold rotational crystal axis, the crystal quasi-angular momentum is conserved. Thus, the scattering of light alters the quasi-angular momentum  $J_z^{EM} + J_z^{ex}$  by  $3N\hbar$ , where  $N$  is an integer. This phenomenon is the rotational analogue of the Umklapp process of discrete translational symmetry in crystals [1]. The phenomenon also determines the polarization selection rules in second-order nonlinear processes [2, 3]. We considered that this threefold rotational symmetry could be exploited for polarization control in both terahertz (THz) generation and second harmonic generation (SHG).

First, we manipulated the magnetization vector of magnons in an antiferromagnetic NiO crystal with a [111] surface. Because of the small random domain structures, the effective crystal symmetry is threefold rotational. We observed magnetic dipole THz radiation, which originates from the magnetization oscillations induced by linearly polarized femtosecond laser pulses. Angular momentum conservation was confirmed from the relationship between the polarization azimuths of the incident light beam and the generated THz wave [4]. Based on this result, we demonstrated the vectorial control of magnon oscillation by using polarization-twisted double pulse excitation [5].

Extending this idea, we then manipulated the polarization of THz radiation by optical rectification using a cubic ZnTe single crystal with a [111] surface. By combining a vectorial pulse shaping technique [6] with *envelope helicity* control [8], we proposed and demonstrated a new method for generating THz waves with arbitrary polarization-shaped waveforms [7]. We also generated broadband THz cylindrical-vector beams using segmented nonlinear crystals with threefold rotational symmetry [9]. Through this technique, we efficiently coupled the propagating broadband THz beams to metal wires [10], which are ideal THz waveguides.

The polarization selection rule in artificial nanostructures with threefold rotational symmetry is an interesting research topic. We attempted helicity control of SHG in a nonlinear metamaterial with this type of symmetry. To date, we have fabricated two-dimensional gratings in a thin metal film. Specifically, we fabricated a threefold symmetric periodic array of triangular holes. Through this apparatus, a circularly polarized fundamental beam generated a counter-circularly polarized SH beam [11]. We also described a general polarization selection rule for nonlinear metamaterials with  $n$ -fold rotational symmetries. By elucidating the effect of rotational symmetry of

nanostructures, we can design nonlinear metamaterials for polarization-controlled SH generation.

- [1] N. Bloembergen, *J. Opt. Soc. Am.* **70** 1429 (1980).
- [2] H. J. Simon and N. Bloembergen, *Phys. Rev.* **171**, 1104 (1968).
- [3] J. Visser, E. R. Eliel, and G. Nienhuis, *Phys. Rev. A* **66**, 033814 (2002).
- [4] T. Higuchi, N. Kanda, H. Tamaru, and M. Kuwata-Gonokami, *Phys. Rev. Lett.* **106**, 047401 (2011).
- [5] N. Kanda, T. Higuchi, H. Shimizu, K. Konishi, K. Yoshioka, and M. Kuwata-Gonokami, *Nature Commun.* **2**, 362 (2011).
- [6] M. Sato, T. Suzuki, and K. Misawa, *Rev. Sci. Instrum.* **80**, 123107 (2009).
- [7] M. Sato, T. Higuchi, N. Kanda, K. Konishi, K. Yoshioka, T. Suzuki, K. Misawa, and M. Kuwata-Gonokami, *Nature Photon.* **7**, 724 (2013).
- [8] T. Higuchi, H. Tamaru, and M. Kuwata-Gonokami, *Phys. Rev. A* **87**, 013808 (2013).
- [9] R. Imai, N. Kanda, T. Higuchi, Z. Zheng, K. Konishi, and M. Kuwata-Gonokami, *Opt. Express* **20**, 21896 (2012).
- [10] Z. Zheng, N. Kanda, K. Konishi, and M. Kuwata-Gonokami, *Opt. Express* **21**, 10642 (2013).
- [11] K. Konishi, T. Higuchi, J. Li, J. Larsson, S. Ishii, and M. Kuwata-Gonokami, *Phys. Rev. Lett.* **112**, 135502 (2014).

## ORGANIC AND HYBRID INTERFACE DYNAMICS UPON PHOTOEXCITATION

Guglielmo Lanzani

*Center for Nano Science and Technology@PoliMi, Istituto Italiano di Tecnologia,*

*Via Giovanni Pascoli, 70/3, 20133 Milano*

*Department of Physics Politecnico di Milano*

*Piazza L. Da Vinci 32 20127 Milano(Italy)*

*Guglielmo.lanzani@iit.it*

The Schokley-Queisser limit of efficiency for silicon photovoltaic cells regards the loss of excess energy due to fast carrier thermalization. The trade-off to obtain highest efficiency is between spectral coverage, extract energy per photon (equal to the semiconductor gap) and heat dissipation. Also in organic solar cell excess energy maybe lost into heat. Here however the physics is substantially different from that of inorganic semiconductors. By using ultrafast pump probe spectroscopy we show that a prototype low band gap polymer quickly dissipates excess energy through non adiabatic internal conversion. In presence of an acceptor however we find that charge separation can be fast enough at high energy to compete with internal conversion. The specific gain of such hot dissociation is discussed in terms of the microscopic charge separation process and the overall cell efficiency. Morphology is another key factor in organic photovoltaic. We study the interface region between donor and acceptor with unprecedented space resolution (5 nm) to unravel the fundamental process occurring upon photoexcitation. We think our results suggest a quite different picture from that universally accepted.

[1] G. Grancini et al. *Nature Materials*, 2013, **12**, 29–33.

## NANOMATERIAL OPTICAL STUDIES IN A TRANSMISSION ELECTRON MICROSCOPE

Dmitri Golberg

*World Premier International Centre for Materials Nanoarchitectonics (WPI-MANA),  
National Institute for Materials Science (NIMS), Namiki 1, Tsukuba, Ibaraki 3050044,  
Japan  
golberg.dmitri@nims.go.jp*

Modern methods of *in-situ* transmission electron microscopy (TEM) allow one to get deep insights into diverse nanomaterial electrical, mechanical and thermal properties [1]. Since recently we have been able to widen the *in-situ* TEM possibilities toward dedicated optical measurements on individual nanostructures, *e.g.* nanotubes, nanowires, nanobelts, nanoparticles and graphene-like inorganic nanosheets. In order to do so, we have designed opto-compatible TEM operations using various wavelength light sources and corresponding optical fibres protruding into the TEM column (Fig. 1). Simultaneous nanomaterial bending/stretching and/or electrical probing inside TEM may be carried out in tandem with the light illumination of nanostructures.

Numerous 1D and 2D nanomaterial systems of our interests are diverse. They include *p*- and *n*-doped Si, ZnS (with and without Cu-doping), ZnO and CdS nanowires, ZnO-ZnS heterostructures, MoS<sub>2</sub> atomically-thin dichalcogenide nanosheets, TiO<sub>2</sub> nanocrystals and many others. The sophisticated optical setup engineering issues, its fine tuning and unique possibilities, and the results of pioneering informative opto-electronic and photovoltaic tests will be discussed during the talk.

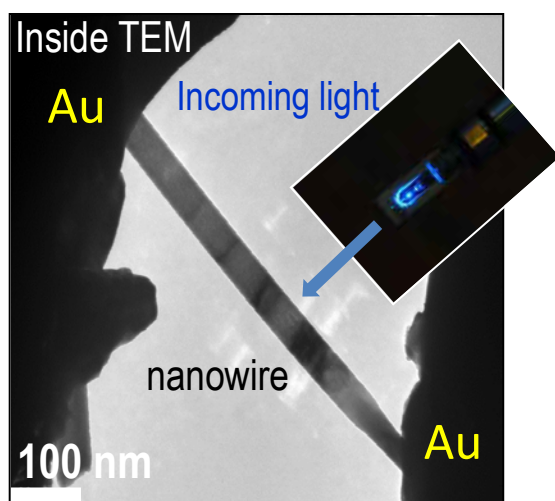


Fig. 1. An individual Zn<sub>1-x</sub>Cu<sub>x</sub>S nanowire stretched between Au electrodes under light illumination in a high-resolution TEM.

The main advantage of the originally designed by us technique is that direct measurements of photocurrents, photovoltages, photoluminescence and cathodoluminescence spectra may be accomplished on individual nanostructures under a full control of their exact crystallography, atomic structure, pre-existing and appearing defects, and spatially-resolved chemistry, and at the highest spatial and temporal resolutions particularly achievable in a high resolution TEM.

This work is carried out under a financial support of MANA-NIMS, Tsukuba, Japan. The author is grateful to Dr. Zhi Xu and Mr. Chao Zhang for the experimental help.

[1] D. Golberg *et al.* *Advanced Materials* **24**, 177 (2102).



## Thursday, July 31





## PURIFICATION OF SINGLE-CHIRALITY CARBON NANOTUBES FOR OPTICAL SPECTROSCOPY STUDIES

Ming Zheng

*National Institute of Standards and Technology, Gaithersburg, Maryland 20899, USA*

*ming.zheng@nist.gov*

Chirality control is one of the most challenging problems in the carbon nanotube field. Over a decade ago, we and others began to explore separation of single-wall carbon nanotubes by exploiting chirality-dependent molecular interactions in liquid phases. By now, efforts from many groups around the world have resulted in a number of effective ways to achieve metal/semiconductor separation and single-chirality purification, enabling fundamental studies and application development. In this presentation, I will review various separation methods developed so far, discuss common physical mechanism underlying these methods, and highlight a polymer-based liquid two-phase extract method we have recently reported [1-2]. I will give examples to illustrate the versatility of the new method, and provide an outlook for its future development to enable optical spectroscopy studies of carbon nanotubes.

[1] Khripin *et al.*, J. Am. Chem. Soc. 135, 6822 (2013)

[2] Fagan *et al.*, Adv. Mat. DOI: 10.1002/adma.201304873 (2014)



## SEPARATION AND OPTICAL PROPERTIES OF SMALL-DIAMETER SINGLE-CHIRALITY SWCNTS

Hiromichi Kataura<sup>1</sup>, Xiaojun Wei<sup>1</sup>, Yasuhiro Ito<sup>1</sup>, Takuya Hirakawa<sup>1</sup>, Shunjiro Fujii<sup>1</sup>,  
Astushi Hirano<sup>1</sup>, Yuhei Miyauchi<sup>2,3</sup>, Kazunari Matsuda<sup>2</sup>, and Takeshi Tanaka<sup>1</sup>

<sup>1</sup> Nanosystem Research Institute (NRI), AIST, Tsukuba, Japan

<sup>2</sup> Institute of Advanced Energy, Kyoto University, Japan

<sup>3</sup> PRESTO, JST, Kawaguchi, Japan

*h-kataura@aist.go.jp*

Because single-wall carbon nanotubes (SWCNTs) are always produced as a mixture of various structures, single-chirality separation is desirable for both fundamental research and applications. Especially, small diameter SWCNTs are very interesting due to their large band gap and strong curvature effects. Previously, we have developed multicolumn gel chromatography method for the precise chirality sorting of semiconducting SWCNTs and have obtained 13 kinds of single-chirality SWCNTs [1]. In this work, we have improved the multicolumn method and optimized it for the small diameter SWCNTs. As a result, we have successfully obtained high-purity (5,4) SWCNTs from HiPco SWCNT. Interestingly, its diameter is smaller than C<sub>60</sub>. In the Raman spectrum of the aqueous solution of (5,4) SWCNT, single radial breathing mode peak at 373 cm<sup>-1</sup> and highly softened TO phonon at 1497 cm<sup>-1</sup> were observed. Moreover, it shows many bright photoluminescence (PL) peaks in an excitation-emission PL map. These new PL peaks can be assigned to emissions from (5,4) SWCNT oxides [2] that were produced in a dispersion process before the separation. These unusual optical properties and chemical reactivity were probably caused by the smallness of diameter, namely the curvature effect of (5,4) SWCNT.

This work was supported by JSPS KAKENHI grant number 25220602.

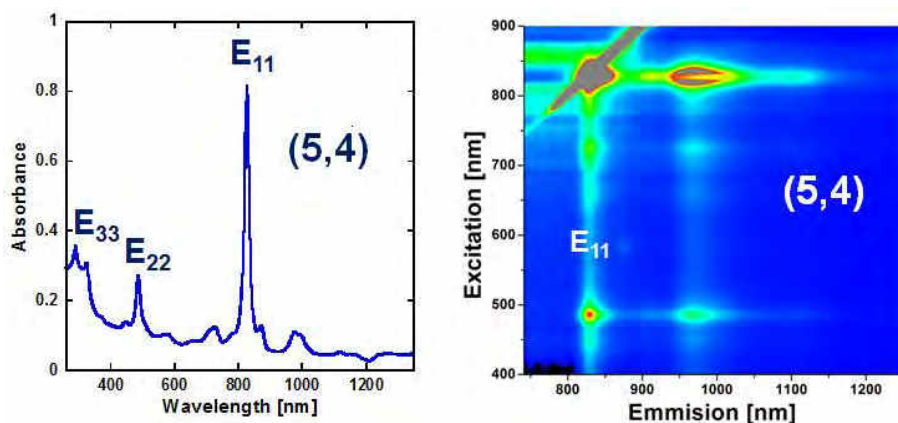


Figure 1. Optical absorption spectrum (left) and PLE map (right) of (5,4) single chirality SWCNTs.

### References

- [1] H. Liu et al. Nat. Commun., 2 (2011) 309.
- [2] Y. Miyauchi et al., Nat. Photonics 6, (2013) 2013547.

## SUPRAMOLECULAR ORGANIZATION OF $\pi$ -CONJUGATED MOLECULES MONITORED BY SINGLE-WALLED CARBON NANOTUBES

L. Alvarez<sup>1,2</sup>, R. Le Parc<sup>1,2</sup>, Y. Almadori<sup>1,2</sup>, P. Dieudonné-George<sup>1,2</sup>,  
R. Aznar<sup>1,2</sup>, B. Jousset<sup>3</sup>, S. Campidelli<sup>3</sup>, J. Cambedouzou<sup>4</sup>,  
F. Fossard<sup>5</sup>, A. Loiseau<sup>5</sup>, T. Saito<sup>6</sup>, and J-L. Bantignies<sup>1,2</sup>

<sup>1</sup>*Université Montpellier 2, Laboratoire Charles Coulomb UMR 5221, F-34095, Montpellier, France*

<sup>2</sup>*CNRS, Laboratoire Charles Coulomb UMR 5221, F-34095, Montpellier, France*

<sup>3</sup>*CEA-Saclay, IRAMIS, NIMBE, Laboratoire d'Innovation en Chimie des Surfaces et Nanosciences (LICSEN), 91191 Gif-sur-Yvette Cedex, France*

<sup>4</sup>*Institut de Chimie Séparative de Marcoule, UMR 5257,*

*CEA/CNRS/ENSCM/Université Montpellier 2, 30207 Bagnols sur Cèze, France*

<sup>5</sup>*Laboratoire d'étude des microstructures, CNRS-ONERA, 92322 Châtillon, France*

<sup>6</sup>*Nanotube Research Center, National Institute of Advanced Industrial Science and Technology (AIST), Tsukuba 305-8565, Japan'*

*Laurent.Alvarez@univ-montp2.fr*

New 1D hybrid nano-systems are elaborated with photo-active  $\pi$ -conjugated molecules (PAM) either encapsulated into the hollow core of single-wall carbon nanotubes or non-covalently functionalized at their outer surface. These nano-materials can display original opto-electronic properties as the chromophores exhibit tunable HOMO-LUMO levels by chemical engineering. Furthermore, the physical properties can be tuned by modifying the structural properties, providing practical routes to fit different requirements for potential applications. Thus, a proper understanding of the PAM supramolecular organizations driven by the host carbon nanotubes is particularly relevant.

In this study, we report some results obtained by functionalizing quathertiophene (4T) and phthalocyanine (Pc) molecules. The structural properties are investigated mainly by x-ray diffraction and/or Transmission Electron Microscopy and Raman spectroscopy. We evidence that the supramolecular organizations of confined oligothiophenes (from 1 to 3 chains into a nanotube section) depend on the nanocontainer size whereas phthalocyanine encapsulation leads the formation of a 1D-phase for which the angle between the molecule ring and the nanotubes axis is close to 32°. Confined Pc molecules display Raman spectra hardly altered with respect to the bulk phase, suggesting a rather weak interaction with the tubes. By contrast, the vibrational properties of the molecules functionalized at the outer surface of tubes display important modifications. We assume a significant curvature of the phthalocyanine induced by the interaction with the tube walls and a change of the central atom position within the molecular ring, in good agreement with our DFT calculations

## CARBON NANOTUBES PHOTONICS: ENHANCEMENT OF S-SWNT PL USING SILICON MICRORING RESONATORS

A. Noury, X. Le Roux, L. Vivien and N. Izard

*Institut d'Electronique Fondamentale, CNRS-UMR 8622, Univ. Paris Sud, Orsay,  
France  
nicolas.izard@u-psud.fr*

Semiconducting Single-Wall Carbon Nanotubes (s-SWNT) are an emerging material for nanophotonics, who have the ability to emit, modulate and detect light in the wavelength range of silicon transparency, and are a promising candidate for active devices in silicon photonics technology.

Few years ago, we have developed an efficient method to extract s-SWNT, using a polyfluorene (PFO) agent in toluene followed by ultracentrifugation steps, allowing obtention of quasi metallic-free s-SWNT samples [1]. PFO wrapped s-SWNT display strong photoluminescence, and an optical gain of  $160 \text{ cm}^{-1}$  was demonstrated in (8,7) nanotube at room temperature [2]. Therefore, it is particularly attractive to couple s-SWNT photoluminescence with optical resonators.

First results used planar cavities [3], but recent works took advantage of the Silicon-On-Insulator (SOI) platform to couple s-SWNT photoluminescence to photonic crystals cavities [4] or silicon microdisk resonators [5]. This approach have the advantage of integration with silicon photonics technology, even if it remains challenging to efficiently couple these structures with silicon waveguides. On the other hand, we recently proposed an integration scheme to couple s-SWNT photoluminescence to silicon waveguides, using evanescent wave from narrow waveguides [6].

We propose to go further by coupling s-SWNT with silicon microring resonators [7]. Sharp and regularly spaced resonance peaks are observed, superimposed to the s-SWNT broad emission peaks. The free spectral range could be easily tuned by adjusting the microring diameter, and the quality factor range from 3000 to 4000. This is among the highest value reported so far for integrated silicon microcavity coupled to carbon nanotubes, which opens bright perspectives for future carbon nanotube based photonics.

- [1] N. Izard *et al.*, Appl. Phys. Lett., **92**, 243112 (2008)
- [2] E. Gaufrès *et al.*, Appl. Phys. Lett., **96**, 231105 (2010)
- [3] E. Gaufrès *et al.*, Opt. Express, **18**, 5740 (2010)
- [4] R. Watahiki *et al.*, Appl. Phys. Lett., **101**, 141124 (2012)
- [5] S. Imamura *et al.*, Appl. Phys. Lett., **102**, 161102 (2013)
- [6] E. Gaufrès *et al.*, ACS Nano, **6**, 3813 (2012)
- [7] A. Noury *et al.*, Nanotechnology, **25**, 215201 (2014)

## COUPLED VIBRATIONS IN INDEX-IDENTIFIED CARBON NANOTUBES

Thierry Michel<sup>1</sup>, Dmitry Levshov<sup>1,2</sup>, Raul Arenal<sup>3</sup>, Matthieu Paillet<sup>1</sup>, Xuan Tinh Than<sup>1</sup>,  
Ahmed-Azmi Zahab<sup>1</sup>, Yuri Yuzyuk<sup>2</sup>, Jean-Louis Sauvajol<sup>1</sup>

*1 Laboratoire Charles Coulomb, University of Montpellier-CNRS, Montpellier, France.*

*2 Faculty of Physics, Southern Federal University, Rostov-on-Don, Russia*

*3 Laboratorio de Microscopias Avanzadas (LMA), Instituto de Nanociencia de Aragon (INA), Universidad de Zaragoza, Zaragoza, Spain.*

*Thierry.Michel@um2.fr*

Combined resonant Raman spectroscopy, high resolution transmission electron spectroscopy and electron diffraction experiments on the same suspended (free-standing) individual carbon nanotubes is an efficient method to determine unambiguously the intrinsic features of phonons in these nano systems.

In this talk, a special attention is focusing on multi-walled carbon nanotubes, mainly on double-walled carbon nanotubes, because they provide a unique model system for studying the role of the coupling between the layers on the phonons.

## OPTICAL SPECTRAL FEATURES OF CUCL@SWCNT HYBRIDES SYNTHESISED VIA GAS-PHASE TECHNIQUE

P. V. Fedotov<sup>1</sup>, A. A. Tonkikh<sup>1</sup>, E. D. Obraztsova<sup>1</sup>

<sup>1</sup> A.M. Prokhorov General Physics Institute, RAS, 38 Vavilov str., Moscow, Russia.  
fedotov@physics.msu.ru

Single-walled carbon nanotubes (SWCNTs) have unique electronic and optical properties which are attractive in various applications. These properties can be further improved by different functionalization techniques, for instance, by filling. In this work, we show that the filling nanotubes with CuCl leads to appearance of the specific optical features and also leads to the enhancement of their optical transmission properties up to outstanding level. The improvement of the transmission coefficient in a wide spectral range is due to the significant p-type doping of the functionalized nanotubes. Such doping leads to the huge increase of the nanotubes charge carrier density and the considerable decrease of the nanotubes absorption via Pauli blocking.

In our work the functionalization was realized via a gas-phase filling of single-walled carbon nanotubes with CuCl. We confirm that this technique is efficient for filling the nanotubes with different diameters (from 1.1 nm up to 2.2 nm) and leads to a much lower level of surface pollution comparing with the other techniques.

We demonstrate that the filling of SWCNTs with CuCl via a gas phase under certain conditions can lead to formation of CuCl@SWCNT hybrids. The optical absorption and Raman spectra of the nanotubes in such hybrid nanomaterial are substantially transformed (Fig. 1). The CuCl@SWCNT hybrids are observed to have a sufficient stability which is proved to be due to the formation of 1D CuCl crystal inside nanotubes. As in case of iodine filling [1], the specific optical features of the hybrids appear due to the formation of various CuCl 1D crystals inside nanotubes and due to the huge charge transfer between the nanotubes surface and the inner CuCl crystal structures [2,3].

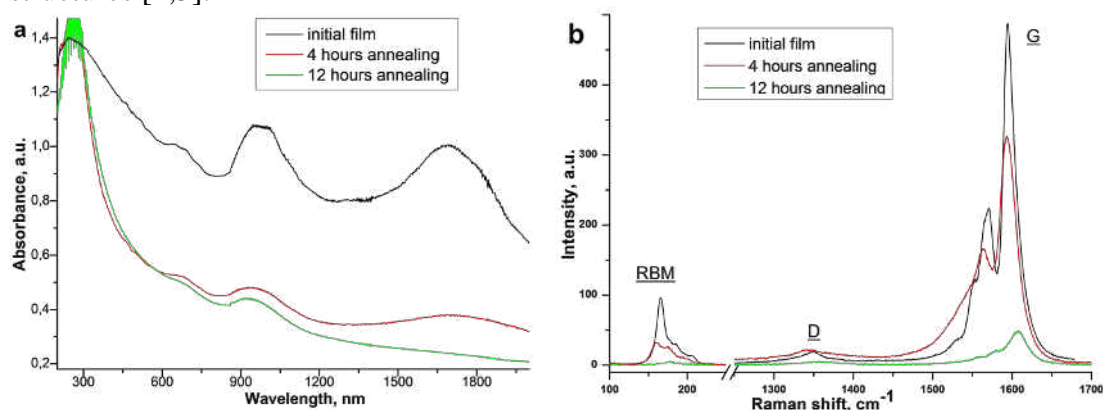


**Fig. 1** The absorption (a) and Raman (b) spectra of initial medium diameter (1.4 nm) SWCNT film and spectra of functionalized SWCNT films treated by CuCl vapour with different exposure times.

[1] A. A. Tonkikh, E. D. Obraztsova, et al., *Physica Status Solidi B* 249 (2012), 2454–2459.

[2] P. V. Fedotov, A. A. Tonkikh, et al., *Physica Status Solidi B* (2014) (*submitted*).

[3] E. D. Obraztsova, A. A. Tonkikh, P. V. Fedotov et al., Abstracts of International Conference "Nanotubes-2014", Los Angeles (USA), June 2014.

*The work is supported by RFBR projects 14-02-31829, 14-02-31818 and 13-02-01354.*

## PHOTO-STIMULATED FIELD EMISSION FROM INDIVIDUAL Si NANOWIRE

A. Derouet<sup>1</sup>, M. Choueib<sup>1,2</sup>, S. C. Cojocar<sup>3</sup>, A. Ayari<sup>1</sup>, P. Vincent<sup>2</sup>, P. Poncharal<sup>1</sup>, S. Perisanu<sup>1</sup>, R. Martel<sup>2</sup> and S. T. Purcell<sup>1</sup>

<sup>1</sup>*Institute Lumière Matière, UMR5306 CNRS, Université de Lyon 1, Villeurbanne, France*

<sup>2</sup>*Département de chimie, Université de Montréal, Montréal, Canada*

<sup>3</sup>*Laboratoire PICM, Ecole polytechnique, Palaiseau, France*  
*r.martel@umontreal.ca, stephen.purcell@univ-lyon1.fr*

There is currently a bound in research on time-modulated field emission (FE) electron sources that has been inspired by both recent high profile optical pulse and modulation experiments [1] and new demands in industry in RF amplifiers, electron microscopy, cathodo-luminescence lighting, accelerator physics, and devices for space applications [2]. As well, though both top down and bottom up silicon nanowires (SiNWs) have been heavily studied over the last decade or more for a wide variety of applications in nanoscience such as transistors, solar cells, photodectors, chemical sensors and nanomechanical systems [3], there has been much less work on their FE behavior even though their semiconducting properties open distinct possibilities compared to metallic and carbon nanotube emitters. In contrast to the exponentially increasing current common for metal emitters and predicted by the Fowler Nordheim theory, for properly controlled semiconducting emitters there can be strong current saturation as a function of applied voltage related to a field-induced depletion zone originating at the emitter apex. The current in the saturation region is highly sensitive to light and temperature, and this is more marked for more pronounced saturation. Here we show that SiNWs can serve as an excellent platform for exploring FE from semiconductors with the added advantage for future applications that they are mass produced.

In-depth FE studies are presented here of individual high quality SiNWs batch-grown by vapor-liquid-solid using Au catalysts with no intentional doping [4]. Extensive I-V, FE microscopy, FE energy spectroscopy and in particular constant and time modulated photo-assisted FE measurements were performed in UHV. Quasi-ideal saturation was found which allowed us to reveal several original FE phenomena such as the ability to vary the degree of saturation by *in situ* cycles of hydrogen passivation and thermal de-passivation [5] and a new double negative resistance in the FE IV characteristics.

[1] Hommelhoff and coworkers - PRL **97**, 247402 (2006), Nature **475**, 78 (2011), Ropers and coworkers - PRL **98**, 043907 (2007), PRL **105**, 147601 (2010), Nature **483**, 190 (2012), Yanagisawa and coworkers - PRL **103**, 257603 (2009), PRL **107**, 087601 (2011).

[2] Legagneux and coworkers, Nature **437**, 968 (2005).

[3] Cui, Y. and Lieber, C. M. Science, **291**, 851(2001); Huang, Y. et al. Science, **294**, 1313 (2001); Beckman, R. et al. Science, **310**, p 465–468 (2005); Patolsky, F. et al. Science, **313**, 1100–1104 (2006); Xiang, J. et al. Nature **441**, 489 (2006); Kelzenberg M. D. et al. Nat. Mater., **9**, 239 (2010).

[4] Lefeuvre E. et al. Thin Solid Films, **519**, 4603 (2011).

[5] Choueib, M. et al., ACS NANO **6**, 7463 (2012).

## FIELD ELECTRON EMISSION FROM SINGLE CRYSTAL DIAMOND NEEDLES

Kleshch V.I.<sup>1</sup>, Purcell S.T.<sup>2</sup>, Obraztsov A.N.<sup>1,3</sup>

<sup>1</sup> *Department of Physics, M. V. Lomonosov Moscow State University, Moscow, Russia*

<sup>2</sup> *Institute Lumière Matière, Université de Lyon 1, Villeurbanne, France*

<sup>3</sup> *Department of Physics and Mathematics, University of Eastern Finland, Joensuu, Finland*

*e-mail: klesch@polly.phys.msu.ru*

Single crystal diamond needles were produced by thermal oxidation of polycrystalline CVD diamond films [1]. Needles had a pyramidal shape with rectangular cross section with length of about 100  $\mu\text{m}$ , thickness at the base of 1  $\mu\text{m}$  and tip apex radius of 10 nm. Field electron emission (FE) measurements were performed using UHV system ( $4 \times 10^{-10}$  Torr) equipped with electron energy analyser [2].

Diamond needles demonstrated excellent stability of emission current in time up to 10  $\mu\text{A}$ . The FE current-voltage characteristics showed strong current saturation that is predicted by the basic theory of the electron emission from semiconductors. In the saturation region, the currents were extremely sensitive to temperature and increased by more than two orders of magnitude with changing of the temperature from 300 to 700 K. Using energy analyser, the total energy distribution (TED) of the emitted electrons was measured as a function of temperature and current. The position of the TED peak gives the voltage drop along the needle. Plotting the emitted current against the voltage drop is equivalent to a two point measurement of a current-voltage characteristic of the needle. This permitted the estimation of activation energy of the saturation current and definition of possible mechanisms of carrier transport.

Obtained results show that despite the large band gap of 5.5 eV of diamond, the needles obtained by thermal oxidation of polycrystalline CVD diamond films without intentional doping can be used as field emitters. Possible applications of diamond needles in vacuum electronics will be discussed.

[1] A. N. Obraztsov, P. G. Kopylov, A. L. Chuvilin, N. V. Savenko, *Diamond and Related Materials*, **18**, 1289 (2009).

[2] M. Choueib, A. Ayari, P. Vincent, M. Bechelany, D. Cornu, S. T. Purcell, *Phys. Rev. B*, **79**, 075421 (2009).

## MOLYBDENUM DISULFIDE COVERED CNT ARRAYS FOR ELECTROCHEMICAL APPLICATIONS

Koroteev Victor, Bulusheva L.G., Okotrub A.V.

*Nikolaev Institute of Inorganic Chemistry SB RAS, Novosibirsk, Russia*

*e-mail: koroteev@niic.nsc.ru*

Combination of low dimensional carbon nanostructures, possessing high electrical conductivity, with semiconducting nanoparticles allows creating new class of hybrid materials with outstanding properties for many applications. Molybdenum disulfide in combinations with carbon-based nanostructures could serve as perfect anode material for lithium storage [1,2]. Theoretical electrochemical capacity of carbon based materials is limited to 372 mAh/g, while the capacity of hybrids could reach 1000 mAh/g.

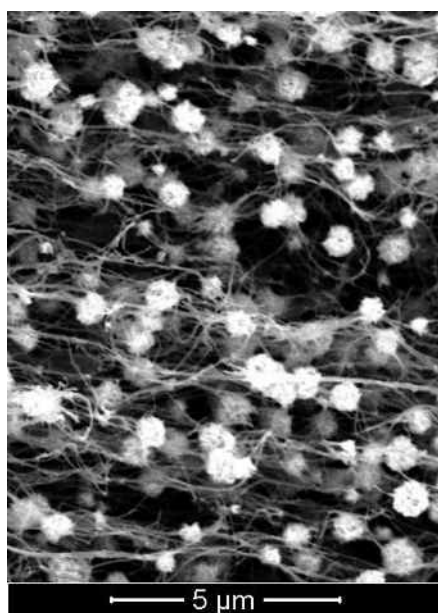


Fig. 1 SEM image of CNT nanotubes with MoS<sub>2</sub> spherical particles attached.

In this work, we develop the approach, which allows the production of carbon nanotube (CNT) arrays and MoS<sub>2</sub> hybrid materials for self-standing Li-battery anode materials. The method is based on postprocessing of CNT arrays produced by CVD. The arrays are treated by molybdates and sulfur containing compounds in autoclaves, which results in removal from silicon substrate and covering with molybdenum disulfide. Typical image of the materials after treatment is presented in fig. 1. MoS<sub>2</sub> spheres are pierced by CNT's, which provide easy electron transport during charge-discharge process, high availability of the particles to electrolyte and mechanical stability.

Materials obtained were studied using Raman spectroscopy, scanning and transmission electron microscopy and x-ray photoelectron spectroscopy, obtaining information about the structure and composition. Li-intercalation study shows that obtained materials perform better than currently available carbon anode materials.

This work was financially supported by the Russian Foundation of Basic Research grant No. 14-03-31633.

[1] Chang K., Chen W., Ma L., Li H., Li H., Huang F., Xu Z., Zhang Q. and Lee J.-Y., *J. Mater. Chem.* **21**, 6251 (2011). DOI: 10.1039/C1JM10174A

[2] Huang G., Chen T., Chen W., Wang Z., Chang K., Ma L.; Huang F., Chen, D. and Lee J.Y., *Small* **9**, 3693 (2013). DOI: 10.1002/sml.201300415



## SIMULATION OF ELECTROMAGNETIC PROPERTIES IN CNTs- AND GRAPHENE-BASED NANOMATERIALS AND NANODEVICES

Yuri Shunin<sup>1,2</sup>, Yuri Zhukovskii<sup>1</sup>, Victor Gopeyenko<sup>2</sup>, Nataly Burluckaya<sup>2</sup>,  
Tamara Lobanova-Shunina<sup>3</sup>, and Stefano Bellucci<sup>4</sup>

<sup>1</sup>*Institute of Solid State Physics, University of Latvia, Latvia*

<sup>2</sup>*Information Systems Management Institute, Latvia*

<sup>3</sup>*Riga Technical University, Aviation Institute, Latvia*

<sup>4</sup>*INFN - Laboratori Nazionali di Frascati, Frascati (Rome), Italy*

Electromagnetic and electromechanical properties of CNTs, graphene nanoribbons (GNRs) and nanofibers (GNFs), CNT- and graphene-based aerogels (CNTBA, GBA), CNT- and graphene-based 3D-nanofoams and carbon-based polymer nanocomposites are critical for various nanotechnology applications, e.g. for engineering of new ultra-light, highly conductive nanomaterials with exceptional mechanical strength, flexibility, and elasticity. These nanomaterials are fundamental for unique nanoelectronic devices and nanosensors [1]. Particular properties of carbon-based nanoporous systems in dependence on porosity extent, morphology and fractal dimension allow finding practically useful correlations between their mechanical and electrical properties.

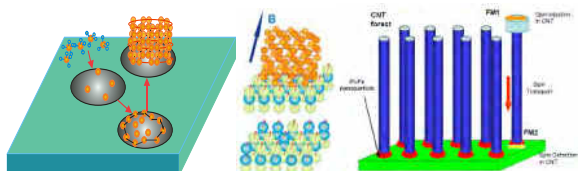


**Fig.1.** Model of CNTs growth in a magnetically controlled CVD process based on Fe-Pt nanodrops catalysts

The model of CNTs growth with the predefined chiralities in a magnetically managed CVD process with the use of magnetically anisotropic  $\text{Fe}_x\text{Pt}_{1-x}$  nanoparticles with various substitutional disorders has been developed (see Fig.1). The model and magnetically controlled conditions, stimulating the CNT growth in a CVD process, aim at the predictable SWCNT diameter and chirality. Quantum chemical and electromagnetic properties of C-Pt-Fe (L10) catalyst interconnects are discussed. The possibilities of CNT forest growth based on FePt nanoparticles for magnetic nanomemory are also evaluated [2].

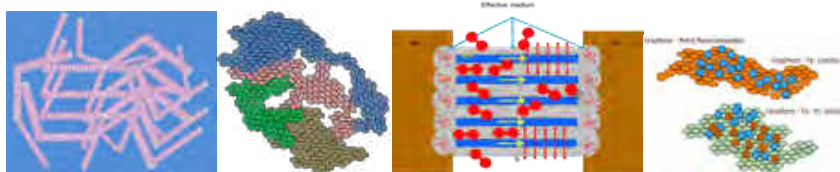


**Fig.2.** A set of simulation models: a) Structural model of CNTBA b) Structural model of GBA; c) GNRs based nanosensor device; d) Graphene-metal nanocomposites- Fe and Fe-Pt coatings

Nanoporous systems are considered as complicated ensembles of basic nanocarbon interconnected elements (e.g., CNTs or GNRs with defects and dangling boundary bonds) within the effective media type environment (see Fig.2). Interconnects are essentially local quantum objects and are evaluated in the framework of the developed cluster approach based on the multiple scattering theory formalism as well as effective medium approximation [3], which allows calculating local electronic densities of states, conductivity, force interaction constants, etc., for the above mentioned nanosized systems.

[1] Shunin Yu N, Zhukovskii Yu F, Gopeyenko V I, Burlutsckaya N, Bellucci S 2012 *Journal of Nanophotonics* **6**(1) 061706-1-16

[2] Shunin Yu N, Bellucci S, Zhukovskii Yu F, Gopeyenko V I, Burlutsckaya N, Lobanova-Shunina T, Capobianchi A, Micciulla F 2014 *Computer Modelling & New Technologies* **18**(2) 7-23

[3] Shunin Yu N, Zhukovskii Yu F, Gopeyenko V I, Burlutsckaya N, Bellucci S 2012 ed Yu Shunin and A Kiv *Nanodevices and Nanomaterials for Ecological Security Series: Nato Science for Peace Series B - Physics and Biophysics* Dodrecht: Springer Verlag 237-262

## CALCULATION OF OPTICAL NONLINEARITIES IN GRAPHENE

J.E. Sipe<sup>1</sup>, JinLuo Cheng<sup>1,2</sup>, and Nathalie Vermeulen<sup>2</sup>

<sup>1</sup>*Department of Physics and Institute for Optical Sciences,  
60 St. George St., Toronto, ON M5S 1A7 CANADA*

<sup>2</sup>*Brussels Photonics Team (B-PHOT), Department of Applied Physics and Photonics  
(IR-TONA), Vrije Universiteit Brussel, Pleinlaan 2, B-1050 Brussel, Belgium*

We present the results of perturbative calculations of the third order optical conductivities of doped graphene, using approximations valid around the Dirac points. In an initial set of calculations we neglect effects due to scattering and electron-electron interactions, and restrict ourselves to zero temperature [1]. In a second set we include interband and intraband relaxation phenomenologically through the inclusion of appropriate relaxation times [2]. Even with the relaxation times included, at zero temperature analytic formulas can be constructed for the conductivities. The effects of finite temperature can be included by an appropriate integration over the chemical potential in the zero temperature results.

The third order effects fall into a number of categories: Third harmonic generation is perhaps the simplest and often the easiest to use to characterize the third order response. The Kerr effect and the two-photon absorption that is associated with it are the main contributions to nonlinear propagation effects. Parametric frequency conversion terms describe the mixing of incident frequencies to yield new frequencies. Two-color coherent control terms describe the interference between one- and two-photon process, leading to the optical injection of currents. Current-induced second harmonic generation describes how the breaking of inversion symmetry due to a current driven by an imposed DC field can lead to the generation of light at double the incident frequency [3].

We review the theoretical predictions for all these phenomena, compare with experimental data where possible, discuss possible reasons for discrepancies, and consider the possibilities for novel nonlinear optics in graphene and graphene-based structures.

[1] J.L. Cheng, Nathalie Vermeulen, and J.E. Sipe, *New Journal of Physics* **16** 053014 (2014).

[2] J.L. Cheng, Nathalie Vermeulen, and J.E. Sipe (in preparation).

[3] J.L. Cheng, Nathalie Vermeulen, and J.E. Sipe, *Optics Express* (in press).

### Acknowledgements

This work has been supported by the EU-FET grant GRAPHENICS (618086), by FWOVlaanderen which provides funding through the FWO project G.A002.13N and the Postdoctoraal Onderzoeker grant for N Vermeulen, by the Natural Sciences and Engineering Research Council of Canada, by VUB-Methusalem, VUB-OZR, and IAP-BELSPO under grant IAP P7-35.

## SINGLE-CARBON-NANOTUBE DEVICES FOR INTEGRATED PHOTONICS

Yuichiro K. Kato

*Institute of Engineering Innovation, The University of Tokyo, Tokyo 113-8656, Japan  
ykato@sogo.t.u-tokyo.ac.jp*

Single-walled carbon nanotubes have unique optical properties as a result of their one-dimensional structure. Not only do they exhibit strong polarization for both absorption and emission, large exciton binding energies allow for room-temperature excitonic luminescence. Furthermore, their emission is in the telecom-wavelengths and they can be directly synthesized on silicon substrates, providing new opportunities for nanoscale integrated photonics.

Here we discuss the use of individual single-walled carbon nanotubes for optical devices that could be integrated in silicon photonics. Their light emission properties can be controlled by coupling to silicon photonic structures such as photonic crystal microcavities [1,2] and microdisk resonators [3]. With the strong absorption polarization at the nanoscale, they allow for unconventional polarization conversion that results in giant circular dichroism [4]. More recently, we have found that excitons can dissociate spontaneously [5], enabling photodetection at low bias voltages. Ultimately, it should be possible to combine these results to achieve generation, manipulation, and detection of photons on a chip.

Work supported by SCOPE, KAKENHI, The Canon Foundation, The Asahi Glass Foundation, KDDI Foundation, and the Photon Frontier Network Program of MEXT, Japan. The devices were fabricated at the Center for Nano Lithography & Analysis at The University of Tokyo.

- [1] R. Watahiki, T. Shimada, P. Zhao, S. Chiashi, S. Iwamoto, Y. Arakawa, S. Maruyama, Y. K. Kato, *Appl. Phys. Lett.* **101**, 141124 (2012).
- [2] R. Miura, S. Imamura, R. Ohta, A. Ishii, X. Liu, T. Shimada, S. Iwamoto, Y. Arakawa, Y. K. Kato, submitted.
- [3] S. Imamura, R. Watahiki, R. Miura, T. Shimada, Y. K. Kato, *Appl. Phys. Lett.* **102**, 161102 (2013).
- [4] A. Yokoyama, M. Yoshida, A. Ishii, Y. K. Kato, *Phys. Rev. X* **4**, 011005 (2014).
- [5] Y. Kumamoto, M. Yoshida, A. Yokoyama, T. Shimada, Y. K. Kato, *Phys. Rev. Lett.*, **112**, 117401 (2014).

## CHIP-INTEGRATED GRAPHENE OPTOELECTRONIC DEVICES

Xuetao Gan<sup>1,2</sup>, Ren-Jye Shiue<sup>2,3</sup>, Kin Fai Mak<sup>4</sup>, Tony F. Heinz<sup>2,4</sup>, Dirk Englund<sup>2,3</sup>

1. School of Science, Northwestern Polytechnical University, Xi'an 710072, China

2. Department of Electrical Engineering, Columbia University, New York, 10027, USA

3. Department of Electrical Engineering and Computer Science, Massachusetts Institute of Technology, Cambridge, MA 02139, USA

4. Department of Physics, Columbia University, New York, NY 10027, USA

xuetaogan@gmail.com

Graphene has attracted great interest in the development of optoelectronic devices due to its broadband optical response, ultrahigh carrier mobility, and potentially CMOS-compatible. Here, we present our recent work on graphene modulators and photodetectors integrated on silicon photonic crystal cavities and channel waveguides.

By electrically gating a graphene monolayer coupled with a planar photonic crystal cavity, electro-optic modulation of the cavity reflection was possible with a contrast in excess of 10 dB and a switching energy of 300fJ, as shown in Fig. 1(a) [1]. Moreover, a novel modulator device based on the cavity-coupled graphene-boron nitride-graphene capacitor was fabricated, showing a modulation speed up to 1.2 GHz [2]. A cavity-coupled graphene photodetector was also demonstrated with an enhancement of the photocurrent by a factor of 26 at resonant wavelengths [3].

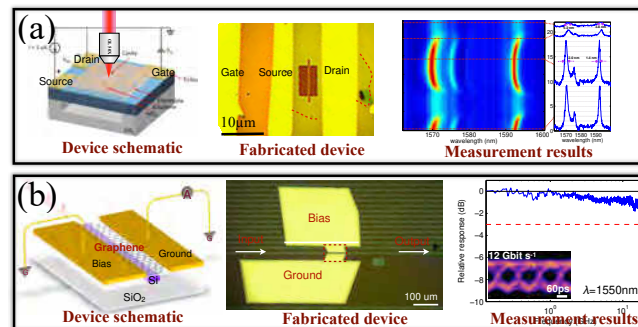


Fig. 1. (a) Graphene modulator integrated on photonic crystal cavity; (b) Graphene photodetector integrated on silicon waveguide.

A waveguide-integrated graphene photodetector that simultaneously exhibits high responsivity, high speed and broad spectral bandwidth has also been reported, as shown in Fig. 1(b) [4]. Using a metal-doped graphene junction coupled evanescently to the waveguide, the detector achieves a photoresponsivity exceeding 0.1 A/W together with a nearly uniform response between 1,450 and 1,590 nm. Under zero-bias operation, a response rate exceeding 20 GHz and an instrumentation-limited 12 Gbit/s optical data link. The demonstrated graphene active devices indicate a new generation of compact, energy-efficient, and ultrafast optoelectronics for on-chip optical communications.

- [1]. X. Gan, R. Shiue, Y. Gao, K. F. Mak, X. Yao, L. Li, A. Szep, D. Walker, J. Hone, T. F. Heinz, and D. Englund, *Nano Lett.* **13**, 691 (2013).
- [2]. X. Gan, R. Shiue, Y. Gao, S. Assefa, J. Hone, and D. Englund, *IEEE, J. Sele. Top. Quant. Electron.* **20**, 6000311 (2014).
- [3]. R. Shiue, X. Gan, Y. Gao, L. Li, X. Yao, A. Szep, D. Walker, J. Hone, D. Englund, *Appl. Phys. Lett.* **103**, 241109 (2013).
- [4]. X. Gan, R. Shiue, Y. Gao, I. Meric, T. F. Heinz, K. Shepard, J. Hone, S. Assefa, and D. Englund, *Nature Photon.* **7**, 883 (2013).



## Poster session II





## EXPERIMENTAL STUDY AND COMPUTER SIMULATION OF THE GROWTH OF SINGLE-CRYSTAL DIAMOND MICRONEEDLES

A. M. Alexeev<sup>1</sup>, F. T. Tuyakova<sup>2,3</sup>, R. R. Ismagilov<sup>1</sup>, A. N. Obraztsov<sup>1,2</sup>

<sup>1</sup>*Department of Physics, Lomonosov Moscow State University, Moscow, Russia*

<sup>2</sup>*Department of Physics and Mathematics, University of Eastern Finland, Joensuu, Finland*

<sup>3</sup>*Moscow State Institute of Radio Engineering, Electronics and Automation, Moscow, Russia;*

*am.alekseev@physics.msu.ru*

Single-crystal diamond microneedles were extracted from (001) textured polycrystalline films. The films were produced using a plasma enhanced chemical vapour deposition (CVD) from a CH<sub>4</sub>/H<sub>2</sub> gas mixture activated by a direct current discharge. The as-grown textured polycrystalline CVD films consist of pyramid-shaped micrometer size diamond crystallites embedded into a nanodiamond ballas-like material. The less ordered fraction of the CVD film material was removed selectively using thermal oxidation. A dependence of the diamond needle shape on the CVD and the oxidation process parameters was revealed via a computer simulation and experimental studies. Ability for mass production of the diamond microneedles of different shapes was demonstrated. The needles are suitable for various applications from microcutting tools to quantum information processing.

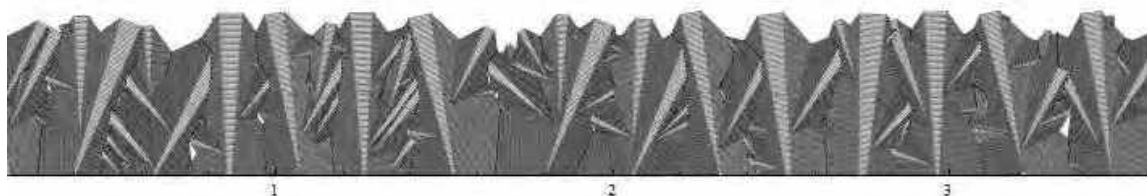


Fig. 1. Schematic image resulting from computer simulation of the process of film growth



## **SYNTHESIS OF LARGE AREA CARBON NANOTUBE ARRAYS ON Cu SUBSTRATE FOR FIELD EMISSION CATHODES**

V. Arkhipov<sup>1</sup>, A. Guselnikov<sup>1</sup>, L. Bulusheva<sup>1</sup>, A. Okotrub<sup>1\*</sup>,  
V. Baryshevsky<sup>2</sup>, P. Kuzhir<sup>2</sup>, S. Maksimenko<sup>2</sup>

<sup>1</sup>*Nikolaev Institute of Inorganic Chemistry SB RAS, 6303090, Novosibirsk, Russia*

<sup>2</sup>*Research Institute for Nuclear Problems, Belarusian State University,  
Bobruiskaya Str. 11, Minsk, 220030, Belarus*

*\*e-mail: spectrum@niic.nsc.ru*

Field-emission cathodes based on oriented carbon nanotubes (CNT) have the prospect for application in devices operating powerful electron fluxes. Aerosol-assisted CVD method is used for the synthesis of CNT arrays on flat substrates with area more than 500 cm<sup>2</sup>. Improve the stability of field emission cathodes was achieved by their synthesis on pre-treated copper substrates. Optimization of the synthesis conditions and parameters of the reaction mixture, temperature and gas flow to synthesize the CNT cathodes consisting of a predetermined length and density. Good adhesion of the CNT array to copper substrate was obtained.

Arrays of aligned multi-walled carbon nanotubes (MWCNT), being 120 micron in length, have been investigated as a working surface of Cu cathode for explosive electron emission. In the diode configuration, we demonstrated the current density as high as 300 A/cm<sup>2</sup> under applied voltage below 400 kV for CNT/copper cathodes with diameter of 50 nm. The Raman measurements reveal that MWCNTs remain structurally the same but just shorter after 21 shoots.

## LASER SYNTHESIS OF 1D POLYNYNIC CARBON CHAINS

N.R. Arutyunyan<sup>1,2</sup>, V.V. Kononenko<sup>1</sup>, E.D. Obraztsova<sup>1,2</sup>

<sup>1</sup>A.M.Prokhorov General Physics Institute, Vavilov 38, 119991 Moscow, Russia

<sup>2</sup>National Research Nuclear University "MEPhI", Kashirskoe sh. 31, 115409 Moscow, Russia

*e-mail: 81natalie@gmail.com*

The first successful attempts of synthesis of one-dimensional carbon chains  $C_{2n}H_2$  (so called carbyne, its chemical structure is shown in Fig.1) were made in the middle of 20<sup>th</sup> century by the group, headed by Dr Sladkov [1]. However, the obtained molecules demonstrated a low stability and a tendency to form chemical bonds between carbon chains, which led to cluster formation. Recently, a method of carbyne synthesis via laser ablation of graphite was proposed [2].

Here, the results on femtosecond laser formation of polyynic chains are presented. To reduce the oxidation and degradation of carbon chains, the synthesis was performed in liquid media. The flakes of graphite were suspended in water and ultrasonicated to obtain a homogeneous suspension of sub-micron graphite particles. This suspension was irradiated by pulses of a Ti:sapph laser. The wavelength of irradiation was 800 nm, with repetition rate 1 kHz and pulse duration 100 fs. The laser beam was focused into the quartz cell.

The threshold of the light intensity in the beam waist for the formation of carbyne was estimated. The intensity value  $4 \cdot 10^{10}$  W/cm<sup>2</sup> was not sufficient for the synthesis of carbon chains, while at  $2 \cdot 10^{11}$  W/cm<sup>2</sup> linear polyynic molecules of various length were produced. The typical optical absorption spectrum of the irradiated graphite suspension is shown in Fig.2. The spectral lines at 189, 199, 215, 225, 262, 276 nm are clearly distinguished. They are attributed to the absorption of the polyynic carbon chains  $C_nH_2$  [3], where  $n = 2 \dots 12$ .



Fig. 1. Chemical structure of polyynic carbon chain.

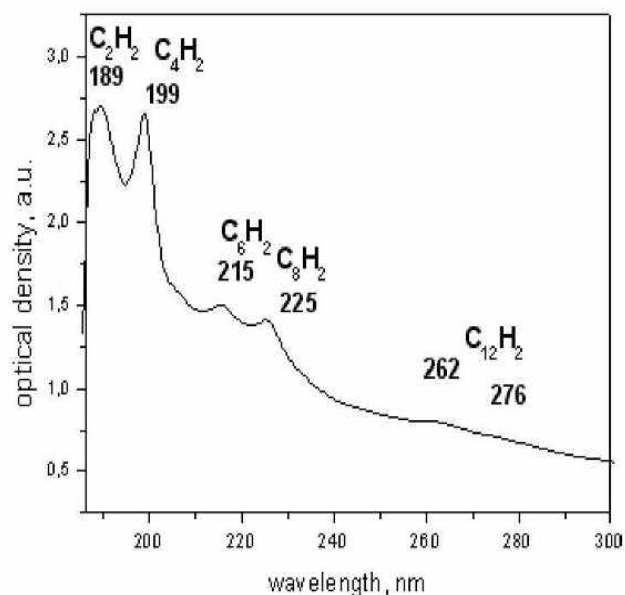


Fig.2. Optical absorption spectrum of the aqueous suspension of polyynic carbon chains.

The stability of the synthesized 1D carbon chains was defined basing on the intensity of the optical absorption bands, and its lifetime was estimated to be 24 hours at 20°C.

[1] A.M.Sladkov, Yu. P. Kudryavtsev, Priroda, **5**, 37 (1969).

[2] M. Tsuji, T. Tsuji, S. Kuboyama et al., ChemPhys Lett, **355**, 101 (2002).

[3] B. D. Anderson and C.M. Gordon, Journal of chemical education, **85** (2008).

## THE SEPARATION OF SINGLE-WALLED CARBON NANOTUBES SYNTHESIZED BY ARC DISCHARGE TECHNIQUE BY TYPE OF CONDUCTIVITY

V. A. Eremina<sup>1,2</sup>, P. V. Fedotov<sup>2</sup>, E. D. Obraztsova<sup>1,2</sup>

<sup>1</sup>Physics Department of M.V. Lomonosov Moscow State University, Moscow, Russia

<sup>2</sup>A.M.Prokhorov General Physics Institute, RAS, Moscow, Russia

erjomina@physics.msu.ru

The existing methods for growing single-walled carbon nanotubes (SWNTs) produce samples with a wide range of structures and electronic properties, but many fundamental and technological applications of SWNTs require nanotube samples with a defined geometry. A number of methods can provide almost single chirality or conductivity separation. Among them there are a gradient density ultracentrifugation, a gel chromatography and other. Recently, a new method has been introduced which provides an easily accessible separation of single-walled carbon nanotubes. An aqueous two-phase separation method is based on formation of two phases (by two polymers - polyethylene glycol and dextran) – top and bottom ones, containing solely metallic or semiconducting nanotubes.

In this work the separation of single-walled carbon nanotubes synthesized by arc discharge technique by type of conductivity has been studied. A well separation of top and bottom phases has been reached by adjusting the concentrations of polymers and surfactants (SDS and SC) (Fig.1). The top phase predominantly contains semiconducting nanotubes and the bottom phase – metallic ones. This can be seen in the absorption spectra in Fig. 2. These fractions will be subsequently used to produce films for optical studies and technological applications.



Fig.1 Photo of top (left) and bottom (right) phases.

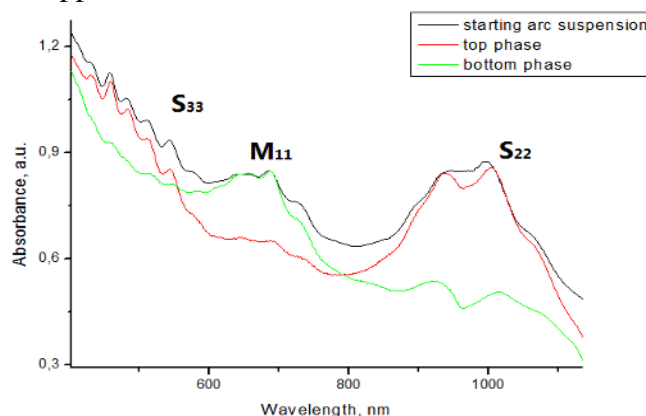


Fig. 2 Absorption spectra of starting arc suspension (black), top phase (red) and bottom phase (green). Spectra were rescaled for easy comparison.

The work is supported by RFBR-13-02-01354. 14-02-31829 and RAS research programs.

[1] Constantine Y Khripin, Jeffrey A. Fagan, and Ming Zheng. *JACS* (2013)

[2] Jeffrey A. Fagan, Constantine Y. Khripin, Carlos A. Silvera Batista, Jeffrey R. Simpson, Erik H. Hároz, Angela R. Hight Walker, and Ming Zheng. *Adv. Mater.* (2014)

## HOT FILAMENT CHEMICAL VAPOR DEPOSITION OF NANOGRAPHITE FILMS

D.I. Finkelstein<sup>1</sup>, A. M. Alexeev<sup>1</sup>, F. T. Tuyakova<sup>2,3</sup>, R. R. Ismagilov<sup>1</sup>,  
A. N. Obraztsov<sup>1,2</sup>

<sup>1</sup>*Department of Physics, Lomonosov Moscow State University, Moscow, Russia*

<sup>2</sup>*Department of Physics and Mathematics, University of Eastern Finland, Joensuu, Finland*

<sup>3</sup>*Moscow State Institute of Radio Engineering, Electronics and Automation, Moscow, Russia;*

*f.davidm@gmail.com*

Nanomaterials with graphite like structures were produced using a Hot Filament Chemical Vapor Deposition (HFCVD) technique. Parameters of the HFCVD process were adjusted to provide carbon condensation from the activated methane-hydrogen gas mixture in form of nanocarbon films with predominantly graphite-type atomic structure. Structural and morphological characteristics of the nanocarbon films were obtained by Raman spectroscopy and scanning electron microscopy (SEM).

The effect of growth parameters and substrate material on characteristics of produced nanocarbon materials was experimentally investigated. Carbon nanostructures of new type were obtained on stainless steel and carbon cloth substrates. Possible formation mechanism of these structures are discussed.

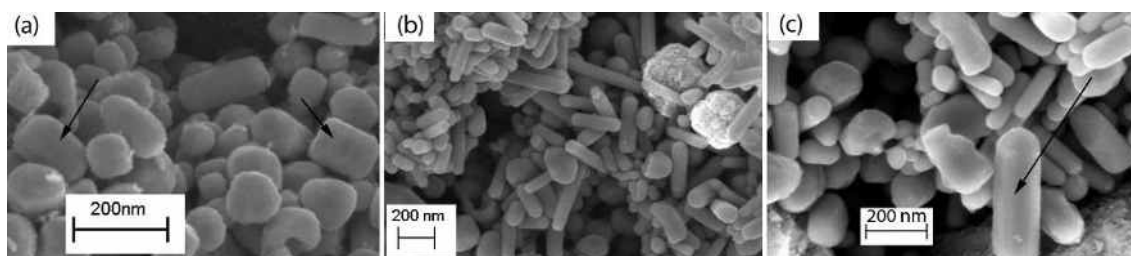


Fig. 1. SEM images of graphite-like capsules deposited on stainless steel. The visible edges of faceted structures are indicated by arrows

## COMPUTER SIMULATION OF SPATIAL-TEMPORAL BEHAVIOUR OF ACTIVE SPECIES IN AN ATMOSPHERIC-PRESSURE DIELECTRIC BARRIER DISCHARGE

R. R. Ismagilov<sup>1</sup>, A. M. Alexeev<sup>1</sup>, F. T. Tuyakova<sup>2,3</sup>, Kuo-Hui Yang<sup>4</sup>,  
A. N. Obraztsov<sup>1,2</sup>

<sup>1</sup>*Department of Physics, Lomonosov Moscow State University, Moscow, Russia*

<sup>2</sup>*Department of Physics and Mathematics, University of Eastern Finland, Joensuu, Finland*

<sup>3</sup>*Moscow State Institute of Radio Engineering, Electronics and Automation, Moscow, Russia;*

<sup>4</sup>*Mechanical and Systems Research Laboratories (MSL), Industrial Technology Research Institute (ITRI), Hsinchu, Taiwan*

*ismagil@polly.phys.msu.ru*

The spatial and temporal behaviors of the activated gas species in ignition region (Dielectric Barrier Discharge (DBD) area) of the plasma jet deposition system were studied with use of a computer simulation. Simulation was conducted for axisymmetric 2D model and Ar diluted gas mixture at atmospheric pressure, activated by electric discharge. Spatial evolution processes of electron density, active species concentration and temperature distribution are investigated. Characteristics of the discharge system in case of applying sinusoidal potential are studied for further understanding and optimization of the DBD jet systems.

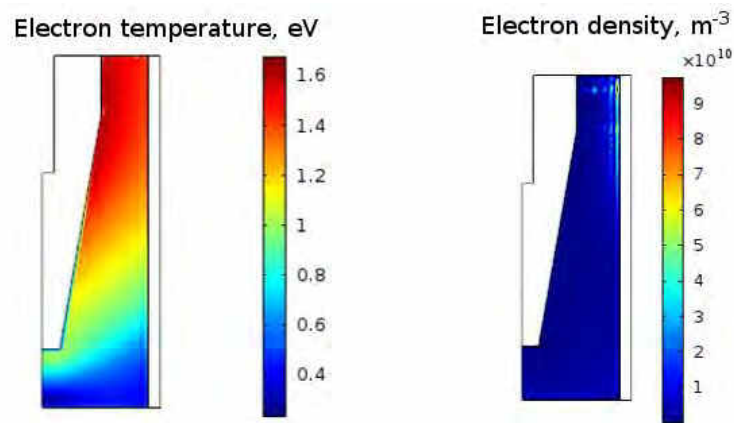


Fig. 1. Typical electron temperature (left) and electron density (right) distributions in activated Ar in case when electric potential equals to 750V and -750V, correspondingly.

## PROPERTIES OF GAS SENSORS BASED ON GRAPHENE AND SINGLE-WALL CARBON NANOTUBES

I.I. Kondrashov<sup>1</sup>, P.S. Rusakov<sup>1</sup>, M.G. Rybin<sup>1</sup>, I.V. Sokolov<sup>1</sup>, A.S. Pozharov<sup>1</sup>,  
R.N. Rizakhanov<sup>2</sup> and E.D. Obraztsova<sup>1</sup>

<sup>1</sup> *A.M. Prokhorov General Physics Institute, Vavilov str. 38, Moscow, Russia, 119991*

<sup>2</sup> *Keldysh Research Center, Moscow, Russia*  
[navi.soul@gmail.com](mailto:navi.soul@gmail.com)

Last years, gas sensors are attracting a tremendous interest because of their widespread applications in industry, environmental monitoring, space exploration, biomedicine, and pharmaceuticals. Depending on gas atmosphere composition the various types of gas sensors are required. The chemical adsorption sensor is the most widely used configuration of gas sensors because of their relatively high compactness, sensitivity and energy efficiency. The adsorption of gases on the active element surface of the adsorption sensor changes its electrical resistance due to the donor or acceptor mechanism for redistributing electrons in the surface layer. An extremely high surface-to-volume ratio and a hollow structure of carbon nanomaterials, such as nanocrystalline and microcrystalline graphite, single-walled or multi-walled nanotubes, fullerenes and graphene, is ideal for gas molecules adsorption and storage. Single-walled carbon nanotubes (SWCNT) and graphene are considered as the most promising materials due to their most pronounced adsorption ability and sensitivity.

In this work we present the detailed investigation of the influence of various gases on the sensory properties of the graphene and SWCNT films. The performance of gas sensor was measured by using a relevant apparatus to obtain the continuous sensor electric resistance change on exposure to different gases and air atmosphere at room temperature. We observed different reactions of the sensor depending on the donor or acceptor mechanism for redistribution of electrons between the gas used and the sensor surface. A good selectivity is very important for leakage detections of explosive gases, and for a real-time detection of toxic or pathogenic gases in industries. It can be achieved via usage of several different sensors at the same time, allowing to determine changes in the gaseous atmosphere composition with a good accuracy.

*The work is supported by RFBR-14-02-31639 grant, project N 611/13 with Keldysh Research Center and RAS research programs.*

## BORON NITRIDE SYNTHESIS IN AFTERGLOW PHASE OF A DISCHARGE IN MOLYBDENUM-DIELECTRIC POWDER

Konchekov E.M., Batanov G.M., Borzosekov V.D., Kharchev N.K., Kolik L.V., Letunov A.A., Malakhov D.V., Milovich F.O., Obratsova E.A., Obratsova E.D., Petrov A.E., Sarkisian K.A., Skvortsova N.N., Stepakhin V.D.  
*Prokhorov General Physics Institute of Russian Academy of Sciences, Russia, 119991, Moscow, Vavilov Str., 38*  
*konchekov@fpl.gpi.ru*

In the paper a synthesis of hexagonal boron nitride (NB) particles is presented. The synthesis occurs at the afterglow phase of discharge that is initiated by gyrotron radiation in molybdenum-dielectric powder mixtures [1,2]. The NB needle and scales structures of micro and nano sizes in the deposited material were found (Fig. 1).

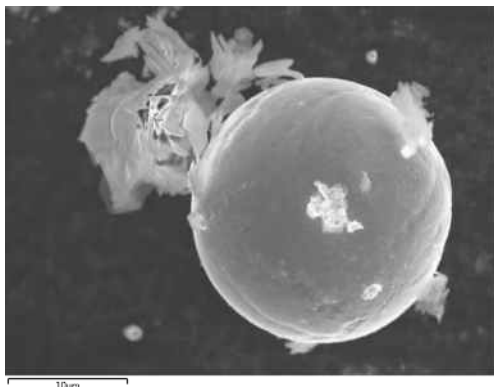


Fig. 1. Molybdenum diboride particle and boron nitride scales

The temperature evolution in several spatial regions of the discharge is also considered. In the initial discharge phase the temperature reaches 5—9 kK on the powder surface and 10—11 kK in the plasma. In some combinations of the mixture components the discharge proceeds to afterglow phase that is characterized by glow duration of tens times longer than gyrotron pulse duration.

It was found that for NB structures synthesis the discharge afterglow phase is required. In this case, at the discharge initial stage in Mo-NB powder the decay and oxidation of the amorphous boron nitride occurs. Then by chemical and plasma-chemical reactions in gas the BN particles (molecules) are synthesized with following quenching via propagation in the reactor volume and deposition on its surfaces.

This study was supported by the Russian Foundation for Basic Research (projects no. 14\_07\_00753\_a and 14\_07\_31278)

[1] G. M. Batanov, N. K. Berezhetskaya, V.D. Borzosekov et al., *JNO*, **8**, 58 (2013).

[2] G. M. Batanov, N. K. Berezhetskaya, V. D. Borzosekov et al., *Third International Workshop "Nanocarbon Photonics and Optoelectronics"*, (Finland, Polvijarvi, 2012)

## SEMIINSULATING 6H-SiC SUBSTRATE FOR GRAPHEN GROWTH.

Lebedev A.A.<sup>1</sup>, Agrinskaya N.V.<sup>1</sup>, Berezovets<sup>1,3</sup>, Lebedev S.P.<sup>1</sup>, Litvin D.P.<sup>1,2</sup>,

Vasil'ev A.V.<sup>2</sup>, Makarov Yu.N.<sup>2</sup>, Nagaluk S.S.<sup>2</sup>, Smirnov A.N.<sup>1</sup>,

<sup>1</sup>*A.F.Ioffe Institute, 194021, St.Petersburg, Polytekhnicheskaya 26 Russia*

<sup>2</sup>*Nitride Crystals Group, 194156 St.Petersburg, Engel'sa pr., 27, Russia*

<sup>3</sup>*International Laboratory of High Magnetic Fields and Low Temperatures, 95 Gajowicka str. 53421 Wroclaw, Poland*

*Shura.lebe@mail.ioffe.ru*

It was develop technology for production of semi-insulating 6H-SiC substrates . It was shown that substrate grown by its parameters are not inferior to similar substrates produced by leading world companies. This substrates were used for formation of graphene layer by sublimation in vacuum. Graphene was synthesized on mechanically polished substrates subjected to a pregrowth thermal treatment at 1300-1400 °C. The annealing modified the surface of a starting substrate: as a result of annealing, defects induced by mechanical polishing were eliminated and atomically smooth steps with height of a unit cell of the 6H polytype were formed ( Fig.1). To obtain graphene layers, samples were again annealed, now in a open growth cell in a high-vacuum chamber at temperatures of 1400--1500°C. After the growth structures of the Hall bar geometry were formed on the graphene film

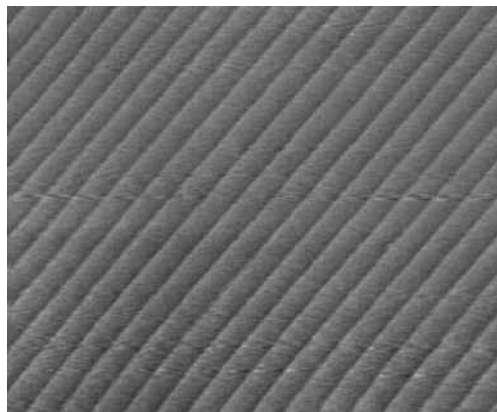


Fig.1 AFM topograph of the SiC surface after its pre-growth annealing.

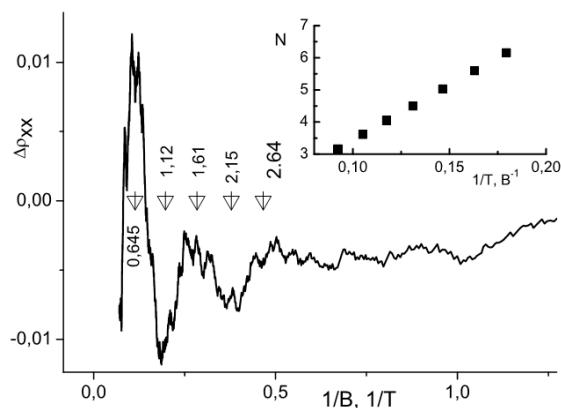


Figure 2. A curve of MR in the scale of inverse magnetic fields. The insert gives the Landau numbers as a function of the positions of SdH maxima for the oscillations of the second type.

Transport properties of grown graphene layers were studied in wide temperature range. It was found that the curves of magnetoresistance and Shubnikov- de Haas oscillations (Fig 2) shown the features, typical for single-layered graphene. The low temperature resistance demonstrated an increase with temperature increase, which also corresponds to a behavior typical for single-layered graphene (antilocalization).

This work was supported by RFBR foundation (project 12-02-00165).



## PRECLEANING OF COPPER FOIL PRIOR TO CVD SYNTHESIS OF GRAPHENE

Changfeng Li<sup>\*</sup>, Wonjae Kim, Harri Lipsanen, and Juha Riikonen  
*Department of Micro and Nanosciences, Aalto University,  
P.O. Box 3500, FI-00076 Aalto, Espoo, Finland  
changfeng.li@aalto.fi*

Graphene has been synthesized by a vast number of scientists on different catalysts using chemical vapour deposition (CVD). Copper foil is a widely utilized substrate and researchers have been focusing on how to improve graphene quality on copper as it offers a way to manufacture high quality monolayer graphene. The surface characteristics of the copper foil play an important role in the graphene synthesis.

Even the high purity copper foils, which are commercially available, tend to have some amounts of surface impurities. Those are obviously critical when synthesizing only one monolayer thick graphene film on the surface. Additionally, copper foils, which are quite typically manufactured by rolling, have striations. Whereas the striations are typical due to manufacturing technique, the surface impurities have different origins depending on the supplier and even on the batch. The striations can lead to enhanced graphene bilayer growth [1], increase the wrinkling or resulting in tearing during the transfer process.

Using energy-dispersive X-ray spectroscopy and scanning electron microscopy we have studied the copper surface prior to any processing, after various cleaning processes and finally subsequent to the graphene growth. Our findings confirm that metals and oxides exist even on the high-purity copper surface. These are typically observed as circular nanostructures after synthesis and are often referred to as 'white dots' among the graphene researchers. As they protrude from the surface they are often seen as nucleation points, increase the bilayer growth, and can create voids in the graphene film [2].

Since sodium oxide can increase the surface roughness of copper [2], we utilize it to remove the silicon oxide and aluminium oxide prior to other treatments. Metal impurities are etched away by diluted nitric acid. The reaction between copper and high concentration of nitric acid generates gas bubbles (NO<sub>2</sub>) which can further enhance the cleaning process by preventing the impurities to reattach to the surface. Finally, the copper foil is immersed into ammonium persulfate in order to remove striations and smoothen the surface.

[1] Fan Yang, Yangqiao Liu, Wei Wu, Wei Chen, Lian Gao and Jing Sun, *Nanotechnology*, **23**, 475705 (2012).

[2] Soo Min Kim, Allen Hsu, Yi-Hsien Lee, Mildred Dresselhaus, Tomas Palacios, Ki Kang Kim and Jing Kong, *Nanotechnology*, **24**, 365602 (2013).

## CHEMICAL VAPOR DEPOSITION OF ISOLATED NANOSCROLLS WITH POLYGONAL CROSS-SECTION

S. A. Malykhin<sup>1</sup>, A. M. Alexeev<sup>1</sup>, F. T. Tuyakova<sup>2,3</sup>, R. R. Ismagilov<sup>1</sup>,  
A. N. Obraztsov<sup>1,2</sup>

<sup>1</sup>*Department of Physics, Lomonosov Moscow State University, Moscow, Russia*

<sup>2</sup>*Department of Physics and Mathematics, University of Eastern Finland, Joensuu, Finland*

<sup>3</sup>*Moscow State Institute of Radio Engineering, Electronics and Automation, Moscow, Russia;*

*sermal92@mail.ru*

Carbon nanoscrolls with polygonal cross-section embedded into nanodiamond films have been synthesized via a plasma-enhanced chemical vapor deposition. Parameters of the CVD process were adjusted to provide carbon condensation from the activated methane-hydrogen gas mixture in form of nanodiamond and nanographite structures. Structural and morphological characteristics of the nanocarbon films were obtained by Raman spectroscopy and scanning electron microscopy (SEM).

Individual scrolls were observed with SEM to evaluate their geometrical and structural characteristics. Obtained experimental results confirm previously proposed empirical structural models of the scrolls.

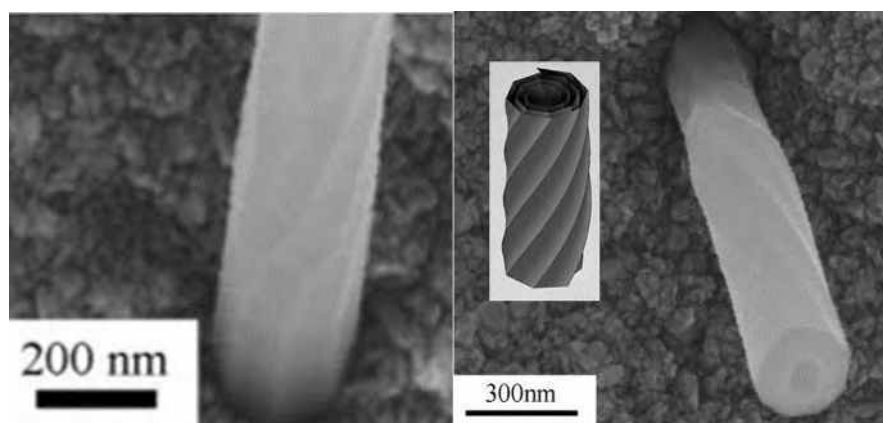


Fig. 1. Typical SEM images of the scrolls embedded into nanodiamond and their structural model

## LIQUID-PHASE EXFOLIATION OF FLAKY GRAPHITE

A.S. Pavlova<sup>1,3</sup>, E.A. Obratsova<sup>2</sup>, C. Monat<sup>3</sup>, P. Rojo-Romeo<sup>3</sup> and E.D. Obratsova<sup>1</sup>

<sup>1</sup>A.M. Prokhorov General Physics Institute, 38, Vavilova str., 119991 Moscow, Russia

<sup>2</sup>Shemyakin–Ovchinnikov Institute of bioorganic chemistry RAS, 16/10, Miklukho-Maklaya str., GSP-7, 117997 Moscow, RUSSIA

<sup>3</sup>Université de Lyon, Lyon Institute of Nanotechnology, Ecole centrale de Lyon, 36, avenue Guy de Collongue, 69131 Ecully, FRANCE  
as.pavlova@physics.msu.ru

The interest in a simple way of graphene fabrication is still challenging. All methods possess different trade-offs. A liquid-phase exfoliation (LPE) of graphite powder can be an answer to a high-yield graphene production [1,2]. To produce the extended graphene flakes the initial graphite in form of flakes can be more advantageous than the graphite powder.

In this work various solvents and surfactants were applied to fabricate graphene flakes from a flaky graphite by a liquid-phase exfoliation technique. This method includes ultrasonication processing of graphite with subsequent ultracentrifugation eliminating large graphite particles.

Ultrasonication is used to disperse graphite, and solvents or surfactants - to stabilize it. Once the suspension was ready the graphene flakes in it were characterized by means of optical microscopy (Fig. 1), Raman spectroscopy (Fig. 1, 2) and scanning electron microscopy (Fig. 3).



Fig. 1. Optical image of drop-casted graphene flakes.

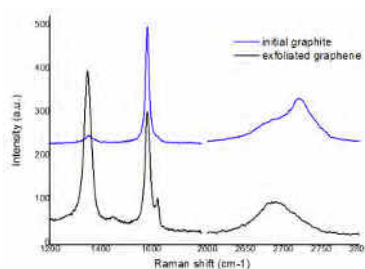


Fig. 2. Raman microscopy spectra from the sample shown in Fig. 1 ( $\lambda=532$  nm).

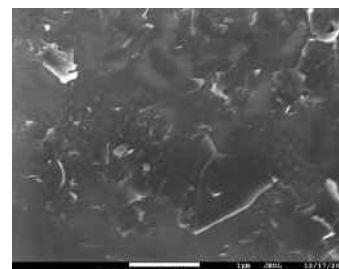


Fig. 3. SEM image of as-fabricated graphene film.

As can it be concluded from Raman data (Fig. 2.) we came up with graphene flakes of about 3-5 carbon layers. The scanning electron microscope (SEM) measurements show that we obtain graphene flakes of size up to 1  $\mu\text{m}$  admixed with a significant amount of small flakes providing a high defect peak in Raman spectra.

A film produced by filtering graphene suspension through Millipore filter is demonstrated on Fig. 3 (SEM image). Such films could be used as saturable absorbers in mode-locked lasers.

*The work was supported by RFBR-14-02-31725, MK-6201.2014.2 and RAS Research programs.*

[1] M. Lotya et al., Liquid Phase Production of Graphene by Exfoliation of Graphite in Surfactant/Water Solutions, *J. Am. Chem. Soc.*, 131 (10), 3611–3620, 2009.

[2] Y. Hernandez et al., High-yield production of graphene by liquid-phase exfoliation of graphite, *Nature Nanotechnology* 3, 563 – 568, 2008.

## GRAVITATIONAL EFFECT ON CHEMICAL VAPOR DEPOSITION OF CARBON MATERIALS IN DIRECT CURRENT GAS DISCHARGE PLASMA

N. O. Skovorodnikov<sup>1</sup>, A. M. Alexeev<sup>1</sup>, F. T. Tuyakova<sup>2,3</sup>, R. R. Ismagilov<sup>1</sup>,  
A. N. Obratsov<sup>1,2</sup>

<sup>1</sup>*Department of Physics, Lomonosov Moscow State University, Moscow, Russia*

<sup>2</sup>*Department of Physics and Mathematics, University of Eastern Finland, Joensuu, Finland*

<sup>3</sup>*Moscow State Institute of Radio Engineering, Electronics and Automation, Moscow, Russia;*

*skovorodnikov.nikolay@gmail.com*

Carbon materials with different atomic structure were synthesized via a plasma-enhanced direct current chemical vapor deposition (PE DCCVD). Parameters of the DC-CVD process were optimized to provide carbon condensation from the activated methane-hydrogen gas mixture. Structural and morphological characteristics of the nanocarbon films were obtained by Raman spectroscopy and scanning electron microscopy (SEM).

Gas mixture activation was conducted with different electrode polarity to evaluate dependence of the CVD process on relative direction of electric and gravitational fields. Obtained results indicate minor gravitational effects in the DC-CVD process except formation of carbon structures of new type. Possible mechanisms of the CVD process and carbon material formation are discussed.



Fig. 1. Photo images of the DC CVD activation region in case of: standard (left), inverted gravity (middle) and inverted electric field (right) configurations.

## CHARACTERIZATION OF GaSe USING RAMAN SPECTROSCOPY AND ATOMIC FORCE MICROSCOPY

Jannatul Susoma, Changfeng Li, Harri Lipsanen and Juha Riikonen

*Department of Micro and Nanosciences, Aalto University,  
P.O. Box 3500, FI-00076 Aalto, Espoo, Finland  
(e-mail: jannatul.susoma@aalto.fi)*

Two-dimensional materials have attracted significant attention from the scientific community in the last years due to their extraordinary transport properties and prospects for technological applications in numerous fields. As a first discovered monolayer material, graphene has been widely studied for its unusual electrical, optical, magnetic, and mechanical properties. The main advantage of graphene-based field-effect transistors (GFET) is the very high carrier mobility reaching values up to  $200,000 \text{ cm}^2 \text{ V}^{-1} \text{ s}^{-1}$  [1]. However, due to absence of a bandgap, it is challenging to establish a high on-off ratio which is essential for transistor applications [2]. Subsequently, considerable efforts have been made to open a bandgap in graphene, for example utilizing graphene nanoribbons, creating sequential defects on monolayer graphene, and using AB stacked bilayer graphene. There has also been an extensive search for other layered 2D materials that would be comparable to graphene with semiconducting characteristics.

GaSe has emerged as one alternative 2D material because of its wide bandgap of 2.10 eV. Very recently, the extraordinary performance of GaSe was demonstrated in applications such as field effect transistor [3] and high performance photodetectors [4] showing impressive quantum efficiency up to  $\sim 1400\%$ . Fundamental research of the basic properties of GaSe is vital while assessing its potential for novel applications. In this point of view, Raman analysis with atomic force microscopy (AFM) and scanning electron microscopy (SEM) is very important. Using scanning confocal  $\mu$ -Raman, we investigated most prominent Raman active modes  $A_{1g}$  ( $214 \text{ cm}^{-1}$ ),  $E_{2g}$  ( $254 \text{ cm}^{-1}$ ) and  $E_{1g}$  ( $309 \text{ cm}^{-1}$ ), where  $A_{1g}$  indicates planar vibration and  $E_{2g}$  and  $E_{1g}$  are associated with the vibration of selenides in the out-of-plane direction [4]. Edge effects, which are important to understand in nanoscale devices, were also investigated by  $\mu$ -Raman mapping. AFM was used to study morphology, defects, and roughness of the GaSe surface as well as to confirm the thickness of the GaSe flakes.

- [1] X. Du, I. Skachko, A. Barker and E. Y. Andrei, Approaching Ballistic Transport in Suspended Graphene, *Nature Nanotechnology*, **3**, 491 (2008).
- [2] F. Schwierz, Graphene Transistors, *Nature Nanotechnology*, **5**, 487 (2010).
- [3] D. J. Late, B. Liu, J. Luo, A. Yan, H. S. S. R. Matte, M. Grayson, C. N. R. Rao, and V. P. Dravid, GaS and GaSe Ultrathin Layer Transistors, *Advanced Materials*, **24**, 3549 (2012).
- [4] P. Hu, Z. Wen, L. Wang, P. Tan, and K. Xiao, Synthesis of Few-Layer GaSe Nanosheets for High Performance Photodetectors, *ACS Nano*, **6**, 5988 (2012).

## MONOCRYSTALLINE DIAMOND PROBES FOR ATOMIC FORCE MICROSCOPY

F.T. Tuyakova<sup>1</sup>, A. N. Obraztsov<sup>1,2</sup>, R. R. Ismagilov<sup>2</sup>, E. A. Obraztsova<sup>3</sup>

<sup>1</sup>*University of Eastern Finland, Finland, Joensuu*

<sup>2</sup>*M.V. Lomonosov Moscow State University, Russia, Moscow*

<sup>3</sup>*A.M. Prokhorov General Physics Institute of RAS, Russia, Moscow*

*feruza.tuyakova@uef.fi*

Diamond is an excellent material for scanning probe microscope applications, but still existing technologies (diamond-coated cantilevers or mounted pieces of monocrystalline diamond) were not able to meet the requirements for affordability, reproducibility and sharpness[1]. Novel monocrystalline diamond probes combine the high aspect ratio geometry with superb mechanical and chemical properties. In this paper we present our innovative results on preparation and testing of the novel diamond probes for scanning probe microscopy applications. Also we will present our results on the effect of selective thermal oxidation on the sharpness of needles.

Monocrystalline diamond probes were prepared by selective thermal oxidation of polycrystalline diamond films grown by chemical vapor deposition [1-5]. The obtained micron-sized single-crystal diamond tips had a pyramidal shape with a radius of curvature of 2-20 nm at the apex. Diamond needle was attached to the console of the cantilever via epoxy glue by electrostatic spraying of liquid. New diamond probes were tested for atomic force microscope. The obtained results revealed comparative advantage of novel probes in comparison with standard silicon probes. The comparatively simple and inexpensive technology for producing the diamond probes opens the way for their mass-production and is promising for use in commercial scanning probe microscopy.

[1] Alexander N. Obraztsov, P. G. Kopylov, B. A. Loginov et al. Single-crystal diamond probes for atomic-force microscopy. *Instruments and Experimental Techniques*, Vol. 53, No 4. (2009), 613–619

[2] Aleksey Zolotukhin, Petr G. Kopylov, Rinat R. Ismagilov, Alexander N. Obraztsov; Thermal oxidation of CVD diamond; *Diamond and Related Materials*, Vol. 19, (2010), 1007-1011.

[3] Alexander N. Obraztsov and Aleksey A. Zolotukhin; *Diamonds in the air*; *Materials Today*, Vol. 15, No 11 (2012), 519.

[4] Aleksey A. Zolotukhin, Rinat R. Ismagilov, Matvei A. Dolganov, and Alexander N. Obraztsov; Morphology and Raman spectra peculiarities of CVD diamond films; *Journal of Nanoelectronics and Optoelectronics*, Vol. 7, No 1. (2012), 22-28.

[5] Aleksey A. Zolotukhin, Matvey A. Dolganov, Alexander N. Obraztsov; Nanodiamond films with dendrite structure formed by needle crystallites; *Diamond and Related Materials* Vol. 37, (2013) 64–67.



## Friday, August 1







## FLOATING CATALYST CVD SYNTHESIS OF SWNTS FOR THIN FILM DEVICES – LESSONS LEARNED AND FUTURE DIRECTIONS

Esko I. Kauppinen

*Department of Applied Physics, Aalto University School of Science*

*Puumiehenkuja 2, P.O. Box 16100, FI-00076 Aalto, Finland*

*esko.kauppinen@aalto.fi*

We discuss  $(n,m)$  distributions of our floating catalyst chemical vapor deposition (FFCVD) synthesis of SWCNTs from CO using Fe catalyst clusters made via direct evaporation using hot wire generator as well as via thermal decomposition of ferrocene, and with the addition of trace amount of CO<sub>2</sub>. Here both the tube diameter as well as length can be tailored by changing the reactor temperature profile as well as CO<sub>2</sub> concentration. Helicity i.e.  $(n,m)$  distributions as determined with ED/TEM are biased towards large chiral angles with the maximum population at about 23 degrees. Then we proceed to explore the effect of carbon source gas, by adding C<sub>2</sub>H<sub>4</sub> together with CO and looking at the effect of temperature when producing catalysts via ferrocene decomposition. We also discuss Cs-corrected HRTEM results to explore the size and structure of the active Fe catalyst particles responsible for the SWNT growth.

We review our earlier results when growing SWNTs from CO with Fe catalyst clusters made via physical vapor deposition (PVD) i.e. evaporation via resistively heating the iron wire. To explore in more detail the effect of Fe catalyst cluster size and concentration in the floating catalyst synthesis, we have developed a novel catalyst particle production method via PVD, based on arc discharge between two electrodes i.e. the spark generator. This method allows to control separately both the catalyst particle size and concentration when fed into the floating catalyst SWCNT synthesis reactor. Controlling the catalyst gas phase concentration allows us to reduce significantly tube-to-tube collisions i.e. bundling. Preliminary results show that when reducing catalyst particle gas phase number concentration, the bundle size of the produced tubes is significantly reduced, and we reduce the tube diameter below 1 nm and narrow the chiral angle distribution towards armchair when reducing synthesis temperature and CO concentration. Interestingly, the SWNT mean diameter does not significantly change when controlling catalyst number mean diameter from 4 nm to 10 nm. We explore also bundle formation during the SWNT deposition processes.

We present the current status of transparent conducting films and field effect thin film transistors manufactured by direct, dry deposition of SWNT networks. Also, we discuss the use of transparent SWNT films in the EMS applications.

## OPTIMIZATION OF MULTI-WALLED CARBON NANOTUBE PROPERTIES VIA VARIATION OF GROWTH CONDITIONS AND POST SYNTHESIS TREATMENTS

Vladimir L. Kuznetsov<sup>1,2</sup>

<sup>1</sup>*Boreshkov Institute of catalysis SB RAS, Lavrentieva ave. 5, 630090, Russia*

<sup>2</sup>*Novosibirsk State University, Pirogova str. 2, 630090, Russia*

*kuznet@catalysis.ru*

Multi-walled carbon nanotubes (MWCNTs) are known as the most perspective components for numerical composite materials because their unique mechanical, chemical, and electronic properties. At the same time properties of MWCNTs significantly depend on their structure (defectiveness, diameter distribution, morphology of agglomerates, concentration of impurities etc.) which in turn depends on the type of process and on reaction parameters used for the production.

For synthesis of MWCNTs by catalytic CVD techniques the nature of catalysts (metals, supports, metal-support interaction, and the effect of promoters) are the most important factors. In this paper I will analyze data concerning the formation of the active component of mono and bimetallic Fe, Co, Fe-Co and Co-Mn catalysts during MWCNT growth versus nanotube properties. This analysis is based on *in situ* synchrotron radiation XRD studies combined with the results of other physical methods (*ex situ* and *in situ* HRTEM, internal field <sup>59</sup>Co NMR, time resolved XPS) which allows the development of kinetic model and the optimization of the synthesis conditions to produce MWCNTs with controlled properties in a fluidized bed reactor. For the first time we have obtained data confirming the stepwise formation of Fe-Co bimetallic alloy. It was found that the cobalt particles are formed at the first stage of catalyst reduction. These primary particles promote the reduction of Fe species with the subsequent formation of the alloy. Mono-component Fe catalyst demonstrates the simultaneous formation of Fe-C alloys with subsequent transformation into stable iron carbide. The *in situ* activation of the Fe-Co catalysts leads to the formation of highly dispersed alloyed particles with bcc structure type. Meanwhile, the stable carbide formation for such systems is not observed. The absence of stable carbides promotes carbon diffusion through metal particle providing much higher activity of bimetallic Fe-Co catalysts compared to that of Fe catalysts. According to the XRD data, catalyst active component is solid or at least contains crystalline core during MWCNT growth.

This paper also reviews MWCNT properties (mechanical, electrical and chemical) especially focusing on their structure. Various parameters influencing the MWCNT growth and properties along with post synthesis treatments influencing the nanotube structure and surface composition are also discussed.

## STM STUDY OF GOLD INTERCALATION PROCESS UNDER GRAPHENE MONOLAYER ON NI(111)

S.L. Kovalenko, B.V. Andryushechkin, and K.N. Eltsov

*A.M. Prokhorov General Physical Institute RAS, 38 Vavilov Stret, 119991 Moscow,*

*Russia*

*eltsov@kapella.gpi.ru*

In the wake of impressive experiments performed at ‘the Manchester group’ on a single atomic sheet of graphite transferred on silicon oxide by means of ‘Scotch Tape technology’ [1,2], the academic community has struggled to create an intelligent technique for graphene layers production on a solid state surface. This issue has not been appropriately addressed so far. Both methods viewed as most promising - high-temperature annealing of hexagonal silicon carbide and cracking of hydrocarbons on surfaces of some metals (Ni, Ru, Re, etc.) – require gold intercalation under graphene to create a quasi-free graphene layer (the Dirac cone waist being at the Fermi level) [3,4]. Also, the graphene electronic structure (the Dirac cone energy position, the formation of a energy band gap, etc.) varies depending on the intercalated metal (Ag, Cu, Si, Cs, etc.). The conditions under which metal intercalation under graphene is possible have been found empirically, while the intercalate atomic structure and the process explaining how alien atoms settle under a graphene layer have remained unknown.

This paper presents the results of a study of the gold intercalation process in the “graphene monolayer on Ni(111) surface” system. The graphene on a Ni(111) surface was formed by a sequence of “propylene adsorption at 300°C / annealing at 500°C” cycles, in which gold was first deposited on a graphene layer at 300°C, and then the entire Au/Gr/Ni(111) system was annealed at 450 °C. We have found that this technique of carbon deposition creates a nearly ideal epitaxial graphene monolayer on the Ni(111) surface. Its lattice orientation is the same as that of the substrate (without any rotation), which is proven by STM and LEED observations. STM images taken at room temperature show that as gold deposits on Gr/Ni(111) as a series of rather large detached 3D islands. As the surface of the Au/Gr/Ni(111) system is then annealed at 450°C, however, the gold morphology changes dramatically. The large islands “melt down” into 2D “pools” retaining a core of the initial island. Structurally, the “pools” represent a network of triangular dislocation loops characteristic of a “gold monolayer on Ni(111) surface” system [5]. We are able to create continuous graphene monolayer on Au /Ni(111). In the paper, we discuss how the intercalated layer forms and what we think its atomic structure is.

Support by the BMBF (project No 05K12OD3) is gratefully acknowledged.

[1] K.S. Novoselov, A.K. Geim, S.V. Morozov *et al*, Science 306 (2004) 666.

[2] K.S. Novoselov, E. McCann, S.V. Morosov, *et al* Nat. Phys. 2 (2006) 177.

[3] M. N. Nair, M. Cranney, F. Vonau, *et al* PHYS. REV. B **85** (2012) 245421.

[4] A. M. Shikin, A. G. Rybkin, D. Marchenko, *et al*, New Journal of Physics 15 (2013) 013016.

## CHIRALITY-CONTROLLED GROWTH OF SINGLE-WALLED CARBON NANOTUBES

Yan Li

*Beijing National Laboratory for Molecular Science, Key Laboratory for the Physics and Chemistry of Nanodevices, State Key Laboratory of Rare Earth Materials Chemistry and Applications, College of Chemistry and Molecular Engineering, Peking University, Beijing 100871, China.  
yanli@pku.edu.cn;*

Chirality-selective growth of single-walled carbon nanotubes (SWNTs) has been a big challenge since 1990s. Recently we developed a strategy to produce SWNTs with specific chirality by using a new family of catalysts, tungsten-based bimetallic alloy nanoparticles of non-cubic symmetry, which have high melting points and consequently are able to maintain their crystal structure during the chemical vapor deposition process, to regulate the chirality of the grown SWNTs. The (12,6) SWNTs are directly synthesized at an abundance of > 92% by using  $W_6Co_7$  catalysts. Experimental evidence and theoretical simulation reveal that the good structural match between the carbon atom arrangement around the nanotube circumference and the arrangement of the atoms in one of the planes of the nanocrystal catalyst facilitates the (n,m) preferential growth of SWNTs. This method is also valid for other tungsten-based alloy nanocatalysts to grow SWNTs of various designed chirality. Employing alloy nanocrystals with unique structure as catalysts paves a way for the ultimate chirality control in SWNT growth and thus may promote the development in SWNT applications.

[1] F. Yang, X. Wang, D. Zhang, J. Yang, D. Luo, Z. Xu, J. Wei, J.-Q. Wang, Z. Xu, F. Peng, X. Li, R. Li, Y. Li, M. Li, X. Bai, F. Ding, Y. Li\*, "Chirality-specific growth of single-walled carbon nanotubes on solid alloy catalysts", *Nature*, DOI 10.1038/nature13434 (2014).

[2] Y. Li, R. Cui, L. Ding, Y. Liu, W. Zhou, Y. Zhang, Z. Jin, F. Peng, J. Liu, "How Catalysts affect the Growth of Single-Walled Carbon Nanotubes on Substrates", *Advanced Materials*, 22, 1508-1515 (2010).

## CARBON NANOTUBE TRANSPARENT CONDUCTORS AND THEIR DEVICE APPLICATIONS

Yutaka Ohno

*Department of Quantum Engineering, Nagoya University,  
Furo-cho, Chikusa-ku, Nagoya 464-8603, Japan  
yohno@nagoya-u.jp*

Transparent conductors are widely used in most of flat-panel displays (FPD) such as liquid crystal displays and recently in organic light-emitting diode (OLED) displays and touch sensors, in which indium-tin-oxide is conventionally used. Recently, carbon nanotube (CNT) transparent conductors are attracting considerable attention because they are free from the resource and price fluctuation problems, and also have various advantages in mechanical, chemical, and optical properties, especially, the flexibility and stretchability enables us to develop various kinds of novel human machine interfaces such as wearable gadgets, head up displays in vehicle, and so on. We recently have realized thin-film transistors and integrated circuits on plastic film by using CNT films, which show good flexibility and optical transparency [1]. The deformation of the devices in various three-dimensional shapes has been demonstrated based on the thermo-pressure moulding process which is widely used to deform plastic materials. We also present low-cost fabrication technique of CNT-based capacitive touch screens [2], and unique characteristics of CNT electrodes for OLED and DUV-LED applications.

- [1] D. M. Sun, M. Y. Timmermans, A. Kaskela, A. G. Nasibulin, S. Kishimoto, T. Mizutani, E. I. Kauppinen and Y. Ohno, *Nat. Commun.* 4, 2302 (2013)
- [2] N. Fukaya, D. Y. Kim, S. Kishimoto, S. Noda and Y. Ohno, *ACS Nano* 8, 3285 (2014)

## TRANSPARENT CONDUCTIVE FILMS BASED ON IODINE- or CuCl-FILLED SINGLE-WALL CARBON NANOTUBES

A.A. Tonkikh<sup>1</sup>, V.I. Tsebro<sup>2</sup>, A.A. Dolgoborodov<sup>3</sup>, E.A. Obraztsova<sup>1</sup>,  
A.G. Nasibulin<sup>4</sup>, E.I. Kauppinen<sup>4</sup>, H. Kataura<sup>5</sup>, K. Suenaga<sup>5</sup>, A.L.Chuvilin<sup>6</sup>, E.D.  
Obraztsova<sup>1</sup>

<sup>1</sup> A.M. Prokhorov General Physics Institute, RAS, 38 Vavilov street, 119991, Moscow, Russia

<sup>2</sup> P.N. Lebedev Physical Institute, RAS, Moscow, Russia

<sup>3</sup> Moscow Engineering Physics Institute, Russia

<sup>4</sup> Aalto University, Espoo, Finland

<sup>5</sup> National Institute of Advanced Science and Technology, Tsukuba, Japan

<sup>6</sup> CIC nanoGUNE Consolider, San Sebastian, Spain

[aatonkikh@gmail.com](mailto:aatonkikh@gmail.com)

One of the most important issues in scientific community is a formation of flexible, highly conductive and transparent films for many applications, for instance, for electrodes. Single-wall carbon nanotubes (SWCNTs) seem to be one of the most promising material for such films providing a prospective to replace the most popular today indium tin oxide (ITO) films.

In this work we present a new way to make the transparent conductive films based on SWCNTs. A net of SWCNTs grown by an aerosol chemical vapor deposition (CVD) technique is used as a framework. To estimate the dependence of electrical resistance on optical transmittance the aerosol-SWCNTs were packed in films of different nanotube density. The films with an average transmittance of 60, 70, 80, 90 and 95 % have been formed. A new approach to increase the electrical conductivity of transparent conductive SWCNTs films is the filling of nanotubes with iodine or CuCl in gas phase. Due to the electron density redistribution (or the charge transfer from NT to filler) the semi-conductive SWCNTs become p-conductors. The effect of charge transfer was observed in UV-vis-IR optical absorption spectra as a suppression of NT electron transitions. Also the film brightening in a spectral range 200 – 3000 nm was observed. The different extent of charge transfer was observed for Iodine and CuCl.

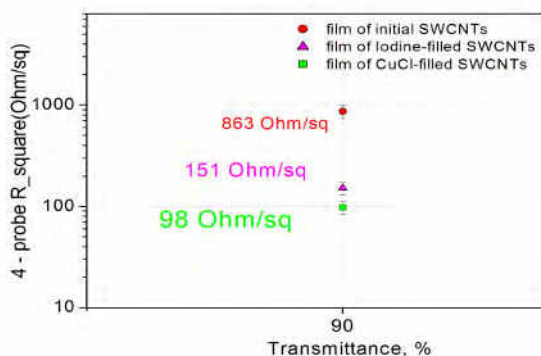


Fig.1. The electrical sheet resistance measured by 4-probe technique versus the average optical transmittance for 3 types of single-wall carbon nanotube films grown by aerosol technique: pristine, iodine-filled and CuCl-filled.

The work was supported by RFBR grants 13-02-01354, 14-02-31818, 14-02-31829, RAS research programs, projects IRSES-295241 and MK-6201.2014.2.

The 4-probe measurements have shown the decrease of sheet resistance by an order of magnitude. The best couple of parameter achieved was the sheet resistance of 98 Ohm/sq at 90% of average optical transmittance (Fig.1). The effect was more pronounced in case of CuCl filling.

## RAMAN SPECTROSCOPY AS A TOOL TO STUDY THE DOPING OF GRAPHENE

Matthieu Paillet<sup>1,2</sup>, Romain Parret<sup>1,2</sup>, Antoine Tiberj<sup>1,2</sup>, Miguel Rubio-Roy<sup>3</sup>, Jean-Roch Huntzinger<sup>1,2</sup>, Périne Landois<sup>1,2</sup>, Mirko Mikolasek<sup>1,2</sup>, Sylvie Contreras<sup>1,2</sup>, Jean-Louis Sauvajol<sup>1,2</sup>, Erik Dujardin<sup>3</sup>, Ahmed-Azmi Zahab<sup>1,2</sup>

<sup>1</sup>*Université Montpellier 2, Laboratoire Charles Coulomb UMR 5221, F-34095, Montpellier, France*

<sup>2</sup>*CNRS, Laboratoire Charles Coulomb UMR 5221, F-34095, Montpellier, France*

<sup>3</sup>*CEMES-CNRS, Université de Toulouse, 29 rue Jeanne Marvig, Toulouse 31055, France*

*Matthieu.Paillet@univ-montp2.fr*

In this communication, we will illustrate how Raman spectroscopy can be used to study the doping of graphene. We will first report data recorded by in situ Raman experiments on single-layer (SLG) graphene during exposure to rubidium vapor. By this way, we have been able to follow continuously the changes of the G and 2D bands features over a broad doping range (up to about  $10^{14}$  electrons/cm<sup>2</sup>). Previous theoretical predictions have shown that the evolution of the G-mode in SLG results from the competition between adiabatic and non-adiabatic effects. We emphasize that a possible substrate pinning effect, which inhibits the charge-induced lattice expansion of graphene layer, can strongly influence the G band position [1].

In the second part, we will show that the charge carrier density of graphene exfoliated on a SiO<sub>2</sub>/Si substrate can be finely and reversibly tuned between electron and hole doping with visible photons. This photo-induced doping happens under moderate laser power conditions but is significantly affected by the substrate cleaning method. In particular, it requires hydrophilic substrates and vanishes for suspended graphene. These findings also suggest that Raman spectroscopy is not always as non-invasive as generally assumed [2].

[1] R. Parret, M. Paillet, J.-R. Huntzinger, D. Nakabayashi, T. Michel, A. Tiberj, J.-L. Sauvajol, A.-A. Zahab, *ACS Nano*, **7**, 165 (2013).

[2] A. Tiberj, M. Rubio-Roy, M. Paillet, J.-R. Huntzinger, P. Landois, M. Mikolasek, S. Contreras, J.-L. Sauvajol, E. Dujardin, A.-A. Zahab, *Scientific Reports*, **3**, 2355 (2013).



## SELF-ASSEMBLING GRAPHENE DEPOSITION TECHNIQUE ON MICRON AND SUB-MICRON SCALE STRUCTURES

Tommi Kaplas, Sepehr Ahmadi, and Yuri Svirko

*Institute of Photonics, University of Eastern Finland, P.O.B. 111, FI-80101, Finland*

[tommi.kaplas@uef.fi](mailto:tommi.kaplas@uef.fi)

Graphene has been utilized in a numerous photonic and optoelectronic applications such as transparent electrodes, saturable absorbers, ultrafast transistors and optical modulators [1]. However, a metallic catalyst is needed for graphene synthesis, while incorporation graphene in to photonic and optoelectronic devices requires deposition graphene directly on insulators and/or semiconductors on the prescribed location. Here we propose a technique for selective graphene growth directly on a pre-patterned dielectric substrate.

In the experiment, we formed grating structures with various periodicities (ranging from 200 nm to 4  $\mu\text{m}$ ) on a silica substrate by electron beam lithography. This pre-patterned substrate was covered by a 180 nm thick copper film and placed in the CVD chamber (see Ref. [2,3] for details). In the CVD process that was carried out at temperature of 950  $^{\circ}\text{C}$ , the Cu film will liquidize and form a pattern prescribed by the morphology of the substrate. A few layer graphene nanostructure, which was grown on the silica/copper interface, can be revealed by etching the copper remains (see Fig. 1).

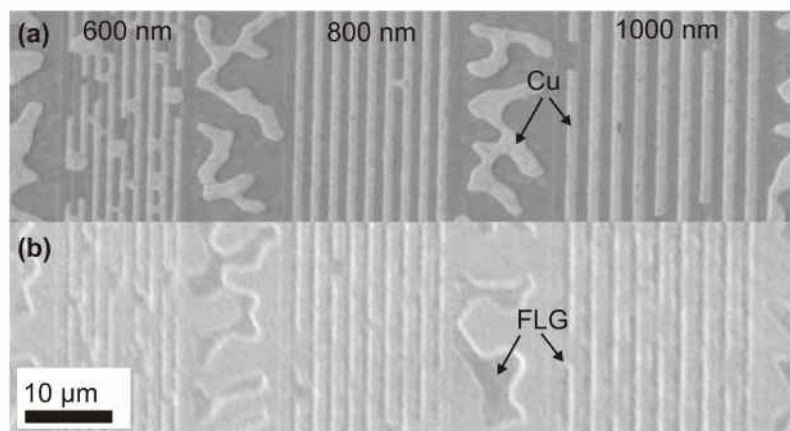


Fig. 1. (a) After the CVD the intact copper layer receded forming copper ribbons aligned by the grating lines (grating line widths 600 nm – 1000 nm). (b) Removing the remaining copper reveals a few layered graphene (FLG) areas beneath copper.

In conclusion we demonstrate a transfer free technique in order to deposit graphene selectively without post patterning. This technique should prove to be useful when pre-patterned structures, such as optical gratings or plane waveguides are needed to coat with graphene.

- [1] F. Bonaccorso, Z. Sun, T. Hasan and A.C. Ferrari, *Nat. Photon.* **4**, 611-622 (2010).
- [2] T. Kaplas, D. Sharma and Y. Svirko, *Carbon* **50(4)**, 1503-1509 (2012).
- [3] T. Kaplas, and Y. Svirko, *Carbon* **70**, 273-278 (2014).

## EFFECTS OF HYDROGEN AND TEMPERATURE ON SCALABLE GRAPHENE GROWTH BY APCVD WITH C<sub>2</sub>H<sub>2</sub>

Mei Qi, Zhaoyu Ren\*, Yixuan Zhou, Weilong Li, Xinlong Xu, and Jintao Bai  
*Institute of Photonics & Photon-Technology, Northwest University, Xi'an 710069, China*  
[qimei0916@163.com](mailto:qimei0916@163.com)

Graphene, a monolayer sp<sup>2</sup>-bonded carbon atoms, has shown great potential for optoelectronic applications [1, 2], such as broadband THz modulator and isolator [3, 4]. In these applications, large area, low defect density, and high uniformity graphene is desirable. Although graphene prepared by mechanical exfoliation has the highest quality, the maximum size on the scale of micron level limited its THz application. Chemical vapor deposition (CVD) on Cu foil is a cost-efficient method for high quality, large-scale graphene. Moreover, CVD graphene can be transferred to any substrate. As a result, CVD graphene shows high potential for the THz applications.

In our work, the graphene was synthesized on Cu foil by APCVD with C<sub>2</sub>H<sub>2</sub>. C<sub>2</sub>H<sub>2</sub> served as the carbon source that can dramatically decrease defects in synthesized graphene due to the healing mechanism of divacancy defects. Effects of H<sub>2</sub> and temperature on graphene growth were studied. High-quality bilayer graphene films are rapidly synthesized with the ratio of H<sub>2</sub> and Ar flow rates (H<sub>2</sub>/Ar) range from 0.010 to 0.111 at 1000 °C [5]. The THz sheet conductivity of the sample is 1.68 mS. In addition, multilayer graphene domains were observed on top of the bilayer graphene under the relatively large H<sub>2</sub> concentration (H<sub>2</sub>/Ar=0.250 and 0.429). The results indicate that H<sub>2</sub> serve as an activator of the surface bound carbon for the bilayer graphene growth, while show an etching effect that control the morphology, nucleation density, and nucleation size of the multilayer graphene domains. And 2 to 5-layer graphene is synthesized with growth temperature range from 1000 °C to 850 °C, indicating that the growth is not self-limiting under low growth temperature with C<sub>2</sub>H<sub>2</sub> concentration in saturation.

The work was supported by National Natural Science Foundation of China (61275105, 61177059, 11374240), International Cooperative Program (201410780), Shaanxi Natural Science Basic Research Plan (2012KJXX-27, 12JK0990), Education Ministry Ph.D. Programs Foundation (20136101110007, 20126101120029), and Key Laboratory Science Research Plan of Shaanxi Education Department (11JS106, 13JS101).

- [1] K. Novoselov, A. Geim, S. Morozov, D. Jiang, Y. Zhang, S. Dubonos, I. Grigorieva and A. Firsov, *Science* **306** (5696), 666-669 (2004).
- [2] F. Bonaccorso, Z. Sun, T. Hasan and A. Ferrari, *Nature Photonics* **4** (9), 611-622 (2010).
- [3] B. Sensale-Rodriguez, R. Yan, M. M. Kelly, T. Fang, K. Tahy, W. S. Hwang, D. Jena, L. Liu and H. G. Xing, *Nature communications* **3**, 780 (2012).
- [4] Y. Zhou, X. Xu, H. Fan, Z. Ren, J. Bai and L. Wang, *Phys. Chem. Chem. Phys.* **15**, 5084-5090 (2013).
- [5] M. Qi, Z. Ren, Y. Jiao, Y. Zhou, X. Xu, W. Li, J. Li, X. Zheng and J. Bai, *The Journal of Physical Chemistry C* **117** (27), 14348-14353 (2013).

## NITROGEN DOPING OF GRAPHENE FILMS GROWN BY CHEMICAL VAPOUR DEPOSITION via AMMONIA PLASMA TREATMENT

Maxim Rybin<sup>1,2</sup>, A. Pereyaslavcev<sup>3</sup>, T. Vasilieva<sup>4</sup>, V. Maysnikov<sup>4</sup>,  
I. Sokolov<sup>1,3</sup>, E. Obraztsova<sup>1,2</sup>

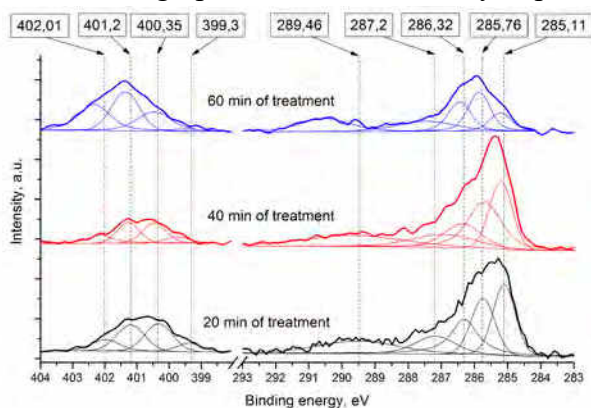
<sup>1</sup> *A.M. Prokhorov General Physics Institute, Moscow, Russia*

<sup>2</sup> *National Research Nuclear University MEPhI (Moscow Engineering Physics Institute), Moscow, Russia*

<sup>3</sup> *The Federal State Unitary Enterprise All-Russia Research Institute of Automatics, Moscow, Russia*

<sup>4</sup> *The Moscow Institute of Physics and Technology, Moscow, Russia*  
*rybmaxim@gmail.com*

Graphene is a two dimensional carbon nanomaterial with unique mechanical, optical, chemical and electronic properties. Moreover, the potential of graphene can be enlarged by its properties changing via chemical functionalization or doping. The second approach is based on some carbon atoms substitution by another ones (boron, nitrogen, sulfur, fluorine etc.) The doping of graphene results in modification of its electronic structure, namely, the Fermi level could be shifted either in conduction zone or in valence zone, depending on electronic structure of dopants. The usual dopants are boron and nitrogen. They are acceptor and donor of electrons for graphene, accordingly. In this work graphene was successfully doped with nitrogen atoms.



XPS spectra of graphene films treated by ammonia plasma for different periods of time.

Here we demonstrate an efficient technique for a large scale production of a high quality graphene. Our process consists of two steps. The first step is synthesis of graphene film on polycrystalline copper foil by a chemical vapor deposition (CVD) method followed by the film transfer onto a silicon substrate covered by a thin (300 nm) silica layer [1, 2]. The second step is treatment of graphene film in ammonia plasma using a radio frequency (RF) plasma reactor [3]. Such combination of two steps guarantees a precise control of

procedure on each step and provides fabrication of N-doped graphene samples with a controllable doping degree. The prepared samples were characterized by XPS (see the figure above), Raman and optical absorption spectroscopy. The presence of C-N bondings has been confirmed by the appearance of new bands in XPS spectra and by the Raman spectra modification.

*The work was supported by RFBR-13-02-12181, 14-02-31639 projects and RAS research programs.*

[1] Rybin et al., PSS C 7 (11–12), 2785 (2010).

[2] Rusakov et al., JNO 8, 78 (2013).

[3] Vasilieva et al., IEEE Transac.Plasma Sci. 38(8), 1903 (2010).

## TiO<sub>2</sub> – NANOGRAFITE COMPOSITE FILM MATERIAL

R. R. Ismagilov<sup>1</sup>, A. M. Alexeev<sup>1</sup>, F. T. Tuyakova<sup>2,3</sup>, A. N. Obraztsov<sup>1,2</sup>

<sup>1</sup>*Department of Physics, Lomonosov Moscow State University, Moscow, Russia*

<sup>2</sup>*Department of Physics and Mathematics, University of Eastern Finland, Joensuu, Finland*

<sup>3</sup>*Moscow State Institute of Radio Engineering, Electronics and Automation, Moscow, Russia;*

*ismagil@polly.phys.msu.ru*

Chemical vapor deposition (CVD) technique was developed to produce nanographite film materials by condensation of carbon from hydrogen-methane gas mixture activated by a direct current discharge [1,2]. A particular feature of the CVD processes consists in ability of obtaining the film material consisting of flaky and tubular graphitic structures of nanometer size.

Atomic layer deposition (ALD) method was used to deposit thin amorphous TiO<sub>2</sub> layer over CVD nanographite film surface.

Obtained composites were studied comprehensively with use Raman scattering, scanning and transmission electron microscopy. Obtained experimental results were used for development of a qualitative model explaining formation mechanisms of the nanographite structures and film morphology.

Potential applications of the TiO<sub>2</sub> – nanographite composites with unique surface morphology, atomic structure and physical characteristics are discussed.

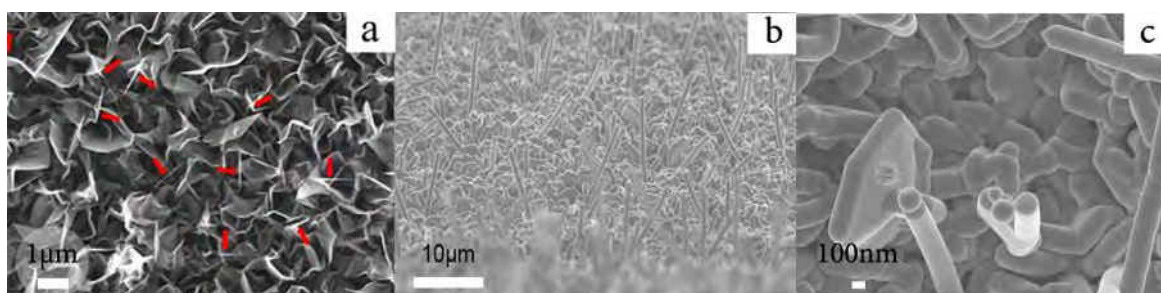


Fig. 1. SEM images of a CVD film composed of graphite sheets and nanoscrolls. (a) plane view, where some nanoscrolls are marked by red arrows. (b) side view of CVD film covered with amorphous TiO<sub>2</sub> by ALD for scrolls visualization. (c) enlarged plane view of CVD film covered with amorphous TiO<sub>2</sub>

[1] A.N. Obraztsov, P.G. Kopylov, A.L. Chuvilin, N.V. Savenko, *Diamond and Related Materials*, **18**, 1289 (2009)

[2] A.L. Chuvilin, V.L. Kuznetsov, A.N. Obraztsov, *Carbon*, **47**, 3099 (2009)

## NANOCARBON BASED COMPOSITES VS FLUORINATED GRAPHENE: DIELECTRIC AND ELECTROMAGNETIC PROPERTIES

N. Valynets<sup>1</sup>, P. Kuzhir<sup>1</sup>, A. Paddubskaya<sup>1</sup>, M. Shuba<sup>1</sup>, S. Maksimenko<sup>1</sup>,  
V. Sysoev<sup>2</sup>, V. Tur<sup>2</sup>, L. Bulusheva<sup>2</sup>, A. Okotrub<sup>2</sup>, J. Macutkevic<sup>3</sup>, J. Banys<sup>3</sup>, F.  
Micciulla<sup>4</sup>, L. Coderoni<sup>4</sup>, S. Bellucci<sup>4</sup>, V. Fierro<sup>5</sup>, V. Ksenevich<sup>6</sup>, N. Gorbachuk<sup>6</sup>, T.  
Veselova<sup>6</sup>, N. Poklonski<sup>6</sup>, A. Wieck<sup>7</sup>, G. Rinaldi<sup>8</sup> A. Celzard<sup>5</sup>

<sup>1</sup>*Research Institute for Nuclear Problems, Belarusian State University,  
Bobruiskaya str., 11, 220030, Minsk, Belarus*

<sup>2</sup>*Nikolaev Institute of Inorganic Chemistry, SB RAS, Russia*

<sup>3</sup>*Department of Radiophysics, Vilnius University, Vilnius, Lithuania*

<sup>4</sup>*Frascati National Laboratory, National Institute of Nuclear Physics, Frascati, Italy*

<sup>5</sup>*IJL – UMR Université de Lorraine – CNRS 7198, ENSTIB, Épinal Cedex, France*

<sup>6</sup>*Department of Physics, Belarusian State University, Nezalezhnastsi ave., 4, 220030,  
Minsk, Belarus*

<sup>7</sup>*Department of Physics and Astronomy, Bochum Ruhr-University, Universitaetstr., 150,  
44780, Bochum, Germany*

<sup>8</sup>*University of Rome "Sapienza", Rome, Italy  
nadezhda.volynets@gmail.com*

Polymer composites with various carbon inclusions, like single- or multi- walled carbon nanotubes (SWCNT and MWCNT), carbon black, graphene nanoplatelets are very attractive for electromagnetic (EM) applications due to possibility to manipulate their properties at nanoscale. We present the comparative study of dielectric and electromagnetic properties of epoxy resin composites filled with different carbon and nanocarbon inclusions and thin films of fluorinated graphene in the wide frequency range (20 Hz - 3 THz) at temperatures from room to 500 K.

In particular, it has been observed that enhancement of the composites' conductivity (epoxy/SWCNT and epoxy/MWCNT, 1 wt%) at the rising of DC bias voltage and temperature is induced by decreasing of height of the energy barriers between separate nanotubes.

The electrical conductivity of epoxy filled with exfoliated graphite above the percolation threshold (2 wt.%) and at low temperatures (below glass transition temperature of pure polymer matrix) is mainly governed by electron tunnelling between graphite particles.

Nanoribbon fluorinated graphene (FG) could be the very promising alternative to epoxy/carbon composites. 10 nm thick layer of FG, been much thinner than the skin depth in microwave range (which is 35-50 micron, depending on the fluorination degree), provides nevertheless non zero EM attenuation, viz 28% at 34-36 GHz. Moreover, the reflectance ability has been observed to be significantly higher in the case of more fluorinated samples (10%).

To conclude, the fluorination, already reported as powerful tool to tune the DC conductivity of graphene [1], can be also very interesting for producing effective EM interference shielding materials, combining reflective (with larger amount of fluorine) and absorptive (with smaller fluorine percentage) nanometrically thin layers.

## INFRARED OPTICAL LIMITING RESPONSE IN DETONATION NANODIAMOND CLUSTERS DISPERSED IN HEAVY WATER

V.V. Vanyukov<sup>1</sup>, T.N. Mogileva<sup>2</sup>, G.M. Mikheev<sup>2</sup>, A.P. Puzyr<sup>3</sup>, V.S. Bondar<sup>3</sup>,  
Y.P. Svirko<sup>1</sup>

<sup>1</sup>*Institute of Photonics, University of Eastern Finland, Joensuu, Finland*

<sup>2</sup>*Institute of Mechanics, Russian Academy of Science, Izhevsk, Russia*

<sup>3</sup>*Institute of Biophysics, Russian Academy of Sciences, Krasnoyarsk, Russia*  
*viatcheslav.vanyukov@uef.fi*

Nonlinear optical materials have attracted much attention of the optical community due to their capability to attenuate potentially dangerous laser radiation while promptly transmitting low-intensity ambient light. These materials can be used in so called optical limiting (OL) devices capable to avoid laser-induced breakdown of sensitive optical components or human eye. We report on the OL the infrared laser radiation with detonation nanodiamond (ND) clusters and on the dependence of the OL properties on the pump wavelength.

In the experiment, we employed suspensions of ND clusters with an average size of 110 nm dispersed in heavy water with concentration 3 wt. %. Heavy water was chosen as a host liquid due to a weak near infrared light absorption. In the OL measurements, we utilized a tunable radiation from 1400 to 1675 nm produced by the optical parametric oscillator/optical parametric amplifier pumped by the second and the first harmonics of Nd: YAG<sup>3+</sup> laser. In order to evaluate the nonlinear attenuation effect in the ND clusters as a function of a wavelength the Z-scan technique was utilized [1].

The nanosecond Z-scan results at the energy of the laser pulses 0.2 mJ show the strong attenuation the near infrared laser radiation in ND suspension. The experimental results reveal that the shorter the wavelength, the lower the nonlinear transmittance of the ND suspension, i.e. the greater the attenuation of the incident radiation. Our findings indicate that the decreasing of the nonlinear transmittance of the ND suspension originates from the nonlinear absorption and an increase of the nonlinear light scattering.

In conclusion, we demonstrate that ND suspensions show strong OL response at the range of 1400÷1675 nm. Recently we have found that ND suspensions show excellent OL performance at wavelengths of 532 [2] and 1064 nm [3] and hence are promising materials for manufacturing of OL devices capable of operating in a broadband spectrum range.

[1] M. Sheik-Bahae, A.A. Said, T.H. Wei, D.J. Hagen, E.W. Van Stryland, *IEEE J. Quantum Electron.* **26**, 760 (1990).

[2] V. Vanyukov, T. Mogileva, G. Mikheev, A. Puzyr, V. Bondar, Y. Svirko, *Applied Optics* **52**, 18 (2013).

[3] V.V. Vanyukov, G.M. Mikheev, T.N. Mogileva, A.P. Puzyr, V.S. Bondar, Y.P. Svirko, submitted to *Optical Materials*, (2014).

## SPIN-ORBIT COUPLING AND QUANTUM CONDUCTANCE IN CARBYNE - THE MOST SIMPLE CARBON NANOMATERIAL

Pavel N. D'yachkov, Vasiliy A. Zaluev

*Kurnakov Institute of General and Inorganic Chemistry of the Russian Academy of  
Sciences, Leninskii pr. 31, 119991 Moscow, Russia  
p\_dyachkov@rambler.ru*

The effect of spin-orbit interaction on the band structures of the monatomic carbon chains, called the carbynes, is calculated in terms of a linear augmented cylindrical wave method [1]. In a cumulenic carbyne with the double bonds, the splitting of  $\pi$  band at the Fermi energy region is equal to 2.4 meV, but the metallic character of band structure is not broken by spin-orbit interaction. In the semiconducting polyynic carbyne with alternating single and triple bonds, the spin-orbit gaps are different for the highest valence band (3.1 meV) and the lowest conduction band (2.1 meV). The spin-orbit gaps in carbyne are about 2 or 3 times smaller than the spin-orbit splitting (6 meV) in the carbon atom. In carbyne, the spin-orbit interaction is larger than that in carbon nanotubes because of the larger curvature of electron orbits encircling the carbyne chains; the larger spin-orbit coupling can be attractive for new experiments and applications. The ballistic electrical conductance of cumulenic and polyynic carbon chains C<sub>40</sub>, C<sub>20</sub>, and C<sub>10</sub> is calculated using the  $\pi$ -electron tight-binding methods [2]. The transmission function and dependences of the current on the length of the carbon chain, the type of carbon bonds, material properties of the electrodes, bias voltage, and temperature are obtained. For small bias voltages, the problem of calculating the transmission function in the cumulenic and polyynic chains is solved analytically by applying the difference schemes approach. In the case of large voltages, we apply an iterative technique. The transmission functions  $\tau(E,V)$  of the cumulenic and polyynic chains of similar composition differ dramatically. The energy regions of very high and low transparency of carbynes for electrons are obtained, and an oscillatory character of the energy dependence of transmission functions is pointed out. The voltage-dependent variations of the  $\tau$  are initially quite weak, but at the higher voltages their effect is a drastic reduction of the carbyne transparency. One important feature of the current-voltage I-V characteristics is that the current initially increases with growth of the bias voltage, reaches a peak, and then drops to give rise to the negative conductance. On the typical I-V curves of the polyynic chains, there are both the peak and local minimum (valley) at higher voltages. Moreover, there are some oscillations of voltage dependences of conductance due to the discrete nature of the C chain electron energy levels. The presence of the negative resistance regions and valley in the curve I-V indicate the possibilities of design of the resonance tunneling devices based on the C chains.

The research was partially supported by the Russian Basic Research Foundation (Grant 14-03-00493) and EU under Project No. FP7-247007 CACOMEL.

[1] P. N. D'yachkov, V. A. Zaluev. Spin-Orbit Gaps in Carbynes. *J. Phys. Chem. C*. 2014, 118 (5), pp 2799–2803. DOI: 10.1021/jp410108f.

[2] P. N. D'yachkov, V. A. Zaluev, E. Yu. Kocherga, and N. R. Sadykov. Tight Binding Model of Quantum Conductance of Cumulenic and Polyynic Carbynes. *J. Phys. Chem. C*. 2013, 117 (32), pp 16306–16315. DOI: 10.1021/jp4038864

## Author index

- Agrinskaya, N. V., 89  
Ahmadi, S., 106  
Alexeev, A. M., 81, 85, 86, 91, 93, 109  
Almadori, Y., 67  
Alvarez, L., 67  
Andryushechkin, B. V., 101  
Anoshkin, I., 27  
Arenal, R., 44, 69  
Arkipov, V., 82  
Arpiainen, S., 16  
Arutyunyan, N. R., 83  
Asanov, I. P., 8, 17  
Avramenko, M. V., 39, 44  
Ayari, A., 71  
Aznar, R., 67
- Bai, J., 46, 49, 107  
Bantignies, J., 67  
Banys, J., 110  
Baryshevsky, V., 82  
Batanov, G. M., 88  
Batrakov, K., 40  
Bautista, G., 57  
Bellucci, S., 74, 110  
Berezovets, 89  
Blau, W. J., 21  
Bokova-Sirosh, S. N., 41  
Bondar, V. S., 111  
Borzda, T., 42, 51, 52  
Borzosekov, V. D., 88  
Bulusheva, L. G., 8, 17, 45, 73, 82, 110  
Burluckaya, N., 74  
Bychanok, D. S., 45
- Cambedouzou, J., 67  
Campidelli, S., 67  
Celzard, A., 110  
Cha, S., 3  
Chehova, G. N., 8  
Chen, Ya, 29  
Cheng, J., 75  
Chernov, A. I., 12  
Chizov, P. A., 35  
Choueib, M., 71  
Chuvilin, A., 17  
Chuvilin, A. L., 104  
Coderoni, L., 110  
Cojocar, S. C., 71
- Contreras, S., 105
- Derouet, A., 71  
Dieudonn-George, P., 67  
Dolgoborodov, A. A., 104  
Dujardin, E., 105  
Dyachkov, P. N., 112
- Eltsov, K. N., 101  
Englund, D., 77  
Eremin, T. V., 43  
Eremina, V. A., 84
- Fasel, R., 6  
Fedotov, P. V., 12, 70, 84  
Ferrari, A., 11  
Fierro, V., 110  
Finkelstein, D. I., 85  
Fossard, F., 67  
Fu, Bo, 29  
Fujii, S., 66
- Gadermaier, C., 34, 42, 51, 52  
Gan, X., 46, 77  
Garnov, S. V., 35  
Generalov, A., 27  
Golberg, D., 61  
Golushko, I. Yu., 39  
Gopeyenko, V., 74  
Gorbachuk, N., 110  
Guselnikov, A., 82
- Heinz, T. F., 77  
Hirakawa, T., 66  
Hirano, A., 66  
Honkanen, S., 14  
Huntzinger, J., 105  
Huttunen, M., 57
- Ishchenko, A. V., 41  
Ismagilov, R. R., 81, 85, 86, 91, 93, 95, 109  
Ito, Y., 66  
Izard, N., 68
- Jiang, Man, 46  
Jorio, Ado, 15  
Jousselle, B., 67
- Kainlauri, M., 16



- Kaplas, T., 40, 106  
Karvonen, L., 14  
Kataura, H., 66, 104  
Kato, Y. K., 76  
Kauppinen, E. I., 12, 99, 104  
Kauranen, M., 57  
Kharchev, N. K., 88  
Kieu, K., 14, 25  
Kim, J. Min, 3  
Kim, W., 16, 90  
Kirilenko, D., 48  
Kleshch, V. I., 72  
Kolik, L. V., 88  
Konchekov, E. M., 88  
Kondrashov, I. I., 87  
Kononenko, V. V., 83  
Koroteev, V., 73  
Kovalenko, S. L., 101  
Krasnikov, D. V., 41  
Ksenevich, V., 110  
Kuwata-Gonokami, M., 58  
Kuzhir, P. P., 26, 40, 82, 110  
Kuznetsov, V. L., 12, 41, 100
- Landois, P., 105  
Lanzani, G., 60  
Lebedev, A. A., 89  
Lebedev, S. P., 89  
Lee, Y. Hee, 28  
Letunov, A. A., 88  
Levshov, D., 44, 69  
Levshov, D. I., 39  
Li, C., 16, 90, 94  
Li, D., 46  
Li, Q., 29  
Li, W., 107  
Li, Yan, 102  
Lim, S. Chu, 28  
Lioubtchenko, D., 27  
Lipsanen, H., 14, 16, 29, 90, 94  
Litvin, D. P., 89  
Liu, Y., 46  
Lobanova-Shunina, T., 74  
Lobiak, E. V., 45  
Loiseau, A., 32, 67
- Mäkitalo, J., 57  
Müller, S., 14  
Macutkevic, J., 40, 110  
Makarov, Yu. N., 89  
Makarova, T. L., 8, 10  
Maki, Kin Fai, 77  
Maksimenko, S. A., 26, 40, 82, 110  
Malakhov, D. V., 88  
Malykhin, S. A., 91  
Martel, R., 71  
Maruyama, S., 23
- Matsuda, K., 66  
Mattila, M., 29  
Mayoral, V. V., 42, 51, 52  
Maysnikov, V., 108  
Mehrarar, S., 14  
Melnikov, L., 30  
Mertelj, T., 42  
Micciulla, F., 110  
Michel, T., 44, 69  
Mihailovic, D., 42, 51, 52  
Mikheev, G. M., 31, 50, 53, 111  
Mikolasek, M., 105  
Milovich, F. O., 88  
Miyauch, Y., 66  
Mogileva, T. N., 111  
Monat, C., 92  
MvGuire, G., 7
- Nagaluk, S. S., 89  
Nashchekin, A., 48  
Nasibulin, A. G., 12, 27, 50, 53, 104  
Nefedov, E., 30  
Nefedov, I., 30  
Norwood, R., 14  
Noury, A., 68
- Obraztsov, A. N., 72, 81, 85, 86, 91, 93, 95, 109  
Obraztsov, P. A., 35  
Obraztsova, E. A., 88, 92, 95, 104  
Obraztsova, E. D., 12, 13, 41, 43, 47, 70, 83, 84, 87, 88, 92, 104, 108  
Ohno, Y., 103  
Okotrub, A. V., 8, 17, 45, 73, 82, 110  
Osadchy, A. V., 13, 47  
Ovchinnikov, V., 27
- Paddubskaya, A., 40, 110  
Paillet, M., 69, 105  
Parc, R. Le, 67  
Pavlov, S., 48  
Pavlova, A. S., 92  
Pereyaslavcev, A., 108  
Perisanu, S., 71  
Petrov, A. E., 88  
Peyghambarian, N., 14  
Pinakov, D. V., 8  
Poklonski, N., 110  
Poncharal, P., 71  
Pozharov, A. S., 87  
Priatelj, M., 51, 52  
Prokhorov, A. M., 70  
Purcell, S. T., 71, 72  
Puzyr, A. P., 111
- Qi, Mei, 49, 107
- Räisänen, A., 27

- Ren, Z., 46, 49, 107  
Riikonen, J., 14, 16, 90, 94  
Rinaldi, G., 110  
Rizakhanov, R. N., 87  
Rochal, S. B., 39  
Rodriquez, R. D., 14  
Rojo-Romeo, P., 92  
Rosenholm, J. M., 7  
Roux, X. Le, 68  
Rubio-Roy, M., 105  
Rusakov, P. S., 87  
Rybin, M. G., 87, 108  
Rybkovskiy, D. V., 13, 47
- Säynätjoki, A., 14, 25  
Saito, T., 67  
Sarksian, K. A., 88  
Saushin, A. S., 50  
Sauvajol, J. L., 44, 69, 105  
Sedelnikova, O. V., 17  
Shelankov, A., 10  
Shenderova, O. A., 7  
Shimano, Ryo, 9  
Shiue, R., 77  
Shlyakhova, E. V., 45  
Shuba, M. V., 26, 110  
Shunin, Y., 74  
Shuvaeva, M. A., 41  
Sipe, J. E., 75  
Skovorodnikov, N. O., 93  
Skvortsova, N. N., 88  
Slepyan, G. Y., 26  
Smirnov, A. N., 89  
Sohn, J., 3  
Sokolov, I. V., 87, 108  
Stepakhin, V. D., 88  
Suenaga, K., 104  
Sun, Z., 24, 29  
Susoma, J., 16, 94  
Svirko, Y., 35, 40, 106, 111  
Sysoev, V., 110
- Tanaka, T., 66  
Tereshchenko, O. E., 35  
Than, X. T., 69  
Tiberj, A., 105  
Tittonen, I., 29  
Tonkikh, A. A., 43, 70, 104  
Topolovsek, P., 42, 51, 52  
Tsebro, V. I., 104  
Tur, V., 110  
Tuyakova, F. T., 81, 85, 86, 91, 93, 109  
Tyakova, F. T., 95
- Valynets, N., 110  
Vanyukov, V. V., 111  
Vasil'ev, A. V., 89  
Vasilieva, T., 108  
Vella, D., 42, 51, 52  
Vermeuleni, N., 75  
Veselova, T., 110  
Vincent, P., 71  
Vivien, L., 68  
Vlasov, I., 7  
Voronovich, S., 40  
Vujicic, N., 42, 51, 52
- Wei, X., 66  
Wieck, A., 110
- Xu, X., 49, 107
- Yang, C., 29  
Yang, He, 29  
Yang, K., 86  
Yong, Z., 29  
Yuzyuk, Y. I., 39, 44, 69
- Zahab, A., 69, 105  
Zahn, D. R. T., 14  
Zaluev, V. A., 112  
Zheng, M., 65  
Zhou, Y., 49, 107  
Zhukovskii, Y., 74  
Zonov, R. G., 50, 53